PPAR Research

PPARs and Metabolic Syndrome

Guest Editors: Lihong Chen, Zhanjun Jia, and Guangrui Yang

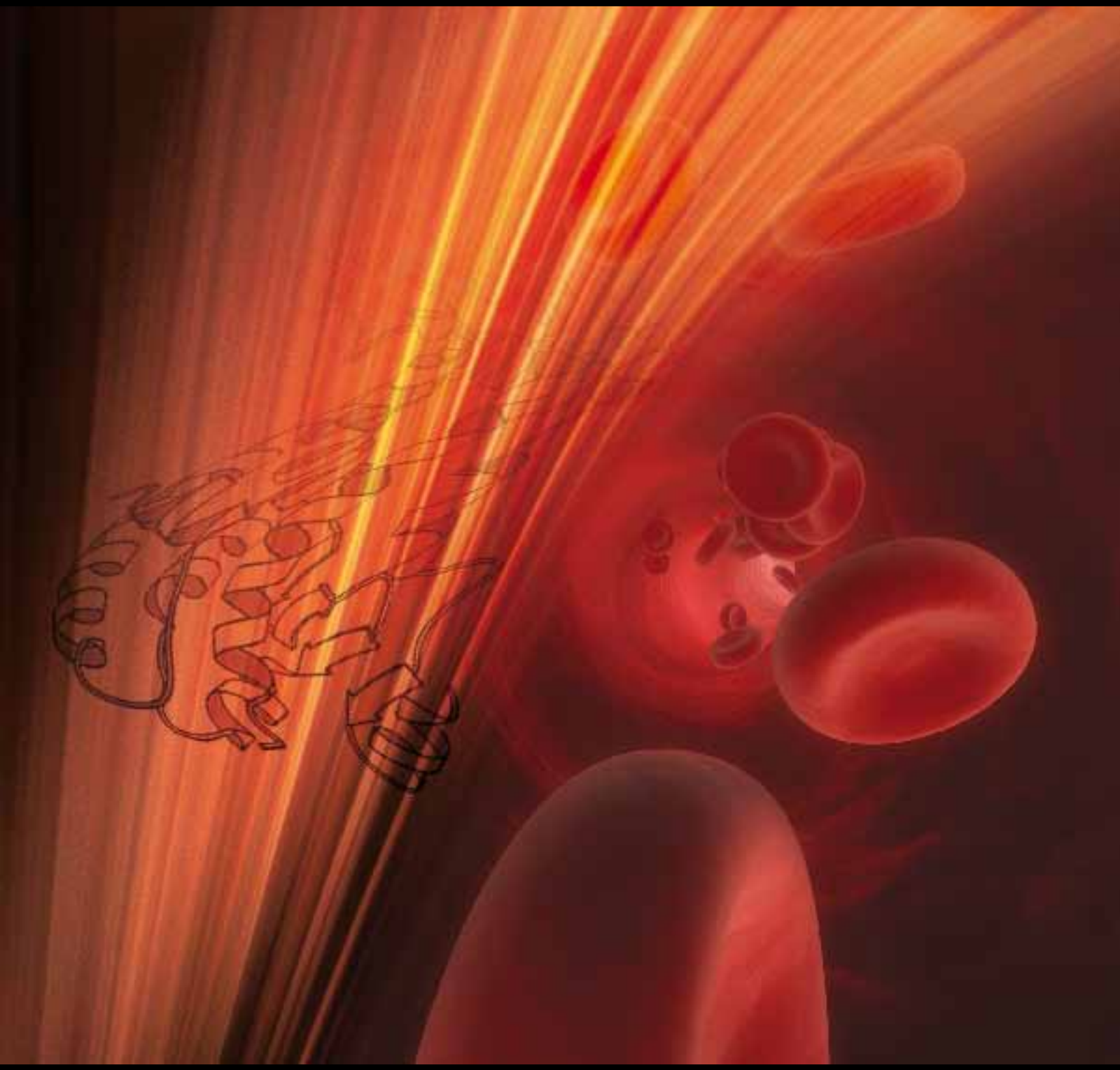

PPARs and Metabolic Syndrome

PPAR Research

PPARs and Metabolic Syndrome

Guest Editors: Lihong Chen, Zhanjun Jia, and Guangrui Yang

Editorial Board

Contents

Hindawi Publishing Corporation
PPAR Research
Volume 2014, Article ID 832606, 2 pages
http://dx.doi.org/10.1155/2014/832606

Editorial
PPARs and Metabolic Syndrome

Lihong Chen,[1] Zhanjun Jia,[2] and Guangrui Yang[1]

[1] *The Institute for Translational Medicine and Therapeutics, University of Pennsylvania, Philadelphia, PA 19104, USA*
[2] *Division of Nephrology and Hypertension, University of Utah, Salt Lake City, UT 84132, USA*

Correspondence should be addressed to Lihong Chen; bjclh2000@163.com and Guangrui Yang; guangrui@mail.med.upenn.edu

Received 25 February 2014; Accepted 25 February 2014; Published 24 March 2014

Peroxisome proliferator-activated receptors (PPARs) exert versatile biological effects, notably in energy metabolism. During the last two decades, numerous studies have demonstrated that PPARs act as pivotal regulators of metabolic syndrome, a series of disorders in energy utilization and storage that are implicated with type 2 diabetes, diabetic nephropathy, and cardiovascular diseases, to mention a few. PPARα and PPARγ are the molecular targets of a number of marketed drugs for the treatment of these diseases, and accumulating evidence suggested PPARβ/δ as a potential therapeutic drug target as well. Although energy metabolism and metabolic syndrome are the most intensively studied domain of PPARs, it has not been addressed specifically in any issue of *PPAR Research* ever since its launch. Here, we gathered 3 reviews and 5 research articles that encompass metabolic syndrome and its complications.

M. Aprile et al. tackled the subject of PPARγ and human adipogenesis in their research article. Rather than focusing on canonical PPARγ transcripts, authors largely emphasized on the critical contribution of PPARγ dominant negative isoforms to adipogenesis and their implied potential role in pathological conditions. In addition, a novel of PPARγ dominant negative transcript, γ1ORF4, was first identified in this study. In regard to nonalcoholic fatty liver diseases, the hepatic expression of the metabolic syndrome, M. Sharif et al. conducted a thorough analysis of previously published data about the steatogenic role of PPARγ and summarized two probable PPARγ ligand-dependent toxicological modes of action: (i) activation of PPARγ in hepatocytes and (ii) inhibition in adipocytes.

Two papers, one review and a research article, by Z. Jia and Y. Sun et al., appraised the role of PPARγ in diabetic nephropathy (DN). Their comprehensive review summarized the limitations of traditional PPARγ agonists, addressed the advantages of newly developed PPARγ agonists, and rendered new insights into the therapeutic potential of PPARγ agonists in the treatment of DN, while the research article suggested that a combination of PPARγ agonists with COX-2/PGE2 inhibitors may be an alternative way of dealing with DN. In another research article, J. Jin et al. analyzed the correlation between PPAR gene polymorphisms and pediatric primary nephrotic syndrome (PNS) by comparing children with PNS against healthy subjects. They found that PPARγ (Pro12Ala) and PGC-1α (Gly482Ser) polymorphisms are associated with abnormal insulin and triglyceride metabolism in pediatric PNS patients, suggesting that these polymorphisms may be relevant to the prognosis of this chronic disease.

The knowledge of the role of PPARα in metabolic disorder-associated cardiovascular diseases was well recognized in this special issue. Z. Jia et al.'s research article asserted the involvement of HMGB1 (high mobility group box 1) in the protective effect of PPARα in cardiac hypertrophy and provided a novel approach to study the pathogenesis of cardiac hypertrophy. Although most studies showed that PPARα activation confers protection against atherogenesis, the intriguing possibility that PPARα might foster atherogenesis is also considered. In this current issue, M. Vechoropoulos et al. found that PPARα mediates the proatherogenic effect of chronic nitric oxide synthesis inhibition and this effect is independent of blood pressure and serum lipids alterations. These data further shaped the view that the role of PPARα in atherosclerosis needs to be reevaluated.

Lastly, in the review article "*PPARs Integrate the Mammalian Clock and Energy Metabolism,*" we collected recent

findings about the role of PPARs in biological clocks. This brand new function of PPARs bridges energy metabolism with circadian rhythm whose relationship has been known for long time, but not well understood. We summarized the circadian function of three PPAR subtypes one by one and concluded that the abnormality of PPARs and circadian rhythm could impinge on each other and thus leads to metabolic disorders. Further investigation of PPARs in this field will give us a new perspective on the therapeutic advances in the treatment of metabolic ailments.

In conclusion, this special issue is packed with intriguing novel breakthroughs and insights into PPARs and metabolic syndrome. We hope that these advances will generate more interest from the scientific community in better understanding of the role of PPARs in metabolic syndrome and associated complications.

Lihong Chen
Zhanjun Jia
Guangrui Yang

Hindawi Publishing Corporation
PPAR Research
Volume 2014, Article ID 537865, 11 pages
http://dx.doi.org/10.1155/2014/537865

Research Article

PPARG in Human Adipogenesis: Differential Contribution of Canonical Transcripts and Dominant Negative Isoforms

M. Aprile,[1] M. R. Ambrosio,[1,2] V. D'Esposito,[2] F. Beguinot,[2,3] P. Formisano,[2,3] V. Costa,[1] and A. Ciccodicola[1]

[1] *Institute of Genetics and Biophysics "Adriano Buzzati-Traverso", National Research Council, 80131 Naples, Italy*
[2] *Department of Translational Medical Sciences, University of Naples "Federico II", 80131 Naples, Italy*
[3] *Institute of Experimental Endocrinology and Oncology, National Research Council, 80131 Naples, Italy*

Correspondence should be addressed to V. Costa; valerio.costa@igb.cnr.it

Received 25 November 2013; Revised 3 February 2014; Accepted 5 February 2014; Published 23 March 2014

Academic Editor: Guangrui Yang

The nuclear receptor PPARγ is a key regulator of adipogenesis, and alterations of its function are associated with different pathological processes related to metabolic syndrome. We recently identified two *PPARG* transcripts encoding dominant negative PPARγ isoforms. The existence of different *PPARG* variants suggests that alternative splicing is crucial to modulate PPARγ function, underlying some underestimated aspects of its regulation. Here we investigate *PPARG* expression in different tissues and cells affected in metabolic syndrome and, in particular, during adipocyte differentiation of human mesenchymal stem cells. We defined the transcript-specific expression pattern of *PPARG* variants encoding both canonical and dominant negative isoforms and identified a novel *PPARG* transcript, γ1ORF4. Our analysis indicated that, during adipogenesis, the transcription of alternative *PPARG* variants is regulated in a time-specific manner through differential usage of distinct promoters. In addition, our analysis describes—for the first time—the differential contribution of three ORF4 variants to this process, suggesting a still unexplored role for these dominant negative isoforms during adipogenesis. Therefore, our results highlight crucial aspects of *PPARG* regulation, suggesting the need of further investigation to rule out the differential impact of all *PPARG* transcripts in both physiologic and pathologic conditions, such as metabolism-related disorders.

1. Introduction

Peroxisome proliferator-activated receptors (PPARs, also known as nuclear receptor family 1C, NR1C) are ligand-dependent transcription factors belonging to the nuclear hormone receptor superfamily. Three members of the PPAR family—known as PPARα, PPARβ/δ, and PPARγ—encoded by different genes located on different chromosomes have been identified [1–3].

Undoubtedly, PPARγ is the most extensively studied and characterized member of PPARs, given its involvement in several physiological states, as well as pathological conditions. Indeed, it modulates the expression of several genes that play a central role in glucose, lipid and cholesterol metabolism, inflammation, angiogenesis, proliferation, and differentiation [4–7]. In particular, PPARγ is the master regulator of adipogenesis, since it regulates the transcription of a wide number of genes involved in cellular differentiation and lipid accumulation [8, 9]. Defects in PPARγ, signaling its altered expression and/or activation, as well as polymorphisms/mutations, are implicated in different pathological conditions occurring in metabolic syndrome, such as insulin resistance, obesity [10], dyslipidemia, and hypertension, that markedly increase the risk of type 2 diabetes [11–13], as well as cardiovascular diseases and cancer [3, 4, 14–17].

The prevalence of metabolic syndrome is increasing to epidemic proportions and, to date, an adequate therapy has not been yet established. Of great clinical interest, synthetic ligands of PPARγ, belonging to the class of thiazolidinediones (TZDs), such as troglitazone, pioglitazone, and rosiglitazone, function as insulin sensitizers and are used for treating hyperglycemia in patients with type 2 diabetes [7, 18–20].

Nevertheless, their use in type 2 diabetes therapy has been limited by untoward effects. Thus, a better understanding of PPARγ signaling is crucial to develop more effective and targeted therapeutic strategies to treat metabolic syndrome and its complications.

However, to fully define the landscape of PPARγ activity, some relevant aspects need to be taken into account. One of the most relevant features is the ability of *PPARG* gene to give rise to different transcripts. Indeed, the human *PPARG* gene consists of nine exons and—by differential promoter's usage and alternative splicing—generates at least four main splice variants (i.e., PPARG1, PPARG2, PPARG3, and PPARG4). These transcripts display different 5′ untranslated regions (UTRs), followed by six coding exons. However, despite the presence of such a variable number of *PPARG* transcripts, this gene encodes only two protein isoforms. Indeed, PPARG1, PPARG3, and PPARG4 encode the same protein PPARγ1—localized in the adipose tissue, liver, heart, and skeletal muscle—whereas PPARG2 yields a protein with 28 additional amino acids at the N-*terminus*, known as PPARγ2, exclusively localized in the adipose tissue [21–23].

Different ability to induce adipogenesis has been shown for PPARγ1 and PPARγ2, indicating a more relevant adipogenic activity for PPARγ2. Although both isoforms are thought to be essential during adipocyte differentiation, their relative contribution is not yet well clarified [24–27].

More recently, our group identified in sporadic colorectal cancers two novel *PPARG* transcripts harboring a read-through in intron 4, named γ2ORF4 and γ3ORF4, displaying the same 5′UTRs of PPARG2 and PPARG3, respectively [28]. The protein products lack the ligand binding domain (LBD) and act as dominant negative toward PPARγ. Although it has been shown that γORF4 plays a role in pathogenesis of colorectal cancer, its presence and expression levels have not yet been investigated in other cells and/or tissues.

To date, accurate analyses of the expression pattern of each *PPARG* transcript are still missing. For instance, to the best of our knowledge, this consideration holds true particularly for the adipogenesis, in which PPARγ is the main driver [4, 7, 29]. Alterations of adipocyte differentiation are strictly associated with obesity and metabolism-related disorders and therefore intimately linked to the physiopathology of the metabolic syndrome [30, 31]. Describing in detail the relative contribution of all currently known *PPARG* transcripts—and its dominant negative isoforms—in adipogenesis, as well as in tissues and cells related to processes altered in metabolic syndrome, will provide a solid basis to rule out if, and how, they may account for metabolism-related diseases.

Here we describe a complete expression analysis of all annotated *PPARG* transcripts—PPARG1, PPARG2, PPARG3, and PPARG4—as well as its dominant negative isoform γORF4 in human tissues and cells affected in metabolic syndrome. In particular, we focus on their differential expression during human adipogenesis, using human mesenchymal stem cells (hMSCs) isolated from the stromal vascular fraction of adipose tissue [32]. After *in vitro* differentiation of hMSCs in adipose cells, by using transcript-specific RT-PCR and Quantitative Real-Time PCR assays, we measured the expression of *PPARG* transcripts at various time points from the induction of adipocyte differentiation, demonstrating the differential contribution of each alternative splice variant. A similar pattern of expression was also observed for total PPARγ and γORF proteins. In addition, here we describe, for the first time, a novel transcript of *PPARG*, named γ1ORF4, similar to the dominant negative γ2ORF4 and γ3ORF4, previously identified [28]. Finally, we evaluated the abundance of all ORF4 variants during adipocytes' differentiation, also suggesting—for the first time—the involvement of these dominant negative isoforms in human adipogenesis.

2. Materials and Methods

2.1. Cell Cultures. Media, sera, and antibiotics for cell culture were from Lonza (Basel, Switzerland). Human Embryonic Kidney 293 cells (HEK239) were cultured in Dulbecco's modified Eagle's medium (DMEM) supplemented with 10% fetal bovine serum (FBS), 2 mmol/L glutamine, 100 units/mL penicillin, and 100 units/mL streptomycin.

Human Mesenchymal Stem Cells (hMSCs) were obtained by abdominal biopsy and cultures established as described previously [33]. The cells were grown in DMEM-F12 (1 : 1) with 10% FBS, 2 mmol/L glutamine, 100 units/mL penicillin, and 100 units/mL streptomycin. Cultures were maintained in a humidified atmosphere of 95% air and 5% CO_2 at 37°C.

2.1.1. Adipocyte Differentiation. Adipocyte differentiation was achieved as previously described [34]. Briefly, hMSCs were seeded (10,000 cells/cm^2) and cultured in six-well plates until confluence. Adipocyte differentiation was induced with a differentiation cocktail consisting of 850 nmol/L insulin, 10 μmol/L dexamethasone, 0.5 mmol/L IBMX (isobutylmethylxanthine), 10 μmol/L pioglitazone, 33 μmol/L biotin, and 17 μmol/L pantothenate in DMEM-F12 (1 : 1) supplemented with 3% FBS, 2 mmol/L glutamine, and antibiotics. After 3 days, the medium was changed to a medium containing only insulin and pioglitazone in DMEM-F12 (1 : 1) supplemented with 10% FBS, glutamine, and antibiotics. Culture medium was then changed every 2 days for another 8 days up to obtain a complete adipocyte differentiation of hMSCs. Lipid accumulation was determined by Oil Red O staining as described by Isakson and colleagues [34]. Adipocyte differentiation from hMSCs was performed in triplicate.

2.2. RNA Extraction and RT-PCR Assays. Total RNA was isolated from HEK239 and hMSCs at different stages of adipocyte differentiation, using TRIzol solution (Invitrogen) according to the manufacturer's instructions. RNA extracted from the other human tissues, heart, liver, and thyroid, and cells, human colon carcinoma, endothelial progenitor (EPCs), macrophages, and breast cancer (MCF7), employed in our analysis, was obtained in previous studies [28, 33, 35, 36]. For each sample, total RNA (1000 ng) was reverse transcribed using "high-capacity cDNA reverse-transcription kit" (Applied Biosystems, Foster City, CA). cDNAs obtained from human tissues and cells were used as template for RT-PCR assays. PCR amplification with specific primer

Table 1: Primer pairs for canonical and dominant negative *PPARG* variants.

Transcript	Oligonucleotide pairs		Size (bp)
	Forward	Reverse	
tPPARG	GAGAAGGAGAAGCTGTTGGC	ATGGCCACCTCTTTGCTCT	272
PPARG1	CGAGGACACCGGAGAGGG	TGTGGTTTAGTGTTGGCTTCTT	69
PPARG2	TTTTAACGGATTGATCTTTTGC	AGGAGTGGGAGTGGTCTTCC	255
PPARG3	TTCTGCTTAATTCCCTTTCC	AGGAGTGGGAGTGGTCTTCC	194
PPARG1/4	CGAGGACACCGGAGAGGG	AGGAGTGGGAGTGGTCTTCC	211/137
tORF4	CTTGCAGTGGGGATGTCTCA	AAACCCAAAACAACTTCCCG	279
γ1ORF4	CGAGGACACCGGAGAGGG	AAACCCAAAACAACTTCCCG	906
γ2ORF4	TTTTAACGGATTGATCTTTTG	AAACCCAAAACAACTTCCCG	950
γ3ORF4	TTCTGCTTAATTCCCTTTCC	AAACCCAAAACAACTTCCCG	889

pairs—designed using Oligo 4.0 and listed in Table 1—was performed using 1 μL of the reverse transcription reaction as template in PCR reactions set up with AmpliTaq Gold (Perkin Elmer). PCR assays have been performed using these amplification conditions: 95°C for 10 minutes, followed by 35 cycles at 95°C for 40 sec, 60°C for 40 sec, 72°C for 30 sec, and 70°C for 7 min. RT-PCR products were of expected length (see Table 1). In each experiment, a sample without reverse transcriptase was used as negative control and it was amplified under the same conditions as the reverse-transcribed RNA.

2.3. Cloning and Sequencing. The multiple PCR products (of about 211 and 137 bp, resp.), obtained in RT-PCR assays of PPARG1/PPARG4, have been cloned into Topo Vector II (Invitrogen) according to the manufacturer's instructions. Clones and other RT-PCR products were directly sequenced by Sanger method, confirming the specificity of reactions.

2.4. Real-Time PCR. Quantitative Real-Time PCRs were performed on cDNA samples of hMSCs and undifferentiated at different stages of adipocyte differentiation (6 hours, 12 hours, 24 hours, 2 days, 4 days, 7 days, and 10 days after induction of the process). Amplification reaction mix contained 1x SYBR Green PCR master mix (Applied Biosystems), 160 nM of each primer, and 50 ng of cDNA (RNA equivalent) as template. Quantitative Real-Time PCR assays were performed in according to the manufacturer's instructions for the 7900HT Real-Time PCR system (Applied Biosystems) in the same conditions described in [37]. Each assay for the 5 analyzed transcripts was performed in three biological replicates for all the time points. For each cell replicate, Real-Time assays were performed in two duplicated wells. Relative gene expression was measured by using $2^{-\Delta\Delta Ct}$ method. For each assay, expression levels were normalized for the reference values (time point at 0 hours or 6 hours) using glyceraldehyde 3-phosphate dehydrogenase (GAPDH) as housekeeping gene. qRT-PCRs data were reported as mean values and standard deviation of three biological replicates and results analyzed by paired Student t test. P value < 0.05 was considered statistically significant.

2.5. Immunoblot Procedure. Total cell lysates were obtained and separated by sodium dodecyl sulfate—polyacrylamide gel electrophoresis (SDS-PAGE) as previously described [38]. Briefly, hMSCs undifferentiated and at different stages of adipocyte differentiation (2 and 10 days) were solubilized for 2 hours at 4°C with lysis buffer containing 50 mM HEPES, 150 mM NaCl, 10 mM EDTA, 10 mM $Na_4P_2O_7$, 2 mM sodium orthovanadate, 50 mM NaF, 1 mM phenyl-methyl-sulfonyl fluoride, 10 μg/mL aprotinin, 10 μg/mL leupeptin, pH 7.4, and 1% (v/v) Triton X-100 (all reagents for lysis buffer were from Sigma-Aldrich, St Louis, MO, USA). The lysates were clarified by centrifugation at 12,000 rpm for 20 min at 4°C. Proteins were separated by SDS-PAGE (Bio-Rad Hercules, CA, USA) and blotted on Immobilon-P membranes (Millipore, Billerica, MA). Membranes were incubated with a polyclonal antibody directed against the N-terminal domain of PPARγ (Santa Cruz Biotechnology, CA, USA) and with antiactin antibodies (Santa Cruz Biotechnology, CA, USA). Detection of blotted proteins was performed by enhanced chemiluminescence (ECL, Amersham Biosciences, Arlington Heights, IL, USA) according to the manufacturer's instructions. Densitometric analysis was performed using Image Lab Software (Bio-Rad, Hercules, CA, USA). For each protein isoform (PPARγ and γORF4), data are shown as pixel density ratio versus control protein (actin).

3. Results

3.1. Expression Profile of PPARG Transcripts. Four main *PPARG* transcripts are currently known, as described by Costa et al. [3]. Additionally, our group has recently identified two isoforms acting asdominant negative toward PPARγ [28], transcribed by the same promoters of PPARG2 and PPARG3 transcripts, respectively (details in Figure 1).

Using specific primers pairs (Table 1), we performed an extensive expression analysis of PPARG1, PPARG2, PPARG3, PPARG4, and ORF4 in tissues and cells related to complications of metabolic syndrome—such as altered glucose and lipids' metabolism (liver), increased inflammatory response (macrophages), atherosclerosis (EPCs, heart, and macrophages), cancer (colon carcinoma and MCF7), and thyroid dysfunction (thyroid)—and in a widely used cell

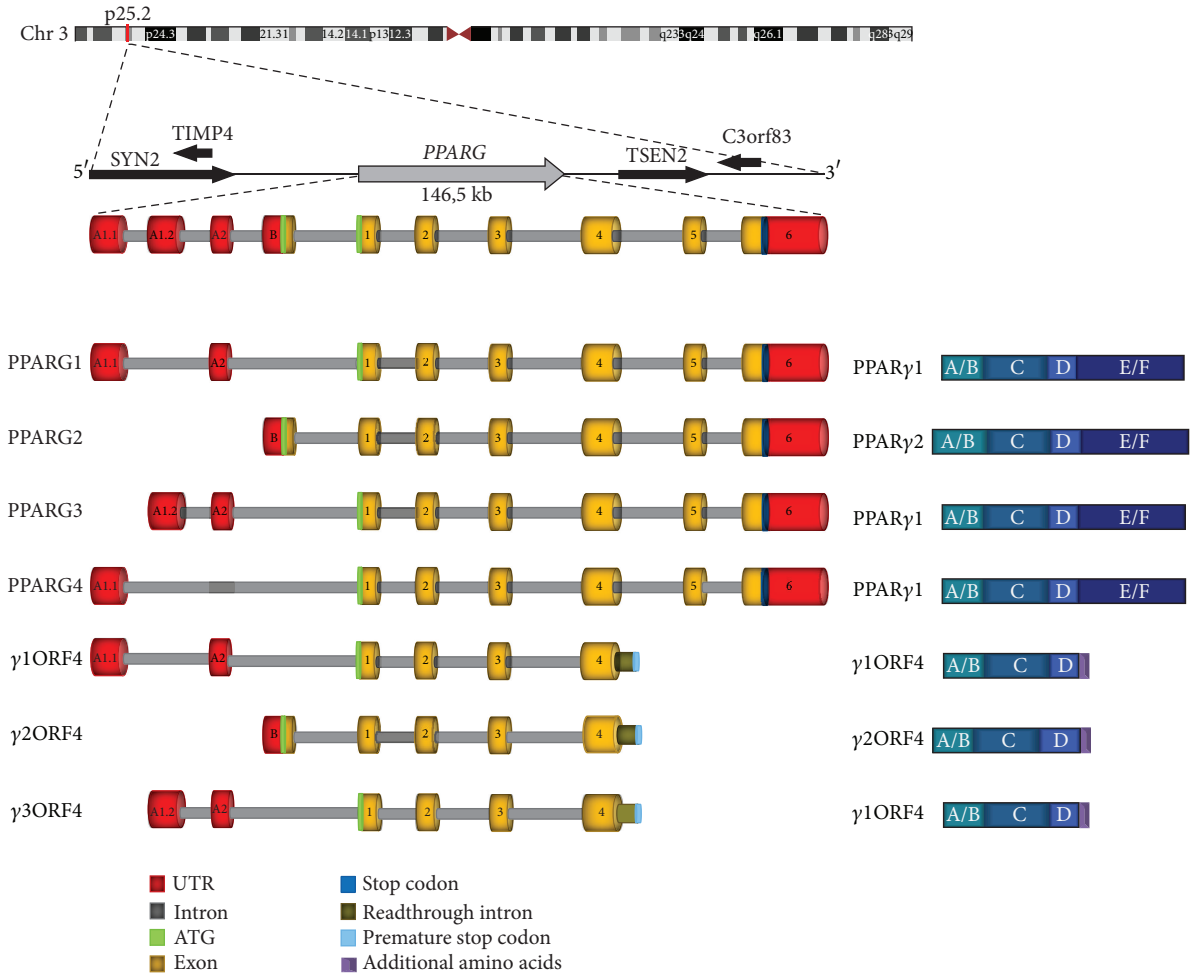

Figure 1: Schematic representation of human *PPARG* gene, transcripts, and protein isoforms. In the upper part the genomic localization of *PPARG* gene is indicated, with chromosome indication, cytogenetic band, and surrounding genes. Below is depicted the exon/intron structure of *PPARG* gene with transcribed splicing variants. Transcripts encoding both the canonical and dominant negative proteins are illustrated in the left panel. The right panel shows a schematic representation of the encoded proteins with the functional domains.

model, HEK293 [3, 6, 17, 39, 40]. Given the high similarity between the 5′UTRs of PPARG1 and PPARG4 transcripts, the primers employed to analyze PPARG4 amplify both variants (distinguishable as PCR products of different size), whereas we could design PPARG1 specific primers.

The tissue-specific expression pattern of *PPARG* alternative variants, including also transcripts encoding the same protein (PPARG1, PPARG3, and PPARG4), is shown in Figure 2. Such analysis revealed that PPARG1 transcript is expressed in all analyzed tissues and cell lines, confirming that it is abundantly and almost ubiquitously expressed in human tissues [21]. Similarly, PPARG4—which is transcribed from the same promoter—is expressed in almost all analyzed samples, albeit at lower levels than PPARG1. Therefore, we demonstrated that, in most of examined samples, PPARG1 and PPARG4 contribute to the translation of PPARγ1 protein, whereas PPARG3 is expressed at low levels only in EPCs and heart. Noteworthy, also PPARG2 transcript is expressed in EPCs, as well as in the heart, whereas its expression is undetectable in other examined tissues and cell lines. This finding—possibly correlated to the anti-inflammatory role of this nuclear receptor in the cardiovascular system [41–43]—suggests that PPARγ2 is predominantly expressed in these adult tissues. Surprisingly, the dominant negative isoform γORF4, till now associated with tumor pathogenesis, is expressed in all analyzed tissues and cell lines, suggesting a not negligible contribute to *PPARG* activity also in other physiologic and pathological cell processes. Of note, the results shown in Figure 2 refer to ORF4 transcripts' total expression.

3.2. Expression of PPARG Variants during Adipogenesis. After *in vitro* induction of hMSCs toward adipogenic differentiation (see Methods), we selected seven different time points (Figure 3). In particular, we investigated the "early stages" of adipocyte differentiation (6, 12, and 24 hours after induction), an intermediate time point (2 days), and "late stages" (4 and 7 days) according to visible changes in cell morphology and an endpoint at 10 days when cells differentiate into adipocytes (Figure 3).

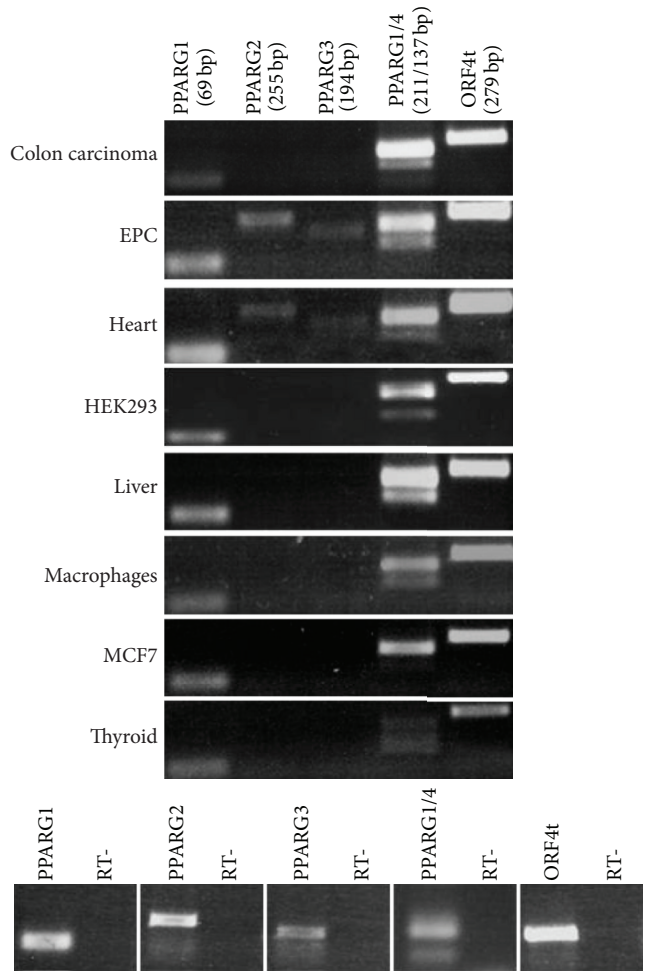

Figure 2: Expression pattern of *PPARG* variants in tissues and cells affected in the metabolic syndrome. For each *PPARG* transcript, specific primer pairs were used for PCR reactions. Given the similarity between PPARG1/4 5′UTRs primers amplifies both variants (distinguishable as PCR products of different sizes). "ORF4t" indicates the entire pool of ORF4 transcripts. Amplicons' sizes are shown (in bp) below transcripts' names. On the bottom panel, negative PCR controls are shown for each primer pair.

RT-PCR assay revealed that, first of all, total *PPARG* expression (i.e., of the entire pool of canonical *PPARG* transcripts) is very high throughout the process. In detail, using variant-specific primers we observed that all *PPARG* transcripts are expressed—albeit at variable levels—in the examined differentiation stages (Figure 4(a)). Interestingly, PPARG2 is not expressed in hMSCs, whereas its expression is remarkably higher in the early stages after induction toward adipocyte differentiation. Particularly, as shown in Figure 4(a), this transcript reaches its highest expression after 2 days from the induction and is completely silenced at the end of the process. Similarly, PPARG3 has a mild but detectable expression only in the intermediate and late stages of cells' differentiation, with its highest expression at 2 days. This analysis revealed that PPARG1 and PPARG4 are the only canonical transcripts contributing to the final expression of PPARγ protein in undifferentiated hMSCs and therefore that these cells express only PPARγ1 isoform. In particular, PPARG1 is expressed at much higher levels than PPARG4 variant and, given the absence of the PPARG3 splice variant, it can be considered as the main contributor to the synthesis of functional PPARγ1 protein in undifferentiated cells (Figure 4(a)).

However, PPARG1 and PPARG4 are expressed also throughout the adipocyte differentiation, although the former is the most expressed *PPARG* transcript at all the stages.

3.2.1. Identification of γ1ORF4 and Analysis of PPARG Dominant Negative Transcripts. Given the existence of two different isoforms of γORF4, previously described as dominant negative of PPARγ [28], we asked whether other ORF4 variants may be transcribed from the promoter upstream the $A_{1.1}$ exon of *PPARG* gene. Thus, using specific primers pairs (described in Table 1), we were able to identify in hMSCs a novel ORF4 variant, named γ1ORF4 (accession number still in process; see Figure 1 for details). Similarly to PPARG1, its 5′UTR consists of $A_{1.1}$ and A_2 exons, whereas its coding region extends from exon 1 to 4, with a read-through in intron 4, identical to the other ORF4 transcripts (structural details in Figure 1).

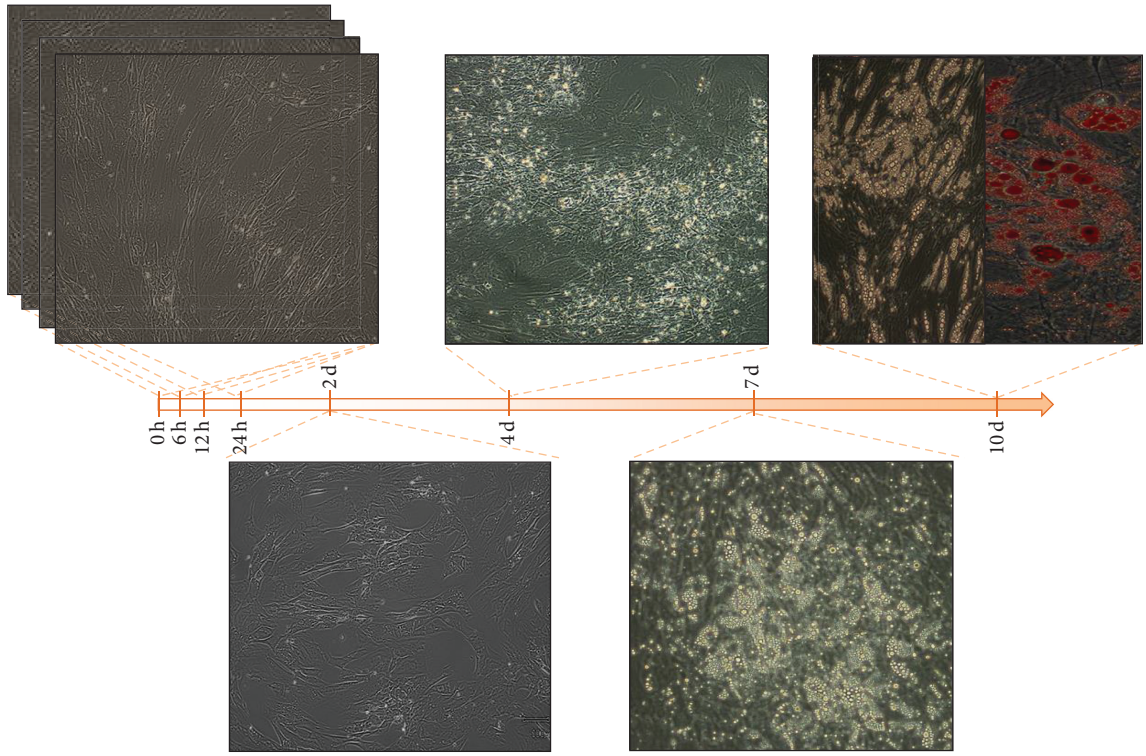

Figure 3: Phenotypic characteristics of undifferentiated, differentiating, and differentiated hMSCs (h = hours; d = days). Adipocyte differentiation was determined at 10 days from adipogenesis induction by Oil Red O staining of lipids vacuoles, as shown.

Given the discovery of such new transcript in hMSCs, we decided to investigate the expression of the entire pool of ORF4 variants (ORF4t in Figure 4(b)) during *in vitro* adipogenesis. Of note, RT-PCR assay revealed that these variants are expressed along adipocytes' differentiation and particularly in the crucial stages of this process (24 hours, 2 and 4 days). Subsequent independent analysis of the three ORF4 transcripts revealed that γ3ORF4 variant is expressed throughout the process, whereas γ2ORF4 mRNA undergoes a dramatic increase at 2 days from differentiation's induction. Noteworthy, the novel variant γ1ORF4—identified in undifferentiated hMSCs—is expressed at variable levels during adipogenesis, although it is undetectable at some stages (Figure 4(b)).

3.3. Quantitative Analysis of Canonical and Dominant Negative PPARG Splice Variants during Adipogenesis. To have a quantitative estimate of *PPARG* transcripts after induction of the adipogenic process, we performed Quantitative Real-Time analysis with specific primer pairs at the time points above described. Such quantitative analysis confirmed the findings of RT-PCR assay, showing that the expression of total *PPARG* increases up to 2 days by adipogenesis induction. Indeed, at this stage, total *PPARG* expression is about 20-fold increase compared to undifferentiated cells and it linearly decreases after 7 days, reaching expression levels comparable to undifferentiated cells (Figure 5(a)).

However, the most relevant findings derive from the canonical transcript-specific analysis. Indeed, it revealed that all PPARG canonical transcripts have a similar trend of expression but exhibit different fold increase during the process (Figure S1 see supplementary materials available online at http://dx.doi.org/10.1155/2014/537865). For PPARG2 and PPARG3 the expression values at 6 hours were used as baseline, since they are not expressed in undifferentiated hMSCs (Figure 5(a)). However, despite their low expression levels, these transcripts exhibit an increase of expression considerably higher than PPARG1. Indeed, at 2 days by differentiations' induction, the expression of PPARG2 and PPARG3 raises of about 110- and 45-fold, respectively, whereas PPARG1 increase is of about 10-fold (Figure 5(a)).

To quantitatively study ORF4 transcripts, the only way to discriminate among the different variants is through the analysis of large PCR amplicons (about 900–1000 bp, Figure 4(b)), unfeasible with qRT-PCR. Thus, quantitative data for ORF4, shown in Figure 5(a), refer to the pool of ORF4 transcripts. Particularly, we observed, for these variants, a different trend of expression throughout the process compared to *PPARG* canonical transcripts, confirming RT-PCR assays (Figure 4(b)). Indeed, ORF4 total expression is significantly downregulated in early stages of differentiation and reaches its highest values at 2 days. Nonetheless, its increase is considerably lower than the canonical transcripts (fold increase = 4; Figure 5(a)).

Finally, pairwise comparison of fold changes' variation, that is, between two subsequent time points, revealed that the most significant increase of the expression values occurs in the transition from day 1 to day 2 upon induction of adipocyte

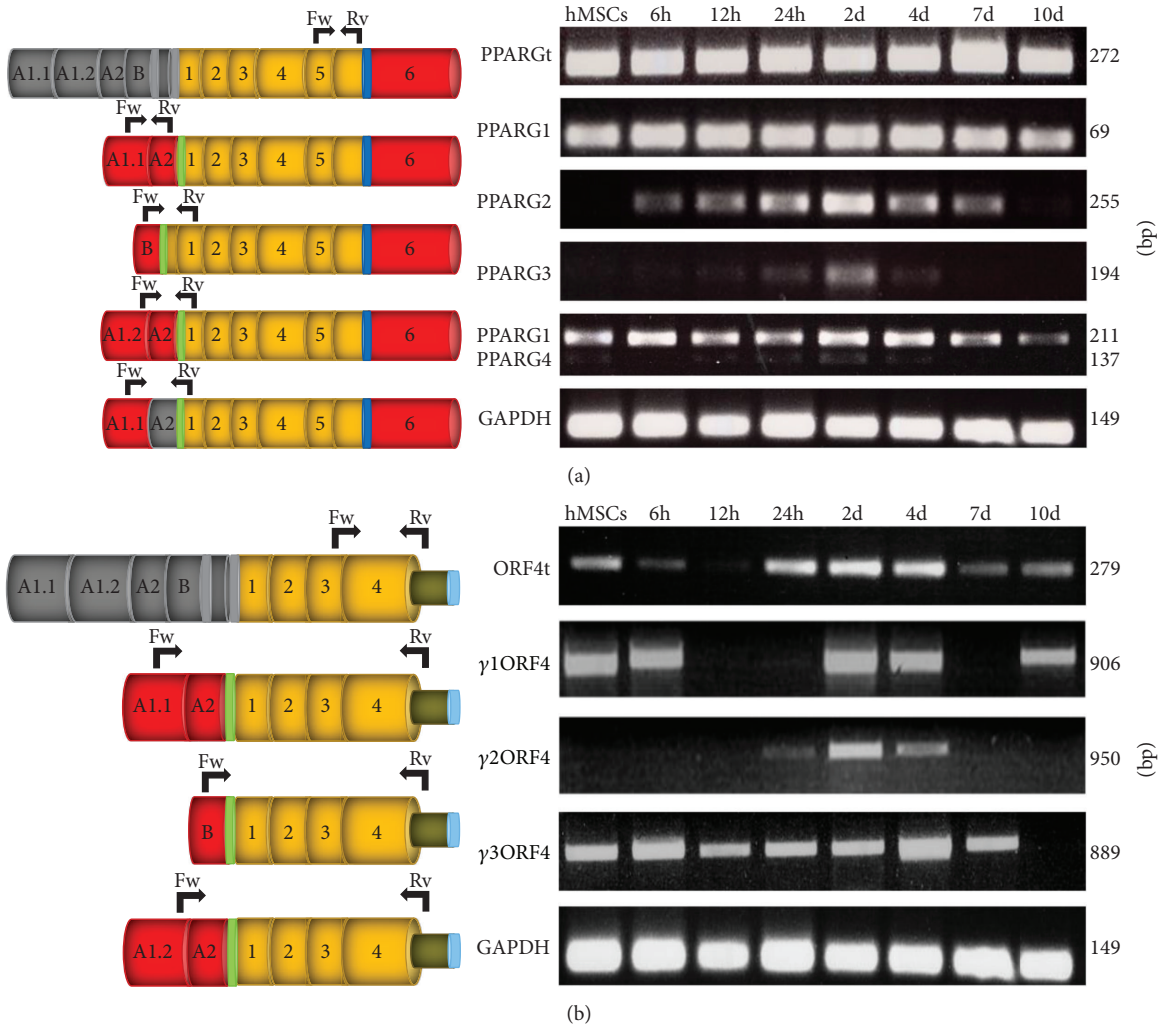

Figure 4: Transcript-specific RT-PCR assays for *PPARG* canonical transcripts (panel (a)) and ORF4 variants (panel (b)) at different time points of the adipogenesis (indicated on the top). On the left, the different *PPARG* transcripts are schematically shown; on the right the related PCR amplicons and their sizes (in bp) are illustrated. "PPARGt" and "ORF4t" indicate the entire pool of canonical *PPARG* and ORF4 transcripts, respectively. Transcript-specific exons are shown in grey and common exons are coloured. Black arrows indicate the specific primer pairs used in this analysis (Fw, forward; Rv, reverse). *GAPDH* was used as internal control.

differentiation (Figure S1). Notably, the most striking increase has been observed for PPARG2 and PPARG3 variants (about 90 and 40 fold, resp.), suggesting the inducible nature of their promoters during this process. On the opposite, highly significant decreases were observed—for these two splice variants—immediately after day 2 from the induction of the process. A common behavior was observed for PPARG1 and ORF4 transcripts. In particular, these variants undergo mild expression changes in the transitions among the stages, showing a quite constant basal expression throughout the adipogenic process (Figure 5(a) and S1). Since the most evident changes in *PPARG* transcripts' abundance were detected after 2 days by differentiation induction, we investigated protein levels on three time points, day 0 (undifferentiated cells), day 2 (i.e., the highest peak of *PPARG* expression), and day 10 (i.e., differentiated cells). As no commercially available antibodies exist for ORF4 protein, we used a polyclonal antibody directed against the N-terminal domain, able to recognize both the canonical and the shortest *PPARG* isoforms. We detected canonical PPARγ at 67 kDa and immunoreactive bands at 40 kDa, the predicted weight of ORF4 protein isoform. As expected, consistently with the changes in mRNA levels, after 2 days by differentiation induction, the expressions of PPARγ—and of the shortest isoforms—were higher compared to both undifferentiated and completely differentiated cells (Figure 5(b)).

4. Conclusions

Epidemiological studies demonstrate that the prevalence of the metabolic syndrome is increasing in the Western world and developing countries, and to date an adequate therapy has not been yet established [17, 44].

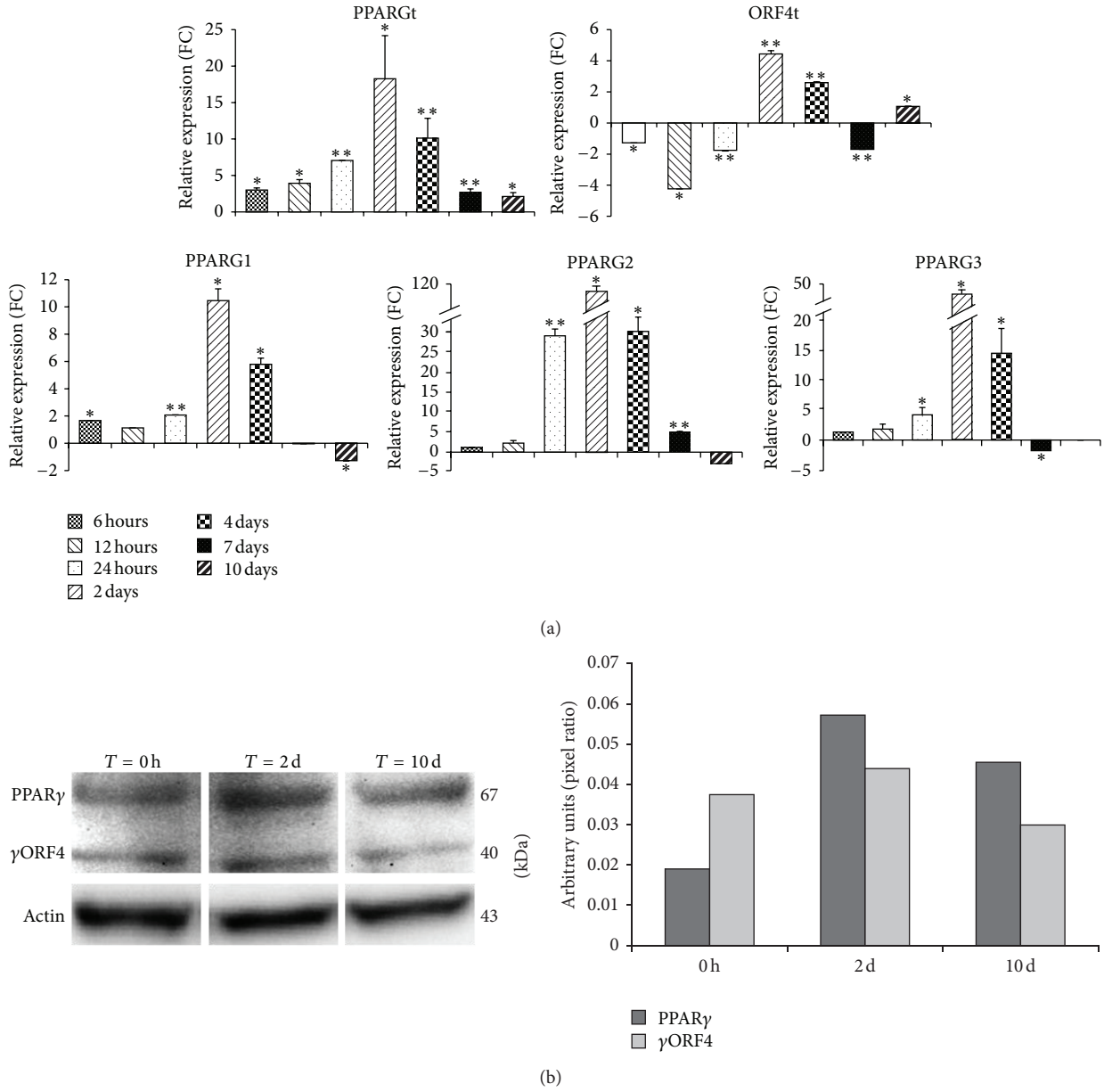

Figure 5: For each analyzed *PPARG* variant, bar graphs in the Panel (a) indicate the relative expression levels at different time points after i*n vitro* adipocyte differentiation. For each assay, expression is normalized for reference samples (time point at 0 or 6 hours) using *GAPDH* as housekeeping gene. Data are reported as mean values, and error bars are also reported. P values < 0.05 are considered statistically significant and indicated by an asterisk. Double asterisks indicate P values < 0.001. In panel (b), total cell lysates of hMSC at day 0, day 2, and day 10 by differentiation induction blotted with anti-PPARγ antibody are shown. To ensure equal protein transfer, membranes were blotted with antiactin antibody. Bar graph indicates the pixel intensity ratio between PPARγ isoforms and actin protein levels, reported as arbitrary units over basal (day 0).

Undoubtedly, *PPARG* is one of the most studied genes accounting for metabolic disorders. Indeed, it modulates the expression of several genes with a crucial role in glucose, lipid and cholesterol metabolism, insulin signaling, and adipokines' production, whose imbalance leads to insulin resistance, obesity, type 2 diabetes, and cardiovascular diseases [3, 4, 7, 14]. PPARγ is also a drug target and, currently, its synthetic ligands are used to treat hyperlipidemia and as insulin-sensitizing antidiabetic agents [18]. Thus, defining *PPARG* activity in tissues and cells related to energy metabolism may provide useful insights to develop new and effective therapeutic strategies to treat the metabolic syndrome and its complications.

It is currently known that—by different promoter usage and alternative splicing—the human *PPARG* gene generates multiple variants encoding two proteins, PPARγ1 and

PPARγ2. Since different *PPARG* splice variants encode the same protein isoform, their differential expression, both spatial and temporal, may reflect a different regulation, translation, mRNA stability, and/or localization. To complicate the picture, the recent identification of γORF4 isoform—able to act as dominant-negative and with a tumorigenic effect [28]—suggests that PPARγ activity is modulated through transcript-specific regulation.

Therefore, our effort has been to investigate *PPARG* expression in different tissues and cells—affected in metabolic syndrome—and during hMSCs' adipocyte differentiation. Other than focusing on canonical *PPARG* transcripts, a particular emphasis was posed toward defining the expression pattern of its variants encoding dominant negative isoforms. In our study we identified γ1ORF4, a novel *PPARG* transcript that, similarly to the previously described γ2ORF4 and γ3ORF4 [28], may act as dominant negative toward PPARγ.

Our expression analysis has clearly demonstrated that the different promoters of *PPARG* have a peculiar transcriptional activity. Such finding is particularly relevant in the adipocyte differentiation, in which PPARγ is a key player [4, 9, 29]. The almost ubiquitous PPARG1/PPARG4 expression, particularly throughout adipogenesis, indicates a more pronounced activity of their promoter compared to the others, suggesting it as the main contributor to PPARγ protein synthesis. Furthermore, the mild expression changes of PPARG1 along adipocyte differentiation strengthen the hypothesis that its promoter provides constitutive levels of *PPARG* messengers. On the opposite, the tissue- and stage-specific PPARG2 expression, as well as its dramatic variations throughout the adipogenesis, clearly demonstrate its inducible nature.

Interestingly, the almost ubiquitous expressions of ORF4 variants in tissues and cells, as well as during adipogenesis, support the hypothesis that *PPARG* regulates itself through dominant negative isoforms. Furthermore, our results suggest that similarly to *PPARG* canonical transcripts, the three ORF4 variants give a different contribution to PPARγ activity. Indeed, whereas γ1ORF4 and γ2ORF4 exhibit stage-specific expression, γ3ORF4 is constantly expressed along adipocyte differentiation but not in mature adipose cells. These findings, strictly correlated with those regarding the canonical isoforms, suggest that (1) the promoter upstream exon B is inducible for both the canonical and ORF4 variants, (2) constitutive levels of *PPARG* variants, encoding dominant negative isoforms, are provided throughout differentiation by the promoter upstream noncoding exon $A_{1.2}$, and (3) it almost exclusively transcribes γ3ORF4 rather than the canonical PPARG3. Therefore, such evidences suggest a relevant—if not exclusive—role of promoter of γ3ORF4 and PPARG3 variants in negative PPARγ regulation. In addition, protein analysis confirmed that after 2 days by differentiation induction PPARγ protein has a higher expression compared to undifferentiated and completely differentiated cells. Moreover, we observed the same trend of expression also for a shorter protein of 40 kDa, corresponding to the predicted weight of ORF4 isoform.

Although the results described herein represent only a starting point to understand the impact of *PPARG* transcripts along human adipogenesis, they support the notion that this generegulates such crucial process through balancing the levels of its different splicing variants. Further studies—particularly taking into account *PPARG* protein products—are strictly required to definitely establish the role of all splicing variants in adipocyte differentiation. Notably, our results shed light on previously underestimated aspects of *PPARG* regulation and propose a yet unexplored role of its dominant negative isoforms during adipogenesis. Indeed, the finding that—during a crucial process in which *PPARG* is a "master gene"—both the transcripts and the proteins encoding dominant negative isoforms are constitutively expressed and/or can be modulated similarly to the canonical *PPARG* variants, enforces the need to investigate toward this direction. Understanding more about *PPARG* activity in the adipogenic process is directly linked to its possible contribution to the onset and progression of metabolism-related pathologies, including the metabolic syndrome and its complications.

Finally, we cannot exclude that the presence of transcripts encoding *PPARG* dominant negative proteins in other human tissues may underlie their interesting roles in physiological processes as well as in other pathological conditions.

Conflict of Interests

The authors declare that there is no conflict of interests regarding the publication of this paper.

Authors' Contribution

M. Aprile and M. R. Ambrosio contributed equally to this work.

Acknowledgments

The authors thank the FLAGSHIP "InterOmics" Project (PB.P05) to A. Ciccodicola, funded and supported by the Italian MIUR and CNR organizations and the Italian Ministry of Education, University and Research (MIUR) Project National Operational Programme for "Research and Competitiveness" 2007–2013 PON01 02460 to A. Ciccodicola, P. Formisano and F. Beguinot. The financial support through the projects ORTO11TSM3 to F. Beguinot and the FIRB project RBNE08NKH7 (MERIT initiative) to F. Beguinot and P. Formisano is gratefully acknowledged. M. Aprile is PhD student in molecular and cellular biotechnology at the Department of Environmental Sciences and Technologies, biological, and pharmaceutical "DISTABiF" at Second University of Naples. M. R. Ambrosio is PhD student in Molecular Oncology and Endocrinology at the Department of Translational Medical Sciences, University of Naples "Federico II".

References

[1] T. M. Willson, P. J. Brown, D. D. Sternbach, and B. R. Henke, "The PPARs: from orphan receptors to drug discovery," *Journal of Medicinal Chemistry*, vol. 43, no. 4, pp. 527–550, 2000.

[2] M. C. Cho, K. Lee, S. G. Paik, and D. Y. Yoon, "Peroxisome proliferators-activated receptor (PPAR) modulators and metabolic disorders," *PPAR Research*, vol. 2008, Article ID 679137, 14 pages, 2008.

[3] V. Costa, M. A. Gallo, F. Letizia, M. Aprile, A. Casamassimi, and A. Ciccodicola, "PPARG: gene expression regulation and next-generation sequencing for unsolved issues," *PPAR Research*, vol. 2010, Article ID 409168, 17 pages, 2010.

[4] E. D. Rosen and B. M. Spiegelman, "PPARγ: a nuclear regulator of metabolism, differentiation, and cell growth," *Journal of Biological Chemistry*, vol. 276, no. 41, pp. 37731–37734, 2001.

[5] W. Ahmed, O. Ziouzenkova, J. Brown et al., "PPARs and their metabolic modulation: new mechanisms for transcriptional regulation?" *Journal of Internal Medicine*, vol. 262, no. 2, pp. 184–198, 2007.

[6] L. Széles, D. Töröcsik, and L. Nagy, "PPARγ in immunity and inflammation: cell types and diseases," *Biochimica et Biophysica Acta—Molecular and Cell Biology of Lipids*, vol. 1771, no. 8, pp. 1014–1030, 2007.

[7] M. Ahmadian, J. M. Suh, N. Hah et al., "PPARγ signaling and metabolism: the good, the bad and the future," *Nature Medicine*, vol. 19, no. 5, pp. 557–566, 2013.

[8] Y. Barak, M. C. Nelson, E. S. Ong et al., "PPARγ is required for placental, cardiac, and adipose tissue development," *Molecular Cell*, vol. 4, no. 4, pp. 585–595, 1999.

[9] E. D. Rosen, P. Sarraf, A. E. Troy et al., "PPARγ is required for the differentiation of adipose tissue in vivo and in vitro," *Molecular Cell*, vol. 4, no. 4, pp. 611–617, 1999.

[10] Y. L. Muller, C. Bogardus, B. A. Beamer, A. R. Shuldiner, and L. J. Baier, "A functional variant in the peroxisome proliferator—activated receptor γ2 promoter is associated with predictors of obesity and type 2 diabetes in Pima Indians," *Diabetes*, vol. 52, no. 7, pp. 1864–1871, 2003.

[11] D. Altshuler, J. N. Hirschhorn, M. Klannemark et al., "The common PPARγ Pro12Ala polymorphism is associated with decreased risk of type 2 diabetes," *Nature Genetics*, vol. 26, no. 1, pp. 76–80, 2000.

[12] H. Mori, H. Ikegami, Y. Kawaguchi et al., "The Pro12 → Ala substitution in PPAR-γ is associated with resistance to development of diabetes in the general population: possible involvement in impairment of insulin secretion in individuals with type 2 diabetes," *Diabetes*, vol. 50, no. 4, pp. 891–894, 2001.

[13] V. Costa, A. Casamassimi, K. Esposito et al., "Characterization of a novel polymorphism in PPARG regulatory region associated with type 2 diabetes and diabetic retinopathy in italy," *Journal of Biomedicine and Biotechnology*, vol. 2009, Article ID 126917, 7 pages, 2009.

[14] J. I. Odegaard, R. R. Ricardo-Gonzalez, M. H. Goforth et al., "Macrophage-specific PPARγ controls alternative activation and improves insulin resistance," *Nature*, vol. 447, no. 7148, pp. 1116–1120, 2007.

[15] S. Azhar, "Peroxisome proliferator-activated receptors, metabolic syndrome and cardiovascular disease," *Future Cardiology*, vol. 6, no. 5, pp. 657–691, 2010.

[16] I. Barroso, M. Gurnell, V. E. F. Crowley et al., "Dominant negative mutations in human PPARγ associated with severe insulin resistance, diabetes mellitus and hypertension," *Nature*, vol. 402, no. 6764, pp. 880–883, 1999.

[17] D. Capaccio, A. Ciccodicola, L. Sabatino et al., "A novel germline mutation in peroxisome proliferator-Activated Receptor γ gene associated with large intestine polyp formation and dyslipidemia," *Biochimica et Biophysica Acta—Molecular Basis of Disease*, vol. 1802, no. 6, pp. 572–581, 2010.

[18] A. Raji and J. Plutzky, "Insulin resistance, diabetes, and atherosclerosis: thiazolidinediones as therapeutic interventions," *Current Cardiology Reports*, vol. 4, no. 6, pp. 514–521, 2002.

[19] M. C. Bragt and H. E. Popeijus, "Peroxisome proliferator-activated receptors and the metabolic syndrome," *Physiology and Behavior*, vol. 94, no. 2, pp. 187–197, 2008.

[20] H. Shahbazian, S. M. Latifi, M. T. Jalali et al., "Metabolic syndrome and its correlated factors in an urban population in South West of Iran.," *Journal of Diabetes & Metabolic Disorders*, vol. 12, no. 1, p. 11, 2013.

[21] L. Fajas, D. Auboeuf, E. Raspé et al., "The organization, promoter analysis, and expression of the human PPARγ gene," *Journal of Biological Chemistry*, vol. 272, no. 30, pp. 18779–18789, 1997.

[22] L. Fajas, J. C. Fruchart, and J. Auwerx, "PPARγ3 mRNA: a distinct PPARγ mRNA subtype transcribed from an independent promoter," *FEBS Letters*, vol. 438, no. 1-2, pp. 55–60, 1998.

[23] C. Knouff and J. Auwerx, "Peroxisome proliferator-activated receptor-γ calls for activation in moderation: lessons from genetics and pharmacology," *Endocrine Reviews*, vol. 25, no. 6, pp. 899–918, 2004.

[24] A. Werman, A. Hollenberg, G. Solanes, C. Bjørbæk, A. J. Vidal-Puig, and J. S. Flier, "Ligand-independent activation domain in the N terminus of peroxisome proliferator-activated receptor γ (PPARγ). Differential activity of PPARγ1 and -2 isoforms and influence of insulin," *Journal of Biological Chemistry*, vol. 272, no. 32, pp. 20230–20235, 1997.

[25] D. Ren, T. N. Collingwood, E. J. Rebar, A. P. Wolffe, and H. S. Camp, "PPARγ knockdown by engineered transcription factors: Exogenous PPARγ2 but not PPARγ1 reactivates adipogenesis," *Genes and Development*, vol. 16, no. 1, pp. 27–32, 2002.

[26] S. Yu, N. Viswakarma, S. K. Batra, M. Sambasiva Rao, and J. K. Reddy, "Identification of promethin and PGLP as two novel up-regulated genes in PPARγ1-induced adipogenic mouse liver," *Biochimie*, vol. 86, no. 11, pp. 743–761, 2004.

[27] E. Powell, P. Kuhn, and W. Xu, "Nuclear receptor cofactors in PPARγ-mediated adipogenesis and adipocyte energy metabolism," *PPAR Research*, vol. 2007, Article ID 53843, 11 pages, 2007.

[28] L. Sabatino, A. Casamassimi, G. Peluso et al., "A novel peroxisome proliferator-activated receptor γ isoform with dominant negative activity generated by alternative splicing," *Journal of Biological Chemistry*, vol. 280, no. 28, pp. 26517–26525, 2005.

[29] A. Chawla, E. J. Schwarz, D. D. Dimaculangan, and M. A. Lazar, "Peroxisome proliferator-activated receptor (PPAR) γ: adipose-predominant expression and induction early in adipocyte differentiation," *Endocrinology*, vol. 135, no. 2, pp. 798–800, 1994.

[30] R. M. Evans, G. D. Barish, and Y. X. Wang, "PPARs and the complex journey to obesity," *Nature Medicine*, vol. 10, no. 4, pp. 355–361, 2004.

[31] S. Kersten, B. Desvergne, and W. Wahli, "Roles of PPARS in health and disease," *Nature*, vol. 405, no. 6785, pp. 421–424, 2000.

[32] A. Armani, C. Mammi, V. Marzolla et al., "Cellular models for understanding adipogenesis, adipose dysfunction, and obesity," *Journal of Cellular Biochemistry*, vol. 110, no. 3, pp. 564–572, 2010.

[33] V. D'Esposito, F. Passaretti, A. Hammarstedt et al., "Adipocyte-released insulin-like growth factor-1 is regulated by glucose and fatty acids and controls breast cancer cell growth in vitro," *Diabetologia*, vol. 55, no. 10, pp. 2811–2822, 2012.

[34] P. Isakson, A. Hammarstedt, B. Gustafson, and U. Smith, "Impaired preadipocyte differentiation in human abdominal obesity: role of Wnt, tumor necrosis factor-α, and inflammation," *Diabetes*, vol. 58, no. 7, pp. 1550–1557, 2009.

[35] V. Costa, I. Conte, C. Ziviello et al., "Identification and expression analysis of novel Jakmip1 transcripts," *Gene*, vol. 402, no. 1-2, pp. 1–8, 2007.

[36] V. Costa, L. Sommese, A. Casamassimi et al., "Impairment of circulating endothelial progenitors in Down syndrome," *BMC Medical Genomics*, vol. 3, article 40, 2010.

[37] V. Costa, C. Angelini, L. D'Apice et al., "Massive-scale rna-seq analysis of non ribosomal transcriptome in human trisomy 21," *PLoS ONE*, vol. 6, no. 4, Article ID e18493, 2011.

[38] A. T. Alberobello, V. D'Esposito, D. Marasco et al., "Selective disruption of insulin-like growth factor-1 (IGF-1) signaling via phosphoinositide-dependent kinase-1 prevents the protective effect of IGF-1 on human cancer cell death," *Journal of Biological Chemistry*, vol. 285, no. 9, pp. 6563–6572, 2010.

[39] S. B. Park, H. C. Choi, and N. S. Joo, "The relation of thyroid function to components of the metabolic syndrome in Korean men and women," *Journal of Korean Medical Science*, vol. 26, no. 4, pp. 540–545, 2011.

[40] H. P. Koeffler, "Peroxisome proliferator-activated receptor γ and cancers," *Clinical Cancer Research*, vol. 9, no. 1, pp. 1–9, 2003.

[41] M. D. Rollins, S. Sudarshan, M. A. Firpo et al., "Anti-inflammatory effects of PPAR-γ agonists directly correlate with PPAR-γ expression during acute pancreatitis," *Journal of Gastrointestinal Surgery*, vol. 10, no. 8, pp. 1120–1130, 2006.

[42] R. B. Clark, "The role of PPARs in inflammation and immunity," *Journal of Leukocyte Biology*, vol. 71, no. 3, pp. 388–400, 2002.

[43] N. Marx, B. Kehrle, K. Kohlhammer et al., "PPAR activators as antiinflammatory mediators in human T lymphocytes: implications for atherosclerosis and transplantation-associated arteriosclerosis," *Circulation Research*, vol. 90, no. 6, pp. 703–710, 2002.

[44] N. Gupta, K. Goel, P. Shah, and A. Misra, "Childhood obesity in developing countries: epidemiology, determinants, and prevention," *Endocrine Reviews*, vol. 33, no. 1, pp. 48–70, 2012.

Hindawi Publishing Corporation
PPAR Research
Volume 2014, Article ID 432647, 13 pages
http://dx.doi.org/10.1155/2014/432647

Review Article

Modes-of-Action Related to Repeated Dose Toxicity: Tissue-Specific Biological Roles of PPARγ Ligand-Dependent Dysregulation in Nonalcoholic Fatty Liver Disease

Merilin Al Sharif, Petko Alov, Vessela Vitcheva, Ilza Pajeva, and Ivanka Tsakovska

Institute of Biophysics and Biomedical Engineering, Bulgarian Academy of Sciences, Acad. G. Bonchev Street, Building 105, 1113 Sofia, Bulgaria

Correspondence should be addressed to Ilza Pajeva; pajeva@biomed.bas.bg and Ivanka Tsakovska; itsakovska@biomed.bas.bg

Received 25 November 2013; Revised 13 January 2014; Accepted 24 January 2014; Published 18 March 2014

Academic Editor: Lihong Chen

Comprehensive understanding of the precise mode of action/adverse outcome pathway (MoA/AOP) of chemicals becomes a key step towards superseding the current repeated dose toxicity testing methodology with new generation predictive toxicology tools. The description and characterization of the toxicological MoA leading to non-alcoholic fatty liver disease (NAFLD) are of specific interest, due to its increasing incidence in the modern society. Growing evidence stresses on the PPARγ ligand-dependent dysregulation as a key molecular initiating event (MIE) for this adverse effect. The aim of this work was to analyze and systematize the numerous scientific data about the steatogenic role of PPARγ. Over 300 papers were ranked according to preliminary defined criteria and used as reliable and significant sources of data about the PPARγ-dependent prosteatotic MoA. A detailed analysis was performed regarding proteins which PPARγ-mediated expression changes had been confirmed to be prosteatotic by most experimental evidence. Two probable toxicological MoAs from PPARγ ligand binding to NAFLD were described according to the Organisation for Economic Cooperation and Development (OECD) concepts: (i) PPARγ activation in hepatocytes and (ii) PPARγ inhibition in adipocytes. The possible events at different levels of biological organization starting from the MIE to the organ response and the connections between them were described in details.

1. Introduction

Multiple or repeated administration of many chemicals may not produce immediate toxic effects but due to their accumulation in tissues or other mechanisms of homeostasis perturbation, results in delayed effects [1]. Repeated dose toxicity comprises these adverse general toxicological effects which occur as a result of repeated daily dosing with or exposure to a substance for a specified period up to the expected lifespan of the test species [2]. The traditional *in vivo* repeated dose toxicity tests, although still widely used, have a number of limitations [3]. The modern toxicology concepts are based on comprehensive knowledge about biological pathways and their relationship to adverse effects at the organ and higher levels. These concepts allow building alternative models (*in vitro* and computational) to describe the adverse effects [4]. They are at the heart of initiatives such as SEURAT-1 (http://www.seurat-1.eu) and TOX21 (http://www.epa.gov/ncct/Tox21/) and are based on the methodology of the Adverse Outcome Pathway (AOP). The AOP regulatory assessment framework has been provided to collect, organize, and evaluate relevant information about chemical, biological, and toxicological effect of chemicals [5]. It supports the use of a mode-of-action (MoA) basis involving description and characterization of the key cytological and biochemical events that are both measurable and necessary to the observed effect.

Liver is one of the organs that are highly exposed to many potentially toxic substances and therefore a frequent target for toxicity. It has a central role in the lipid homeostasis and its primary function is fat redistribution instead of storage, the latter being typical for adipose tissue (Figure 1). The liver damage can be a result of direct hepatocyte damage, hepatic tumor, and/or accumulation of lipids or phospholipids (fatty liver disorder). The nonalcoholic fatty liver disease (NAFLD) is a medical condition characterized by significant lipid deposition in the hepatocytes [6]. NAFLD is a common cause of

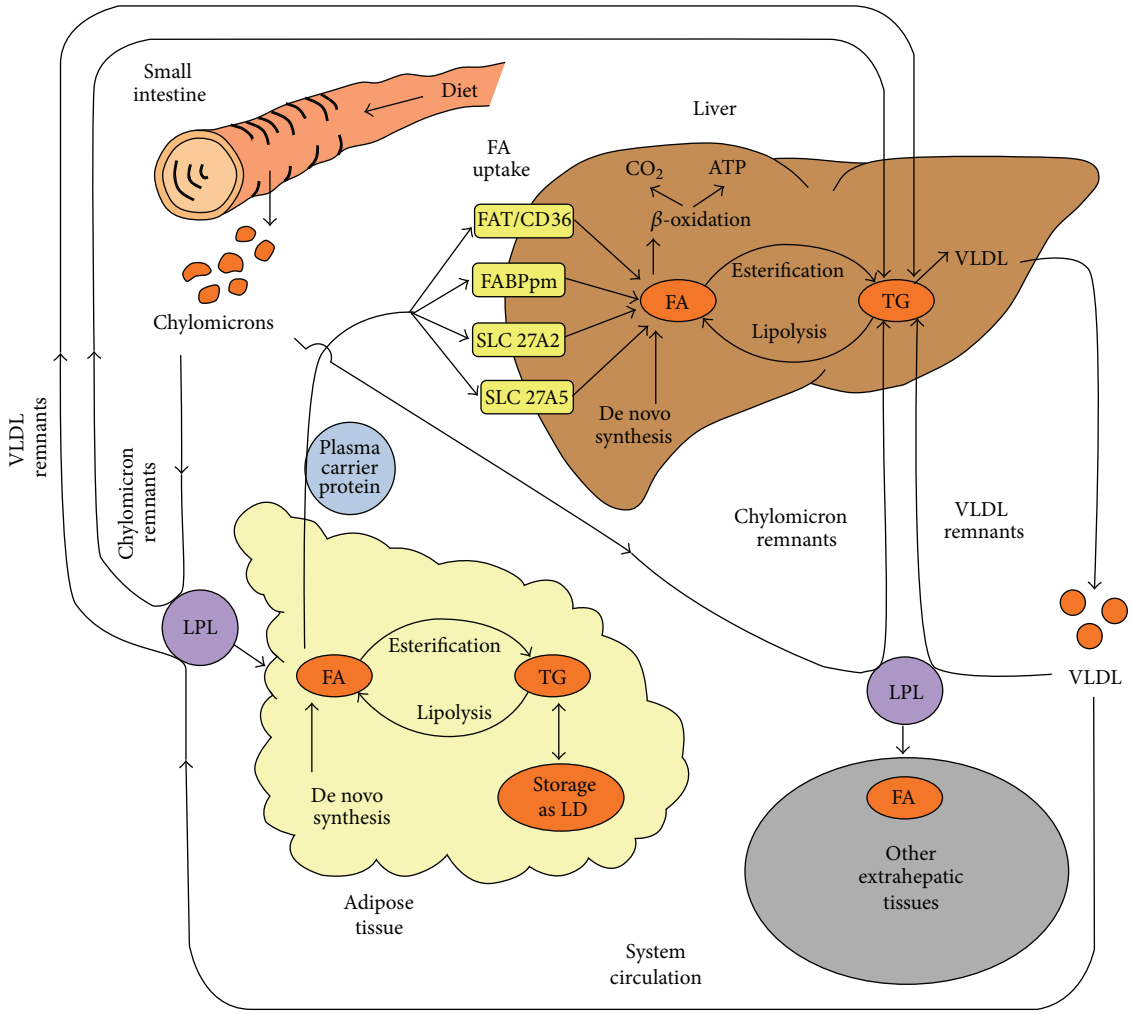

Figure 1: A simplified presentation of the fatty acids transport, metabolism, and fate in the human organism. FAT/CD36: fatty acid translocase/cluster determinant 36; FABPpm: plasma membrane fatty acid binding protein; SLC 27A2: solute carrier family 27 (fatty acid transporter), member 2; SLC 27A5: solute carrier family 27 (fatty acid transporter), member 5; FA: fatty acids; TG: triglycerides; VLDL: very low-density lipoprotein; LPL: lipoprotein lipase; LD: lipid droplet.

chronic liver injury; thus, in view of repeated-dose hepatotoxicity, its pathogenesis is of particular interest, with emphasis on the mode and site of action of potential chemical inducers. Different molecular initiating events (MIEs) influence the onset and progression of these toxic effects [7].

Peroxisome proliferator-activated receptor gamma (PPARγ) has been recently proposed as one of the receptors involved in the MIE for liver steatosis (the early manifestation of NAFLD) [7]. PPARγ is responsible for the regulation of adipogenesis (adipocyte proliferation and differentiation), lipid and glucose homeostasis, inflammatory responses, vascular functions, and placental development [8–10]. The modulation of PPARγ function by ligand binding reflects on its genomic activity (transactivation and transrepression). The up-regulated genes are associated with lipid transport, metabolism, storage, and adipogenesis [11, 12]. The down-regulated genes typically include those involved in adaptive inflammatory responses. Several transrepression mechanisms have been reported [12].

PPARγ has two isoforms, PPARγ1 and PPARγ2, differing by a thirty amino acid N-terminal extension present in PPARγ2. While PPARγ1 is expressed in multiple tissues including liver, adipocytes are the most likely site of PPARγ2 expression [13, 14].

In this study, we present a comprehensive analysis of the data reported in the scientific literature about the role of PPARγ in the pathogenesis of NAFLD. Based on these data and according to the OECD guidelines [5], the main possible MoAs starting from xenobiotic interaction with PPARγ as a MIE, passing through downstream transcriptional dysregulation, and resulting in the first two stages of NAFLD, namely, liver steatosis and nonalcoholic steatohepatitis (NASH), are outlined.

2. Methodology of the Analysis

In order to clarify the role of PPARγ ligand binding in the MoA of NAFLD, we have summarized and analyzed

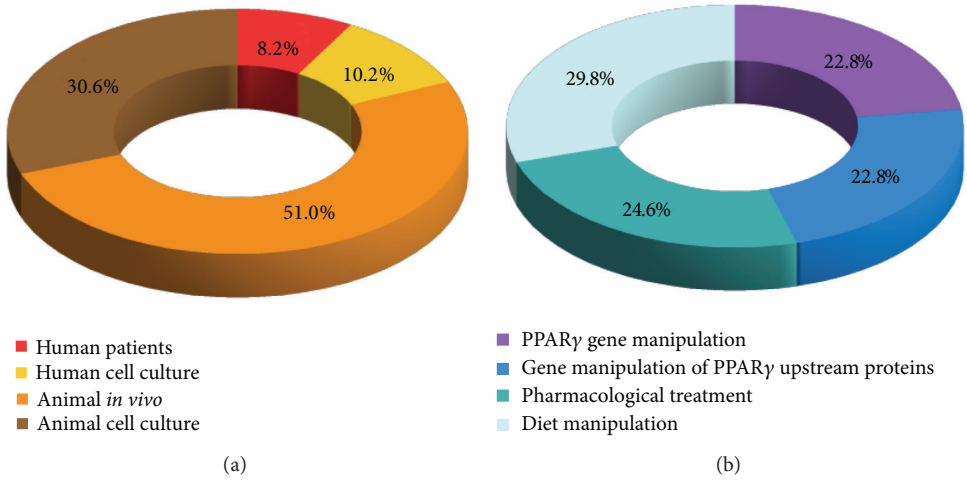

Figure 2: Major categories of subjects (a) and experimental approaches (b) in the selected papers.

the experimental data from studies on hepatocytes, as well as adipocytes.

Over 300 papers retrieved from NIH PubMed system (http://www.ncbi.nlm.nih.gov/pubmed) were screened and ranked according to the following general criteria:

(i) completeness of the model description: type of experiment (*in vivo* or *in vitro*), species or cell line used, and genetic properties of the studied subjects which could support a causal link between the MIE and the adverse outcome;

(ii) relevance of the presented experimental evidence to studied MoA: availability of results from biochemical, histological, or other assays that are qualitatively or quantitatively associated with commonly accepted markers of NAFLD;

(iii) availability of sufficient data for categorization of the experimental observations as key molecular events (initiating or intermediate) of studied MoA: experimentally-induced (by diet, pharmacological treatment, or genetic techniques) changes in PPARγ activity and/or expression accompanied by changes in the expression of PPARγ target proteins.

The analysis of the collected papers was done in several steps. First, the initial pool was filtered for availability of information about potential toxicity pathways and target proteins related to them and all papers containing such data were scored. Next, scores were given depending on the investigated subjects (humans or animals) with a higher score for papers reporting human data. The papers that met at least one of the following criteria were selected for further evaluation: evidence for PPARγ dysregulation, relation to the selected endpoints (steatosis or steatohepatitis), or intermediate events preceding these endpoints. The selected papers constituted the core set, which was further extended by additional more specific literature search on PPARγ, the target protein, and the toxicity pathway. The final set contained 72 papers, among them 26 reviews. Supplementary Table 1 in Supplementary Material (available online at http://dx.doi.org/10.1155/2014/432647) classifies the available data in all 72 papers in relation to: the studied subjects (human patients, human cell cultures, animals *in vivo*, and animal cell cultures), the experimental approaches (PPARγ overexpression, PPARγ overexpression and pharmacological treatment; PPARγ knockout/knockdown; PPARγ knockout/knockdown and pharmacological treatment; pharmacological treatment; diet manipulation; gene manipulation of PPARγ upstream proteins; gene manipulation of PPARγ upstream proteins and pharmacological treatment). The papers dealing with the AOP methodology, reviews, and research articles containing background information (receptor structure, up- and downstream proteins' functions, etc.) are given in the last two columns. Figure 2 summarizes the data in Supplementary Table 1.

The analysis of the selected papers served as a basis for building the blocks in the proposed MoA. Table 1 exemplifies a summary of the main findings in these papers related to one of the most studied PPARγ target proteins CD36.

3. Results and Discussion

The coordinated cellular regulation of the lipid metabolism pathways and the dynamic balance of the intertissue lipid exchange are crucial for the whole-body lipid homeostasis. NAFLD stems from abnormalities such as increased fatty acid (FA) uptake; increased *de novo* FA synthesis; decreased FA oxidation; or impaired VLDL secretion [15, 25, 26].

The effects of PPARγ dysregulation on the liver remain under debate, with some studies showing that it promotes hepatic steatosis through up-regulation of genes involved in lipid uptake and storage and others showing that it prevents hepatic steatosis and fibrosis, possibly by sequestering FAs in adipose tissue and preventing hepatic stellate cell activation [13, 14]. However, growing evidence stresses on the importance of PPARγ in pathogenesis of NAFLD [16, 25, 27–30]. *In vitro* and *in vivo* experiments on animal models have confirmed that hepatic overexpression and/or activation of the receptor by an agonist triggers undesirable up-regulation of

Table 1: Main findings extracted from selected scientific papers supporting the prosteatogenic role of FAT/CD36 in the MoA from PPARγ dysregulation to NAFLD.

Species	PPARγ related strain characteristics	Diet	Experiment type	Gene manipulation	Pharmacological treatment		Endpoints			Reference
					Agent	Type	PPARγ	CD36	NAFLD biomarkers	
Human	NASH patients							+	+	[15]
Mouse	Wild type	HFD					+		+	[16]
	Liver PPARγ deficient line	HFD					0		0	
	Wild type	CD		PPARγ transfected			+	+	+	
	Liver PPARγ deficient line	CD		PPARγ transfected			+	+	+	
Mouse			**Hepatocytes**	**PPARγ transfected**	**Rosiglitazone**	**Synthetic agonist**	+ / + / +	+ / ++ / ++	+ / ++ / ++	
					Palmitate	**Endogenous metabolite**	+	++	++	
Mouse	Functional PPARγ	HFD					+	+	+	[17]
	PPARγ knockout	HFD					0/+	0/+	0/+	
Mouse	**Functional PPARγ**		**Tissue slices**		**Oleic acid**	**Endogenous agonist**			+	
	Functional PPARγ				**Rosiglitazone**	**Synthetic agonist**			+	
	PPARγ knockout				**Oleic acid**	**Endogenous agonist**			**0**	
	PPARγ knockout				**Rosiglitazone**	**Synthetic agonist**			**0**	
	Functional PPARγ		**Hepatocytes**		**BADGE**	**Synthetic antagonist**			–	
	Functional PPARγ				**Oleic acid + BADGE**	**Endogenous agonist +Synthetic antagonist**			**0**/+	
Mouse	Insulin-resistant mice	CD					+	+	+	[18]
	Control mice	CD			Pioglitazone	Synthetic agonist			0	
	Insulin-resistant mice	CD			Pioglitazone	Synthetic agonist	0	+	++	

Table 1: Continued.

Species	PPARγ related strain characteristics	Diet	Experiment type	Gene manipulation	Pharmacological treatment		Endpoints			Reference
					Agent	Type	PPARγ	CD36	NAFLD biomarkers	
Mouse	Wild type	HFD-safflower oil					0/+	0	0/+	[19]
	Wild type	HFD-butter					+	+	+	
	Wild type	HFD-safflower oil		PPARγ2 knockdown			+	0/+	0/+	
	Wild type	HFD-butter		PPARγ2 knockdown			+	0/+	0/+	
	Wild type	CD		PPARγ transfected			+	+	+	
Mouse	JAK2L-tyrosine kinase deficient	CD					+	++	++	[20]
	Wild type	CD			GW9662	Synthetic antagonist	0	0	0	
	JAK2L-tyrosine kinase deficient	CD			GW9662	Synthetic antagonist	+	+	+	
Mouse	Liver SMS2-overexpressing transgenic line	CD						+	0/+	[21]
	lSMS2-deficient knockout line	CD						−	0/−	
	Wild type	HFD					1	1	+	
	Liver SMS2-overexpressing transgenic line	HFD					+	+	++	
	lSMS2-deficient knockout line	HFD					−	−	−	
	Liver SMS2-overexpressing transgenic line	HFD			GW9662	Synthetic antagonist			−	
Human			**Huh7 hepatoma cells**		**Ceramide**	**Endogenous suppressor**	−	−		

Table 1: Continued.

Species	PPARγ related strain characteristics	Diet	Experiment type	Gene manipulation	Pharmacological treatment		Endpoints			Reference
					Agent	Type	PPARγ	CD36	NAFLD biomarkers	
Mouse	Wild type	CD		Fbw7 knockdown			+	+	++	[22]
	Wild type	CD		Fbw7/PPARγ2 double knockdown			0/−	0/+	+	
	Wild type	CD		Fbw7 transfected			−	−	0/−	
Mouse	**Wild type**		**Hepatocytes**	**Fbw7 knockdown**			+	+	+	
Mouse	Wild type	HFD					+	+	+	[23]
	Wild type	HFD, liquid, overfeeding					++	++	++	
Mouse	Wild type	HFD					0/+	0/+	0/+	[24]
	Obese, hypercholesterolemic, diabetic foz/foz mice	CD					+	+	0/+	
	Obese, hypercholesterolemic, diabetic foz/foz mice	HFD					+	++	+	

Legend: Bold: *in vitro* experiments; CD: control diet, HFD: high-fat diet; endpoints: empty cells: endpoint not determined, +: increase, −: decrease, 0: no effect, 1: controls taken for 100%; 0/+ and 0/− are used in cases where a clear-cut decision about the reported effects could not be done.

various lipogenic target genes [16–18]. Recently, it has been demonstrated that liver-specific knockout of PPARγ could prevent fatty liver down-regulating genes coding for lipogenic and fatty acid transport proteins [17]. PPARγ knockdown by interfering RNA also reduces the liver concentration of triglycerides (TG) [19]. Detrimental hepatic PPARγ expression as a consequence of genetic alterations has been reported, where receptor activation was shown to initiate massive liver steatosis and hepatocyte proliferation [31]. PPARγ gene nucleotide variations have also been reported to affect hepatic steatosis, often in relation to partial lipodystrophy [11, 32].

In the ideal scenario, the MIE as a primary anchor or "the foundation" of the AOP should be well-defined. However, not only the potential of a chemical to elicit that event should be recognized but also the likely site of action (in terms of the receptor tissue localization) should be noted [5]. In this particular case, PPARγ dysregulation by ligand-dependent activation or inhibition may result in the same adverse outcome but the site of action could be different (hepatocyte versus adipocyte).

3.1. PPARγ Ligand-Dependent Activation in Hepatocytes. The relevance of the PPARγ ligand-dependent activation as a MIE in NAFLD-related toxicity pathways has been supported by data about prosteatogenic effects of PPARγ agonists (synthetic: rosiglitazone and pioglitazone; endogenous: palmitate and oleate) and/or overexpression of PPARγ in the liver [16, 17, 27, 30] as well as by the observed protective effect against hepatic steatosis of PPARγ antagonists (BADGE, GW9662) or hepatocyte-specific PPARγ knockout or knockdown [20, 30].

On the basis of the literature data reviewed, four main toxicity pathways from hepatic PPARγ ligand-dependent activation to NAFLD were outlined for inclusion in MoA: uptake of FA, *de novo* synthesis of FA, TG synthesis, and lipid storage. The results of the literature analysis are summarized in Figure 3.

The lipogenic PPARγ target proteins include enzymes involved in different rate limiting stages of the synthesis of FAs (FAS, ACC, SCD1) and TGs (MGAT1, DGAT1, DGAT2) [16, 17, 21, 22, 24]. Among the lipid droplet-associated proteins (LD proteins) considered to be prosteatotic are FSP27/CIDE-C, Plin 1, 2, 4, Caveolin 1 [21, 25, 29, 33–35]. The group of lipid transport/binding proteins includes ApoCIV, aP2, Caveolin 1, and FAT/CD36 [15–24, 35–37]. The analysis of the studies regarding the target proteins that could be up-regulated in response to this MIE points to CD36, aP2, and FSP27 as the most completely characterized prosteatotic factors.

The FAT/CD36 (FA translocase/cluster determinant 36) protein is a member of the class B scavenger receptor family. It is known for its role in the uptake of oxidized low-density lipoprotein by macrophages and uptake of FAs by adipose tissues, skeletal muscle, and heart. Equally important function of CD36 in the uptake of FAs in the liver and the pathogenesis of fatty liver disease has recently been outlined [25]. Thus, CD36 and its transcriptional regulators can represent novel therapeutic targets for the prevention and management of fatty liver disease. Additionally, plasma soluble CD36 has recently been proposed as a new biomarker of a phenotype of insulin resistance, carotid atherosclerosis, and fatty liver in a study of healthy nondiabetic subjects [38].

CD36 localizes on the cell surface caveolae, as well as on intracellular vesicles and mitochondria, where it interacts with carnitine palmitoyl transferase 1, the key mitochondrial enzyme regulating FA transport, and oxidation in mitochondria. Mitochondrial CD36 content correlates with mitochondrial FA oxidation in human muscle and is increased by treatment with rosiglitazone [39–41]. To date, several transcriptional regulators of CD36 are reported, including ligand-sensing and lipogenic transcriptional factors, such as cytosolic aryl hydrocarbon receptor (AhR), and several nuclear hormone receptors such as pregnane X receptor (PXR), liver X receptor (LXR), and PPARγ [25]. In particular, adipogenic transformation of liver and exacerbation of steatosis have been strongly associated with the PPARγ-mediated elevation of CD36 mRNA and protein levels [15, 19, 37].

A model describing the CD36 mediated toxicity pathway from hepatic PPARγ ligand-dependent activation to increased TG accumulation is presented in Figure 4 as follows: (1) in the absence of ligands (agonists), the heterodimer of PPARγ with retinoid X receptor alpha (RXRα) is associated with corepressors turning off gene transcription; (2) the agonist binding induces conformational changes in the receptor followed by replacement of corepressors by coactivators that triggers gene transcription; (3–6) the overexpression and translocation of CD36 to the plasma membrane markedly increase the hepatic uptake of FAs from the circulation; (7) the enhanced esterification of these fatty acids results in increased TG storage in LDs.

An early hypothesis about the mechanism of long-chain FAs transmembrane passage emphasized the interactions of FAT/CD36 and FABPpm (plasma membrane fatty acid binding protein). The latter has been suggested to act as a receptor for long-chain FAs, facilitating the diffusion of the fatty acid-albumin complex through the unstirred fluid layer, while FAT/CD36 was supposed to facilitate FAs flip-flop across the bilayer [42]. The concept about CD36 being a simple transporter was recently questioned as real-time fluorescence measurements revealed a CD36-dependent enhancement of intracellular FA metabolism (e.g., esterification). Thus, a rate increase of FAs uptake mediated by their extensive incorporation into TGs instead of catalyzing the FA translocation across the plasma membrane has been proposed. Although the precise molecular mechanism of the long-chain FAs uptake is still under debate, there is no doubt that CD36 is central to the TG accumulation as HEK293 cells overexpressing CD36 have been shown to accumulate more and larger LDs [43].

Along with the FAs uptake, other key intermediate events are included in the toxicity pathways (Figure 3). They are associated with increased FA synthesis, TG synthesis, and TG storage, all together leading to microvesicular (increased number of LD) or macrovesicular (increased size of LD) steatosis [16, 18–20]. However, LDs are not considered merely as storage depots for superfluous intracellular lipids in times of hyperlipidemic stress, but they are metabolically active organelles involved in cellular homeostasis [44, 45].

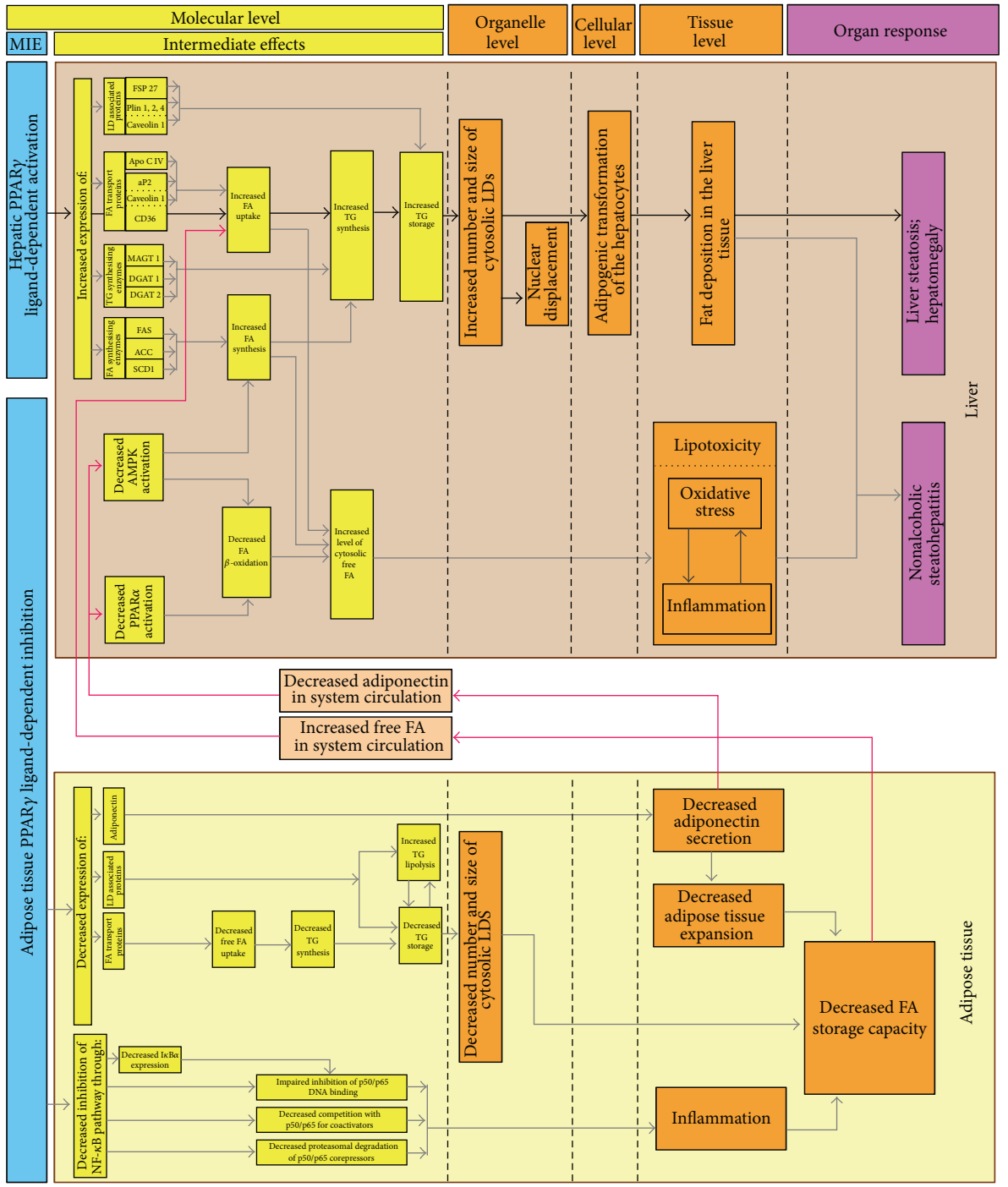

FIGURE 3: Probable MoAs leading from tissue-specific ligand-dependent PPARγ dysregulation to NAFLD. FSP27/CIDE-C: fat-specific protein 27/cell death-inducing DFF45-like effector; Plin 1, 2, 4: Perilipins 1, 2, and 4; ApoCIV: apolipoprotein C IV; aP2: adipose fatty acid binding protein; FAT/CD36 (or just CD36): fatty acid translocase/cluster determinant 36; FAS: fatty acid synthase; ACC: acetyl-CoA carboxylase; SCD1: stearoyl-CoA desaturase1; MGAT1: monoacylglycerol O-acyltransferase 1; DGAT1: diglyceride acyltransferase 1; DGAT2: diglyceride acyltransferase 2.

Following excessive fat deposition at tissue level, liver steatosis with significant hepatomegaly [20–22] was underlined as one possible organ response, while NASH was incorporated in the MoA as combination of hepatic steatosis and inflammation, the latter stemming from lipotoxicity [20, 23].

3.2. PPARγ Ligand-Dependent Inhibition in Adipocytes. PPARγ2 isoform is expressed predominantly in the adipocytes. Its role in fatty acid uptake into adipocytes and adipocyte differentiation has been well defined in experiments with thiazolidinediones and other insulin-sensitizing agents that are potent PPARγ agonists. Activation of PPARγ promotes

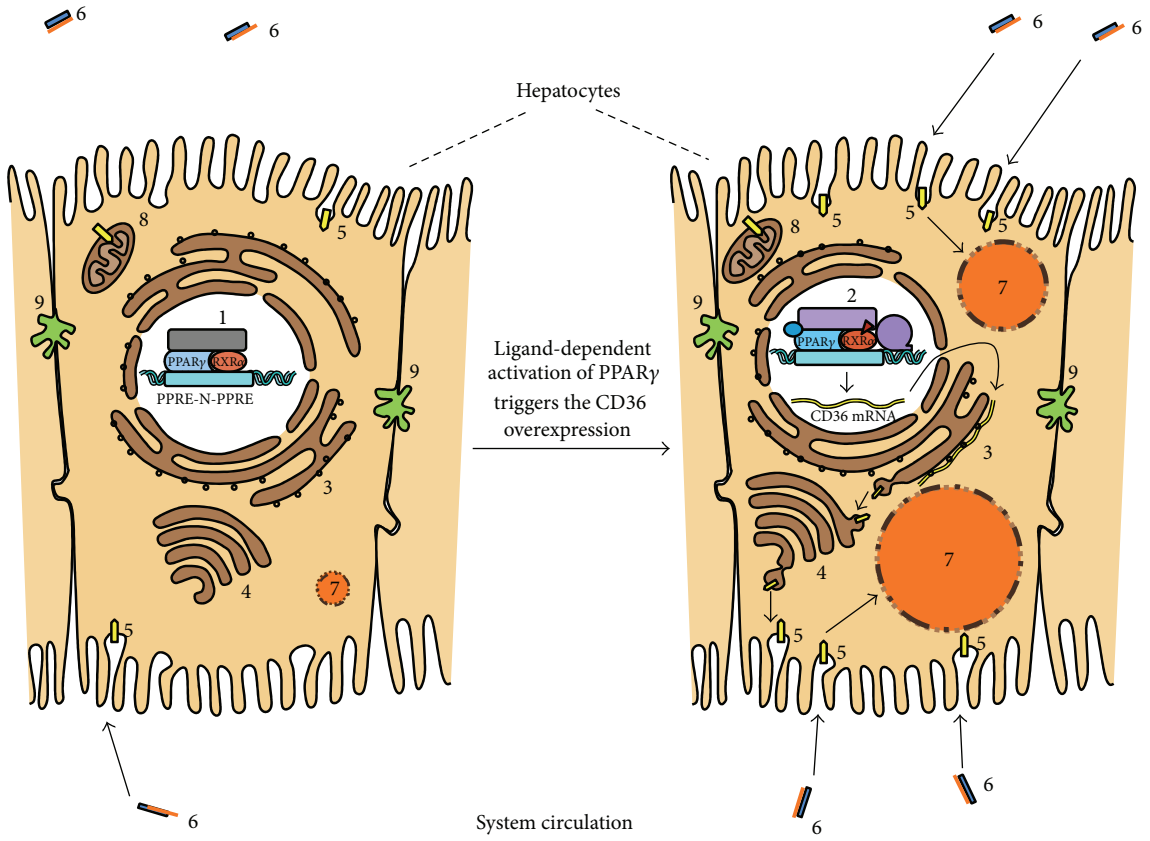

Figure 4: Model of ligand-dependent PPARγ activation as a potential MIE for liver steatosis through CD36 mediated excessive FA uptake and consequent hepatic TG accumulation. (1): PPARγ-RXRα-heterodimer interacting with the PPARγ response elements (PPRE-N-PPRE) and transcriptional corepressor complex; (2): ligand-activated PPARγ-RXRα heterodimer with transcriptional coactivator complex and RNA pol II; (3): rough endoplasmic reticulum; (4): Golgi complex; (5): FAT/CD36 (fatty acid translocase); (6): plasma fatty acid binding protein (in blue) carrying fatty acid (in orange); (7): growing lipid droplet storing triglycerides and coated with LD associated proteins; (8): mitochondria; (9): bile canaliculus.

sequestration of lipids into adipose tissue that has been recognized to affect circulating levels of triglyceride and free FA, with secondary decrease of hepatic lipid uptake and lipotoxicity in the liver [46–48].

Natural occurrence of mutant PPARγ alleles that impair its native function has been considered extremely informative for the consequences of PPARγ loss of function. Mutations in human PPARγ-coding sequence have been found to cause lipodystrophy (an underdevelopment of adipose tissue). The substantial reductions in adipose tissue mass have been associated with severe insulin resistance and often with hepatosteatosis [8, 32]. An insufficient adipose tissue capacity to buffer dietary FAs, with consequent lipotoxicity due to deposition of TG and acyl-CoA in insulin-sensitive tissues, has been underlined as causative factor for insulin resistance [32]. Moreover, adipose tissue loss has been considered critical for the development of hepatic steatosis in JAK2L mice [20] and in mouse models of severe lipodystrophy [49, 50]. A number of reviewed studies support the correlation between general PPARγ-deficiency and severe lipodystrophy accompanied by insulin resistance and hypotension. Insulin resistance, impaired adipogenesis, elevated levels of plasma free FAs and TGs, and decreased levels of both plasma leptin and adiponectin have been observed also in different mouse models of adipocyte-specific PPARγ-knockout [9].

Targeting drosophila tribbles homologue 3 (Trib3), which *in vitro* prevents PPARγ activation, by antisense oligonucleotide (ASO) has been shown to increase white adipose tissue mass by 70%, improving insulin sensitivity primarily in a PPARγ-dependent manner. Cotreatment with the PPARγ antagonist BADGE blunted the expansion of white adipose tissue and abrogated the insulin-sensitizing effects of Trib3 ASO [51]. Recently, Tsukahara et al. connected the reduced adipogenesis and lipid accumulation in 3T3-L1 cells with the inhibition of PPARγ-mediated reporter gene expression by the endogenous PPARγ antagonist cyclic phosphatidic acid (CPA) that binds to the nuclear receptor with nanomolar affinity and high specificity [52]. Moreover, scoparone which decreased TG accumulation in the mature adipocytes has been reported to suppress the differentiation of 3T3-L1 preadipocytes through down-regulation of adipogenic genes by PPARγ inhibition. It has been shown also to inhibit the rosiglitazone-mediated overexpression of PPARγ target genes to near that observed in cells treated with GW9662 [53].

Based on experimental studies reflecting the importance of PPARγ inhibition for the reduced lipid storage capacity of

the adipose tissue, we have developed also a toxicity pathway emphasizing the linkage between this MIE and NAFLD (Figure 3). Among the possible intermediate effects is the decreased expression of adiponectin. The regulation of adiponectin, a hormone exclusively expressed in adipose tissue and recognized by hepatic adiponectin receptors 1 and 2, is under PPARγ control. Besides the improvement of insulin signaling via IRS-1 (insulin receptor substrate 1), adiponectin exerts its effect by enhanced β-oxidation of fatty acids through activation of PPARα and phosphorylation of AMPK (5′-adenosine monophosphate-activated protein kinase). The last has been implicated both in reduction of malonyl-CoA-mediated inhibition of β-oxidation and in lowering of triglyceride and cholesterol synthesis via suppression of SREBP-1 (Sterol regulatory element-binding protein-1) and ChREBP (Carbohydrate-responsive element-binding protein) [54]. Adiponectin-dependent activation of the AMPK signaling pathway and its role for the lipid metabolism have been confirmed to promote lipid oxidation, suppress lipid synthesis, and reduce hepatic lipid accumulation also in bovine hepatocytes cultured *in vitro* [55]. More importantly, hepatic steatosis has been associated with hypoadiponectinemia. In a study on obese adolescents, hypoadiponectinemia and significantly decreased expression of PPARγ2 in the subcutaneous adipose tissue were associated with high liver fat content, as well as with insulin resistance. An inverse relationship was observed between plasma adiponectin or PPARγ2 expression and hepatic fat content. Adiponectin expression was also positively related to PPARγ2 expression [56]. Shrinkage and reduced secretion of adiponectin by adipose tissue have been shown to initiate a dramatic partitioning of lipid into livers of foz/foz mice [24]. Treatment with 4-hydroxynonenal has been reported to increase adiponectin gene expression, which paralleled elevated PPARγ gene expression and transactivity. As T0070907 (PPARγ antagonist) has been shown to reverse both effects, a critical role of the receptor in this process has been proposed [57]. Recently, it has been reported that eicosapentaenoic acid (EPA) and its metabolite 15d-PGJ_3 could increase adiponectin secretion in 3T3-L1 adipocytes, partially mediated by PPARγ [58].

In addition to impaired adiponectin secretion, other toxicity pathways in adipocytes have been outlined within the proposed MoA. As already discussed, LD proteins are known to play important regulatory roles in the remodeling (fragmentation, shrinkage, expansion, and/or fusion) of LDs. Reduced expression of LD proteins, transcriptionally regulated by PPARγ (FSP27/CIDEC, Plin1), has been linked to increased adipocyte lipolysis leading to elevated concentration of circulating FAs, insulin resistance, and ectopic lipid deposition in hepatocytes [44, 59].

Gaemers et al. [23] reported the role of the compromised metabolic function of inflamed white adipose tissue in overfeeding mouse models of NAFLD with significant decrease in the expression of PPARγ and its target proteins involved in lipid uptake: CD36 and aP2. Recently, various plant-derived agents (scoparone and extracts from *Zanthoxylum piperitum DC* and *Petalonia binghamiae thalli*) have been shown to inhibit *in vitro* adipocyte differentiation as well as TG accumulation in the mature adipocytes by decreasing the expression of PPARγ [60] and its adipocyte-specific target genes (aP2, CD36/FAT) [53, 61]. Lactic acid bacteria isolated from Korean pickled fish markedly decreased the expression level of PPARγ, aP2, and CD36 and significantly decreased intracellular TG storage [62]. Nuclear factor erythroid 2-related factor 2 has been shown to decrease PPARγ and aP2 expression in mouse embryonic fibroblasts, while in Lep (ob/ob) mice, it inhibited the lipid accumulation in white adipose tissue, suppressed adipogenesis, induced insulin resistance, and increased hepatic steatosis [63].

PPARγ has been recently shown to play a regulatory role in inflammatory and immune responses. Luconi et al. [12] reviewed different mechanisms of action of PPARγ some of which included repression of NFkB pathway. PPARγ has been shown to interfere with transcription of target genes either by direct interaction with NFkB preventing its binding to specific responsive elements on target genes, or by competing for common coactivators. PPARγ maintained inflammation-related genes in a repressed state through blocking the pro-inflammatory stimulus-induced clearance of corepressor complexes on target genes. Ligand-dependent SUMOylation of PPARγ has been reported to induce the expression of IKBα (the inhibitory subunit of the NF-κB complex in the cytoplasm) [12, 46]. PPARγ-dependent down-regulation of NF-κB pathway explained the anti-inflammatory action of the PPARγ activator resolvin D1 in lung, partially reversed by GW9662 [64]. Recently, PPARγ activation by bezafibrate has been implicated in the reduction of white adipose tissue inflammatory state [65].

All these data support the prosteatotic role of PPARγ inhibition in adipose tissue, as a possible MIE leading to NAFLD. The decreased adipogenesis and the resulting undesirable changes in adipose lipid-buffering capacity result in changes of plasma free FA and adiponectin levels. These changes were underlined as causative factors for decreased hepatic FA oxidation, increased FA synthesis, and elevated flow of FA into the liver. As already discussed, excessive liver triglyceride accumulation could be a consequence of elevated FA uptake. The latter could also increase the cytosolic free FA pool—an intermediate event preceding the generation of multiple fatty acids—derived mediators of lipotoxicity [54, 66]. The resulting oxidative stress and inflammation comprise a manifestation of the lipotoxic hepatocellular injury associated with NASH [67].

4. Concluding Remarks and Perspectives

The concerns about the safety profile of PPARγ-targeting xenobiotics of either synthetic or natural origin are rooted in the risk of developing adverse outcomes upon prolonged treatment. Both agonists and antagonists could reinforce improper and/or ectopic induction/suppression of PPARγ-responsive genes related to lipid metabolism and inflammation with consequent development of NAFLD. The better understanding of the MIE would allow for the definition of the properties of chemicals inducing the perturbation, such as bioavailability, structural requirements (especially for receptor binding), and metabolic transformation [5]. In this regard,

an important question to deal with is to identify the primary site of action of toxicants at a tissue level. We propose two probable toxicological MoAs from PPARγ ligand binding to nonalcoholic fatty liver disease: (1) PPARγ activation in hepatocytes and (2) PPARγ inhibition in adipocytes. Increased cellular free FA uptake, exceeding the adaptive pathways of hepatic lipid export and catabolism, could be a prerequisite for adipogenic transformation of hepatocytes. Among the PPARγ target proteins, CD36 is outlined as an essential prosteatotic factor confirmed by most experimental evidence. In adipocytes, PPARγ ligand-dependent inhibition may decrease FA storage capacity of adipose tissue with secondary effects on hepatic FA uptake, synthesis, and β-oxidation, facilitating development of NAFLD. The activity of PPARγ apart from its transcriptional regulation, cell-specific expression pattern of its cofactors and their insufficiently understood interactions, depends also on the posttranslational modifications of the receptor, availability of RXRα (forming a heterodimer with PPARγ), status of the target genes' promoters, presence of endogenous ligands, regulation of the receptor degradation, and its cellular localization [13, 68–71]. Combination of all these dependencies with the complex cross-talk between different signal transduction pathways makes the evaluation of PPARγ-mediated toxicity pathways within the established MoAs a challenging task. Developing of MoA/AOP as dynamic entities that can be continually updated and refined [5] is the first step towards the building of new generation predictive models of liver toxicity. Development of such models and their application to chemicals lacking extensive *in vivo* testing regarding NAFLD strongly depends on the presence of test results from *in vitro* and/or *in silico* assays as well as of datasets that detail the effects of these chemicals on the whole organisms [72]. Collectively, the reviewed *in vivo* and *in vitro* studies suggest that until a critical evaluation of potential adverse health hazards is performed, extreme caution should be exerted in long-term application of PPARγ modulators. The transcriptional networks and the affected metabolic and signaling pathways in pathological conditions, such as NAFLD, deserve to be further addressed in order to improve risk assessment by the PPARγ targeting strategies. Other major tasks would be the description of pathways from additional transcriptional regulators controlling PPARγ expression or activity as well as gaining insights into the molecular basis and the pathophysiological relevance of different coactivator recruitment following the ligand-binding.

Conflict of Interests

The authors declare that they have no conflict of interests.

Acknowledgments

The funding from the European Community's 7th Framework Program (FP7/2007–2013) COSMOS Project under Grant agreement no. 266835 and from Cosmetics Europe is gratefully acknowledged.

References

[1] National Research Council (NRC), *Toxicity Testing in the 21st Century: A Vision and A Strategy*, National Academies Press, Washington, DC, USA, 2007.

[2] ECHA, *Guidance on Information Requirements and Chemical Safety Assessment, Chapter R. 7a-Endpoint Specific Guidance*, ECHA, Helsinki, Finland, 2013.

[3] P. Prieto, E. Testai, M. Cronin, and C. Mahony, "Current state of the art in repeated dose systemic toxicity testing," in *Towards the Replacement of In Vivo Repeated Dose Systemic Toxicity TestIng*, T. Gocht and M. Schwarz, Eds., vol. 1, pp. 38–46, 2011.

[4] M. T. D. Cronin and A. N. Richarz, "Mode of action working group: use of mode of action related to repeated dose systemic toxicity—a framework for capturing Information," in *Towards the Replacement of In Vivo Repeated Dose Systemic Toxicity TestIng*, T. Gocht and M. Schwarz, Eds., vol. 2, pp. 284–289, 2012.

[5] OECD, *Guidance Document on Developing and Assessing Adverse Outcome Pathways*, Series on Testing and Assessment No. 184, OECD, Paris, France, 2013.

[6] D. A. Sass, P. Chang, and K. B. Chopra, "Nonalcoholic fatty liver disease: a clinical review," *Digestive Diseases and Sciences*, vol. 50, no. 1, pp. 171–180, 2005.

[7] B. Landesmann, M. Goumenou, S. Munn, and M. Whelan, "Description of prototype modes-of-action related to repeated dose toxicity," Reference Report By the Joint Research Centre of the European Commission, Institute for Health and Consumer Protection, 2012.

[8] S. Virtue and A. Vidal-Puig, "Adipose tissue expandability, lipotoxicity and the metabolic syndrome-an allostatic perspective," *Biochimica et Biophysica Acta*, vol. 1801, no. 3, pp. 338–349, 2010.

[9] S. Azhar, "Peroxisome proliferator-activated receptors, metabolic syndrome and cardiovascular disease," *Future Cardiology*, vol. 6, no. 5, pp. 657–691, 2010.

[10] T. Fournier, V. Tsatsaris, K. Handschuh, and D. Evain-Brion, "PPARs and the placenta," *Placenta*, vol. 28, no. 2-3, pp. 65–76, 2007.

[11] V. Costa, M. A. Gallo, F. Letizia, M. Aprile, A. Casamassimi, and A. Ciccodicola, "PPARG: gene expression regulation and next-generation sequencing for unsolved issues," *PPAR Research*, vol. 2010, Article ID 409168, 17 pages, 2010.

[12] M. Luconi, G. Cantini, and M. Serio, "Peroxisome proliferator-activated receptor gamma (PPARγ): is the genomic activity the only answer?" *Steroids*, vol. 75, no. 8-9, pp. 585–594, 2010.

[13] M. Ahmadian, J. M. Suh, N. Hah et al., "PPARγ signaling and metabolism: the good, the bad and the future," *Nature Medicine*, vol. 19, no. 5, pp. 557–566, 2013.

[14] V. Chandra, P. Huang, Y. Hamuro et al., "Structure of the intact PPAR-γ-RXR-α nuclear receptor complex on DNA," *Nature*, vol. 456, no. 7220, pp. 350–356, 2008.

[15] L. Zhu, S. S. Baker, W. Liu et al., "Lipid in the livers of adolescents with nonalcoholic steatohepatitis: combined effects of pathways on steatosis," *Metabolism*, vol. 60, no. 7, pp. 1001–1011, 2011.

[16] Y. J. Lee, E. H. Ko, J. E. Kim et al., "Nuclear receptor PPARγ-regulated monoacylglycerol O-acyltransferase 1 (MGAT1) expression is responsible for the lipid accumulation in diet-induced hepatic steatosis," *Proceedings of the National Academy of Sciences of the USA*, vol. 109, no. 34, pp. 13656–13661, 2012.

[17] E. Morán-Salvador, M. López-Parra, V. García-Alonso et al., "Role for PPARγ in obesity-induced hepatic steatosis as determined by hepatocyte- and macrophage-specific conditional knockouts," *FASEB Journal*, vol. 25, no. 8, pp. 2538–2550, 2011.

[18] H. Satoh, N. Ide, Y. Kagawa, and T. Maeda, "Hepatic steatosis with relation to increased expression of peroxisome proliferator-Activated receptor-γ in insulin resistant mice," *Biological and Pharmaceutical Bulletin*, vol. 36, no. 4, pp. 616–623, 2013.

[19] T. Yamazaki, S. Shiraishi, K. Kishimoto, S. Miura, and O. Ezaki, "An increase in liver PPARγ2 is an initial event to induce fatty liver in response to a diet high in butter: PPARγ2 knockdown improves fatty liver induced by high-saturated fat," *Journal of Nutritional Biochemistry*, vol. 22, no. 6, pp. 543–553, 2011.

[20] B. C. Sos, C. Harris, S. M. Nordstrom et al., "Abrogation of growth hormone secretion rescues fatty liver in mice with hepatocyte-specific deletion of JAK2," *Journal of Clinical Investigation*, vol. 121, no. 4, pp. 1412–1423, 2011.

[21] Y. Li, J. Dong, T. Ding et al., "Sphingomyelin synthase 2 activity and liver steatosis. An effect of ceramide-mediated peroxisome proliferator-activated receptor γ2 suppression," *Arteriosclerosis, Thrombosis, and Vascular Biology*, vol. 33, no. 7, pp. 1513–1520, 2013.

[22] S. Kumadaki, T. Karasawa, T. Matsuzaka et al., "Inhibition of ubiquitin ligase F-box and WD repeat domain-containing 7α (Fbw7α) causes hepatosteatosis through Krüppel-like Factor 5 (KLF5)/Peroxisome Proliferator-activated Receptor γ2 (PPARγ2) pathway but not SREBP-1c protein in mice," *Journal of Biological Chemistry*, vol. 286, no. 47, pp. 40835–40846, 2011.

[23] C. Gaemers, J. M. Stallen, C. Kunne et al., "Lipotoxicity and steatohepatitis in an overfed mouse model for non-alcoholic fatty liver disease," *Biochimica et Biophysica Acta*, vol. 1812, no. 4, pp. 447–458, 2011.

[24] C. Z. Larter, M. M. Yeh, D. M. Van Rooyen et al., "Roles of adipose restriction and metabolic factors in progression of steatosis to steatohepatitis in obese, diabetic mice," *Journal of Gastroenterology and Hepatology*, vol. 24, no. 10, pp. 1658–1668, 2009.

[25] J. He, J. H. Lee, M. Febbraio, and W. Xie, "The emerging roles of fatty acid translocase/CD36 and the aryl hydrocarbon receptor in fatty liver disease," *Experimental Biology and Medicine*, vol. 236, no. 10, pp. 1116–1121, 2011.

[26] Y. Kawano and D. E. Cohen, "Mechanisms of hepatic triglyceride accumulation in non-alcoholic fatty liver disease," *Journal of Gastroenterology*, vol. 48, no. 4, pp. 434–441, 2013.

[27] L. A. Videla and P. Pettinelli, "Misregulation of PPAR functioning and its pathogenic consequences associated with nonalcoholic fatty liver disease in human obesity," *PPAR Research*, vol. 2012, Article ID 107434, 14 pages, 2012.

[28] H. Nagasaka, T. Miida, A. Inui et al., "Fatty liver and antioxidant enzyme activities along with peroxisome proliferator-activated receptors γ and α expressions in the liver of Wilson's disease," *Molecular Genetics and Metabolism*, vol. 107, no. 3, pp. 542–547, 2012.

[29] K. Matsusue, "Novel mechanism for hepatic lipid accumulation: a physiological role for hepatic PPARγ-fsp27 signal," *Yakugaku Zasshi*, vol. 132, no. 7, pp. 823–829, 2012.

[30] T. Okumura, "Role of lipid droplet proteins in liver steatosis," *Journal of Physiology and Biochemistry*, vol. 67, no. 4, pp. 629–636, 2011.

[31] G. Panasyuk, C. Espeillac, C. Chauvin et al., "PPARγ contributes to PKM2 and HK2 expression in fatty liver," *Nature Communications*, vol. 14, no. 3, pp. 672–680, 2012.

[32] R. K. Semple, V. K. K. Chatterjee, and S. O'Rahilly, "PPARγ and human metabolic disease," *Journal of Clinical Investigation*, vol. 116, no. 3, pp. 581–589, 2006.

[33] R. J. Flach, H. Qin, L. Zhang, and A. M. Bennett, "Loss of mitogen-activated protein kinase phosphatase-1 protects from hepatic steatosis by repression of cell death-inducing DNA Fragmentation Factor A (DFFA)-like effector C (CIDEC)/fat-specific protein 27," *Journal of Biological Chemistry*, vol. 286, no. 25, pp. 22195–22202, 2011.

[34] K. Matsusue, "A physiological role for fat specific protein 27/cell death-inducing DFF45-like effector C in adipose and liver," *Biological and Pharmaceutical Bulletin*, vol. 33, no. 3, pp. 346–350, 2010.

[35] L. Bai, Y. Jia, N. Viswakarma et al., "Transcription coactivator mediator subunit MED1 Is required for the development of fatty liver in the mouse," *Hepatology*, vol. 53, no. 4, pp. 1164–1174, 2011.

[36] E. Kim, K. Li, C. Lieu et al., "Expression of apolipoprotein C-IV is regulated by Ku antigen/peroxisome proliferator-activated receptor γ complex and correlates with liver steatosis," *Journal of Hepatology*, vol. 49, no. 5, pp. 787–798, 2008.

[37] C. Z. Larter, M. M. Yeh, J. Williams, K. S. Bell-Anderson, and G. C. Farrell, "MCD-induced steatohepatitis is associated with hepatic adiponectin resistance and adipogenic transformation of hepatocytes," *Journal of Hepatology*, vol. 49, no. 3, pp. 407–416, 2008.

[38] A. Handberg, K. Højlund, A. Gastaldelli et al., "Plasma sCD36 is associated with markers of atherosclerosis, insulin resistance and fatty liver in a nondiabetic healthy population," *Journal of Internal Medicine*, vol. 271, no. 3, pp. 294–304, 2012.

[39] A. Ring, S. Le Lay, J. Pohl, P. Verkade, and W. Stremmel, "Caveolin-1 is required for fatty acid translocase (FAT/CD36) localization and function at the plasma membrane of mouse embryonic fibroblasts," *Biochimica et Biophysica Acta*, vol. 1761, no. 4, pp. 416–423, 2006.

[40] R. Ehehalt, R. Sparla, H. Kulaksiz, T. Herrmann, J. Füllekrug, and W. Stremmel, "Uptake of long chain fatty acids is regulated by dynamic interaction of FAT/CD36 with cholesterol/sphingolipid enriched microdomains (lipid rafts)," *BMC Cell Biology*, vol. 9, p. 45, 2008.

[41] X. Su and N. A. Abumrad, "Cellular fatty acid uptake: a pathway under construction," *Trends in Endocrinology and Metabolism*, vol. 20, no. 2, pp. 72–77, 2009.

[42] A. Chabowski, J. Górski, J. J. F. P. Luiken, J. F. C. Glatz, and A. Bonen, "Evidence for concerted action of FAT/CD36 and FABPpm to increase fatty acid transport across the plasma membrane," *Prostaglandins Leukotrienes and Essential Fatty Acids*, vol. 77, no. 5-6, pp. 345–353, 2007.

[43] S. Xu, A. Jay, K. Brunaldi, N. Huang, and J. A. Hamilton, "CD36 enhances fatty acid uptake by increasing the rate of intracellular esterification but not transport across the plasma membrane," *Biochemistry*, vol. 52, no. 41, pp. 7254–7261, 2013.

[44] S. Manteiga, K. Choi, A. Jayaraman, and K. Lee, "Systems biology of adipose tissue metabolism: regulation of growth, signaling and inflammation," *Wiley Interdisciplinary Reviews Systems Biology and Medicine*, vol. 5, no. 4, pp. 425–447, 2013.

[45] Y. Guo, K. R. Cordes, R. V. Farese Jr., and T. C. Walther, "Lipid droplets at a glance," *Journal of Cell Science*, vol. 122, no. 6, pp. 749–752, 2009.

[46] A. Rogue, C. Spire, M. Brun, N. Claude, and A. Guillouzo, "Gene expression changes induced by PPAR gamma agonists in animal and human liver," *PPAR Research*, vol. 2010, Article ID 325183, 16 pages, 2010.

[47] G. Musso, R. Gambino, and M. Cassader, "Recent insights into hepatic lipid metabolism in non-alcoholic fatty liver disease

(NAFLD)," *Progress in Lipid Research*, vol. 48, no. 1, pp. 1–26, 2009.

[48] C.-Y. Park and S. W. Park, "Role of peroxisome proliferator-activated receptor gamma agonist in improving hepatic steatosis: possible molecular mechanism," *Journal of Diabetes Investigation*, vol. 3, no. 2, pp. 93–95, 2012.

[49] Z. He, H. H. Zhu, T. J. Bauler et al., "Nonreceptor tyrosine phosphatase Shp2 promotes adipogenesis through inhibition of p38 MAP kinase," *Proceedings of the National Academy of Sciences of the USA*, vol. 110, no. 1, pp. E79–E88, 2013.

[50] W. Chen, B. Chang, P. Saha et al., "Berardinelli-seip congenital lipodystrophy 2/seipin is a cell-autonomous regulator of lipolysis essential for adipocyte differentiation," *Molecular and Cellular Biology*, vol. 32, no. 6, pp. 1099–1111, 2012.

[51] D. Weismann, D. M. Erion, I. Ignatova-Todorava et al., "Knockdown of the gene encoding Drosophila tribbles homologue 3 (Trib3) improves insulin sensitivity through peroxisome proliferator-activated receptor-γ (PPAR-γ) activation in a rat model of insulin resistance," *Diabetologia*, vol. 54, no. 4, pp. 935–944, 2011.

[52] T. Tsukahara, R. Tsukahara, Y. Fujiwara et al., "Phospholipase D2-dependent inhibition of the nuclear hormone receptor PPARγ by cyclic phosphatidic acid," *Molecular Cell*, vol. 39, no. 3, pp. 421–432, 2010.

[53] J.-R. Noh, Y.-H. Kim, J.-H. Hwang et al., "Scoparone inhibits adipocyte differentiation through down-regulation of peroxisome proliferators-activated receptor γ in 3T3-L1 preadipocytes," *Food Chemistry*, vol. 141, no. 2, pp. 723–730, 2013.

[54] N. Anderson and J. Borlak, "Molecular mechanisms and therapeutic targets in steatosis and steatohepatitis," *Pharmacological Reviews*, vol. 60, no. 3, pp. 311–357, 2008.

[55] H. Chen, L. Zhang, X. Li et al., "Adiponectin activates the AMPK signaling pathway to regulate lipid metabolism in bovine hepatocytes," *Journal of Steroid Biochemistry and Molecular Biology*, vol. 138, pp. 445–454, 2013.

[56] R. Kursawe, D. Narayan, A. M. G. Cali et al., "Downregulation of ADIPOQ and PPARγ2 gene expression in subcutaneous adipose tissue of obese adolescents with hepatic steatosis," *Obesity*, vol. 18, no. 10, pp. 1911–1917, 2010.

[57] Z. Wang, X. Dou, D. Gu et al., "4-Hydroxynonenal differentially regulates adiponectin gene expression and secretion via activating PPARγ and accelerating ubiquitin-proteasome degradation," *Molecular and Cellular Endocrinology*, vol. 349, no. 2, pp. 222–231, 2012.

[58] J. Lefils-Lacourtablaise, M. Socorro, A. Géloën et al., "The eicosapentaenoic acid metabolite 15-deoxy-δ(12,14)-prostaglandin J3 increases adiponectin secretion by adipocytes partly via a PPARγ-dependent mechanism," *PloS ONE*, vol. 8, no. 5, Article ID e63997, 2013.

[59] A. S. Greenberg, R. A. Coleman, F. B. Kraemer et al., "The role of lipid droplets in metabolic disease in rodents and humans," *Journal of Clinical Investigation*, vol. 121, no. 6, pp. 2102–2110, 2011.

[60] S. Y. Gwon, J. Y. Ahn, T. W. Kim, and T. Y. Ha, "*Zanthoxylum piperitum* DC ethanol extract suppresses fat accumulation in adipocytes and high fat diet-induced obese mice by regulating adipogenesis," *Journal of Nutritional Science and Vitaminology (Tokyo)*, vol. 58, no. 6, pp. 393–401, 2012.

[61] S.-I. Kang, M.-H. Kim, H.-S. Shin et al., "A water-soluble extract of *Petalonia binghamiae* inhibits the expression of adipogenic regulators in 3T3-L1 preadipocytes and reduces adiposity and weight gain in rats fed a high-fat diet," *Journal of Nutritional Biochemistry*, vol. 21, no. 12, pp. 1251–1257, 2010.

[62] J.-E. Park, S.-H. Oh, and Y.-S. Cha, "Lactobacillus plantarum LG42 isolated from gajami Sik-Hae inhibits adipogenesis in 3T3-L1 adipocyte," *BioMed Research International*, vol. 2013, Article ID 460927, 7 pages, 2013.

[63] J. Xu, S. R. Kulkarni, A. C. Donepudi, V. R. More, and A. L. Slitt, "Enhanced Nrf2 activity worsens insulin resistance, impairs lipid accumulation in adipose tissue, and increases hepatic steatosis in leptin-deficient mice," *Diabetes*, vol. 61, no. 12, pp. 3208–3218, 2012.

[64] Z. Liao, J. Dong, W. Wu et al., "Resolvin D1 attenuates inflammation in lipopolysaccharide-induced acute lung injury through a process involving the PPARγ/NF-κB pathway," *Respiratory Research*, vol. 13, p. 110, 2012.

[65] D. C. Magliano, T. C. Bargut, S. N. de Carvalho, M. B. Aguila, C. A. Mandarim-de-Lacerda, and V. Souza-Mello, "Peroxisome proliferator-activated receptors-alpha and gamma are targets to treat offspring from maternal diet-induced obesity in mice," *PLoS ONE*, vol. 8, no. 5, Article ID e64258, 2013.

[66] B. A. Neuschwander-Tetri, "Hepatic lipotoxicity and the pathogenesis of nonalcoholic steatohepatitis: the central role of nontriglyceride fatty acid metabolites," *Hepatology*, vol. 52, no. 2, pp. 774–788, 2010.

[67] G. Serviddio, F. Bellanti, and G. Vendemiale, "Free radical biology for medicine: learning from nonalcoholic fatty liver disease," *Free Radical Biology and Medicine C*, vol. 65, pp. 952–968, 2013.

[68] S. Polvani, M. Tarocchi, and A. Galli, "PPAR and oxidative stress: Con(β) catenating NRF2 and FOXO," *PPAR Research*, vol. 2012, Article ID 641087, 15 pages, 2012.

[69] A. Bugge and S. Mandrup, "Molecular mechanisms and genome-wide aspects of PPAR subtype specific transactivation," *PPAR Research*, vol. 2010, Article ID 169506, 12 pages, 2010.

[70] M. Schupp and M. A. Lazar, "Endogenous ligands for nuclear receptors: digging deeper," *Journal of Biological Chemistry*, vol. 285, no. 52, pp. 40409–40415, 2010.

[71] E. Burgermeister and R. Seger, "MAPK kinases as nucleo-cytoplasmic shuttles for PPARγ," *Cell Cycle*, vol. 6, no. 13, pp. 1539–1548, 2007.

[72] K. A. Houck, A. M. Richard, R. S. Judson, M. T. Martin, D. M. Reif, and I. Shah, "ToxCast: predicting toxicity potential through high-throughput bioactivity profiling," in *High-Throughput ScreenIng Methods in Toxicity TestIng*, P. Steinberg, Ed., pp. 1–31, John Wiley & Sons, Hoboken, NJ, USA, 2013.

Hindawi Publishing Corporation
PPAR Research
Volume 2014, Article ID 653017, 6 pages
http://dx.doi.org/10.1155/2014/653017

Review Article

PPARs Integrate the Mammalian Clock and Energy Metabolism

Lihong Chen and Guangrui Yang

The Institute for Translational Medicine and Therapeutics, Translational Research Center, University of Pennsylvania, 3400 Civic Center Boulevard, Building 421, Philadelphia, PA 19104-5158, USA

Correspondence should be addressed to Lihong Chen; bjclh2000@163.com and Guangrui Yang; guangrui@mail.med.upenn.edu

Received 25 November 2013; Accepted 17 December 2013; Published 19 February 2014

Academic Editor: Zhanjun Jia

Peroxisome proliferator-activated receptors (PPARs) are a group of nuclear receptors that function as transcription factors regulating the expression of numerous target genes. PPARs play an essential role in various physiological and pathological processes, especially in energy metabolism. It has long been known that metabolism and circadian clocks are tightly intertwined. However, the mechanism of how they influence each other is not fully understood. Recently, all three PPAR isoforms were found to be rhythmically expressed in given mouse tissues. Among them, PPARα and PPARγ are direct regulators of core clock components, Bmal1 and Rev-erbα, and, conversely, PPARα is also a direct Bmal1 target gene. More importantly, recent studies using knockout mice revealed that all PPARs exert given functions in a circadian manner. These findings demonstrated a novel role of PPARs as regulators in correlating circadian rhythm and metabolism. In this review, we summarize advances in our understanding of PPARs in circadian regulation.

1. Introduction

1.1. The PPAR Family. Peroxisome proliferator-activated receptors (PPARs) are transcription factors, belonging to the nuclear receptor superfamily, a group of proteins that are usually activated by their respective ligands and function within the cell nuclei for controlling metabolism, development, and homeostasis of the organism. PPARs heterodimerize with the retinoid X receptor (RXR) and bind to PPAR responsive element (PPRE) in the regulatory region of target genes that function in diverse biological processes, such as lipid metabolism, adipogenesis, insulin sensitivity, immune response, and cell growth and differentiation [1, 2]. PPARs also participate in the pathogenesis of a cluster of human diseases, for example, metabolic syndrome that includes insulin resistance, glucose intolerance, obesity, dyslipidemia, hypertension, atherosclerosis, and microalbuminuria [3–6].

PPARs have 3 isoforms in mammals, namely, α, β/δ, and γ. Although they share structural similarity and exhibit high homology in amino acid sequence, the three isoforms are differentially expressed among tissues [7]. In general, PPARα is abundant in the liver, brown adipose tissue, heart, and kidney; PPARγ is mainly enriched in the adipose tissue and PPARβ/δ is ubiquitously expressed throughout the body [8]. Their differential distributions as well as different affinities to ligands attribute to their distinct roles. PPAR ligands vary from endogenous fatty acids to industrial chemicals and pharmaceutical drugs. Synthetic PPARα agonists such as fenofibrate and clofibrate are clinically proven lipid-lowering drugs [9]. A class of PPARγ ligands called thiazolidinediones (TZDs), such as rosiglitazone and pioglitazone, has been introduced in clinical practice for improving glycemic control via insulin sensitization in patients with type 2 diabetes [10]. Increasing evidence also points to a potential role of PPARβ/δ activators in improving insulin resistance and dyslipidemia [11]. In addition, some PPAR ligands are also potential therapeutic agents for treating hypertension, atherosclerosis, and diabetic nephropathy [1, 12, 13]. The development and use of PPAR ligands in the past decades have greatly advanced our understanding of physiological and pathological role of PPARs and the therapeutic implication of targeting them.

1.2. Circadian Rhythm. Circadian rhythm is any biological process displaying endogenous and entrainable oscillations of about 24 hours. In mammals, for example, sleep-awake

pattern, blood pressure and heart rate, hormone secretion, body temperature, and energy metabolism exhibit circadian oscillation. These endogenous responses have significant relevance to human health and diseases [14]. Disruption of circadian rhythm has become an exacerbating factor in metabolic syndrome [15–19]. This is exceptionally important in developed countries due to frequent shift working, exposure to artificial light, travel by transmeridian air flight, and involvement in social activities. Some reports have shown that night-shift workers exhibit a higher incidence of obesity and other aspects of metabolic syndrome [15, 20, 21]. Recently, Hatori and colleagues found that temporal restriction of calorie consumption limits mouse weight gain on a high fat diet via enhancing oscillation of clock genes and their target genes [22]. Deletion of the clock gene Bmal1 (brain and muscle aryl-hydrocarbon receptor nuclear translocator-like 1) in adipose tissue causes mice to become obese via shifting their eating behavior [23]. These evidence suggested when you eat may be as important as what you eat.

Circadian rhythm is driven by a group of genes called clock genes and has been widely observed in plants, animals and even in bacteria. In mammals, the core clock genes are rhythmically expressed in the SCN (suprachiasmatic nucleus), the master clock residing in the hypothalamus, and most peripheral tissues such as liver, fat, muscle, heart, and blood vessels [14]. These genes form a tightly regulated system with interlocking feedback and feedforward loops (Figure 1). BMAL1 and CLOCK (Circadian Locomotor Output Cycles Kaput), or its paralog NPAS2 (neuronal PAS domain protein 2), form a heterodimer. This BMAL1:CLOCK/NPAS2 complex binds to E-box elements in the promoters of Period (PER1-3) and Cryptochrome (CRY1 and CRY2) genes and activates their transcription. Upon accumulation in the cytoplasm to a critical level, the proteins of PER and CRY dimerize and translocate into the nucleus to repress the transcriptional activity of BMAL1:CLOCK/NPAS2 complex, thereby shutting down their own transcription. This core loop is interconnected with additional regulatory loops involving nuclear receptors, RAR-related orphan receptor (ROR), and REV-ERB, whose transcription is driven by BMAL1 and in turn to enhance and suppress BMAL1 transcription, respectively [24]. These feedback loops also control numerous target genes (termed clock controlled genes, CCG) in a circadian manner. Recently, all PPAR isoforms in mouse tissues were found to be rhythmically expressed [25]. Furthermore, PPARα and PPARγ have direct interactions with the core clock genes [26–28], suggesting that they may act as molecular links between circadian rhythm and energy metabolism.

2. PPARα and Circadian Clock

The expression of PPARα has a diurnal rhythm in mouse liver, heart, kidney, and, to a lesser extent, in the SCN [25, 29]. This circadian pattern might be partially controlled by some hormonal factors, such as glucocorticoids and insulin, whose secretions display diurnal variations [29, 30]. More recently, several reports showed a direct link between PPARα and the circadian clocks. Firstly, PPARα was identified as a direct target gene of BMAL1 and CLOCK via an E-box-dependent mechanism [31]. The expression level of PPARα in the liver was decreased and its circadian oscillation was abolished in BMAL1 knockout mice or CLOCK-mutant mice [27, 31]. Reciprocally, PPARα-null mice showed altered oscillation of BMAL1 and PER3 in the liver. *In vitro* experiments revealed that PPARα directly regulates the transcription of BMAL1 and REV-ERBα via binding to PPRE sites in their respective promoter regions [27, 32]. Besides transcriptional regulation, PPARα could modulate PER2 activity by direct physical interactions [33].

Fenofibrate, a PPARα agonist and anticholesterol drug, was able to increase transcription and reset rhythmic expression of BMAL1, PER1, PER3, and REV-ERBα in mouse livers [27] and cultured hepatocytes [32]. Bezafibrate, another PPARα agonist, was shown to phase-advance the circadian expression of BMAL1, PER2, and REV-ERBα in multiple mouse peripheral tissues [34, 35]. Interestingly, bezafibrate did not alter the phase of core clock genes in the SCN, although it was able to affect circadian behavior, for example, alleviating delayed sleep phase syndrome caused by clock mutation [34]. In addition, clock gene expressions were also found unaltered in the SCN of PPARα knockout mice [27]. These results imply that PPARα is involved in circadian regulation independently of the central clock and that PPARα could be a potent target for treating sleep disorders.

More importantly, as a mediator of circadian regulation of lipid metabolism, PPARα also regulates the expression of numerous genes involved in lipid and cholesterol metabolism and energy homeostasis. Many of these genes, such as sterol regulatory element binding protein (SREBP), fatty acid synthase (FAS), and HMG-CoA reductase, display daily fluctuations in mouse liver; however, their amplitudes are attenuated or abolished in PPARα knockout mice [36, 37]. Kersten et al. showed that PPARα mRNA is induced during fasting in wild-type mice to accommodate the increased requirement of hepatic fatty acid oxidation. PPARα-null mice, however, showed a massive accumulation of lipid in their livers when fasted [38], which indicates a pivotal role of PPARα in the management of energy storage during fasting. Oleoylethanolamide (OEA), an endogenous PPARα agonist, is synthesized diurnally in the gut epithelium [39]. Administration of OEA produced satiety and reduced weight gain in wild-type mice, but this response was abolished in PPARα-null mice [40], suggesting that PPARα regulates the feeding behavior and may be a potential target for treating eating disorders.

PPARα is also abundant in the heart where it serves a role in normal cardiac metabolic homeostasis via regulating enzymes involved in fatty acid beta-oxidation [41]. Its higher expression level during early dark phase is consistent with the circadian variation of heart function. Wu et al. found that both PPARα and its target gene glucose transporter type 4 (Glut4) and acetyl-coA synthetase (Acs1) were significantly downregulated in the activity phase in mouse heart when cardiac tissue overexpressed PPARγ coactivator 1α (PGC-1α). The disrupted circadian expression of PPARα was accompanied by abolished diurnal variation of ejection fraction and shortening fraction [42], indicating that PPARα

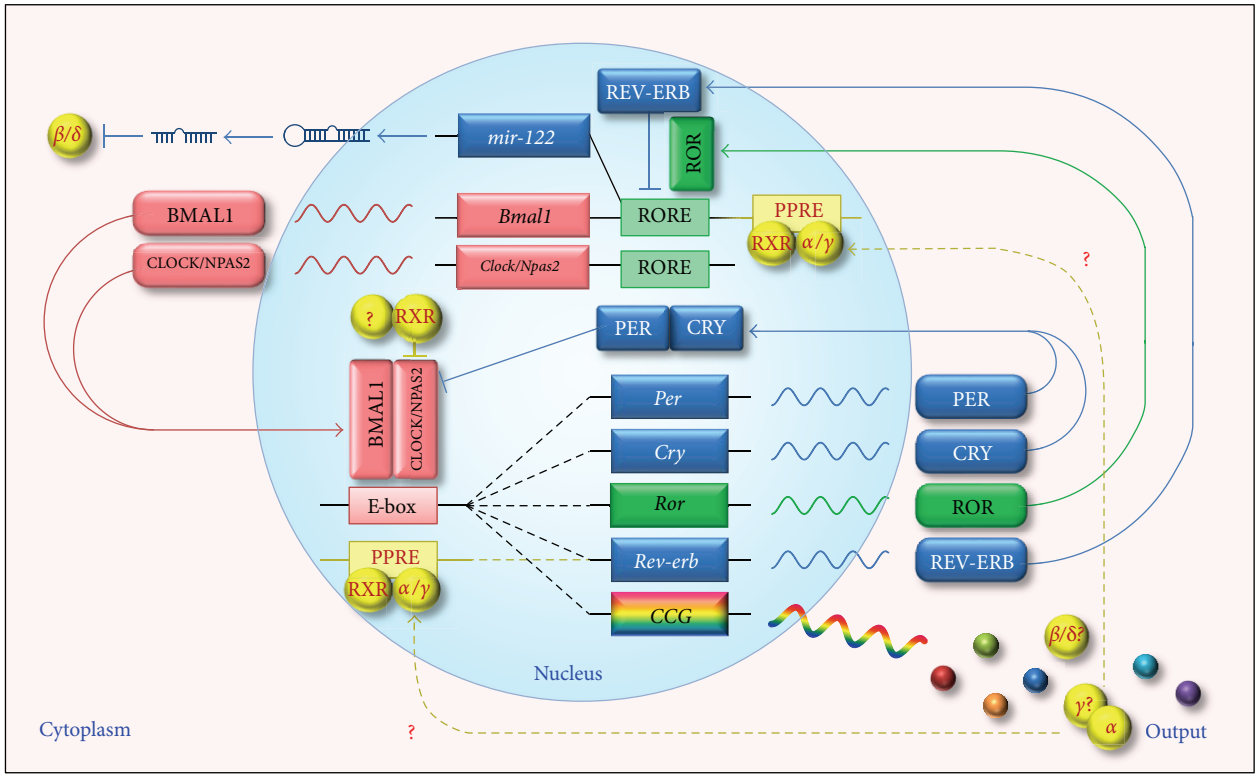

α: PPARα. β/δ : PPAR β/δ.
γ: PPARγ. CCG: clock controlled gene.

Figure 1: Involvement of PPARs in the transcriptional feedback loops of the mammalian circadian clock. BMAL1:CLOCK/NPAS2 heterodimer activates transcription of PER, CRY, ROR, and REV-ERB via binding to E-box in their promoters. Upon accumulation, PER and CRY dimerize and translocate into the nucleus to repress BMAL1:CLOCK/NPAS2 activity and therefore their own transcription. ROR activates and REV-ERB represses RORE-mediated transcription. These interlocking loops also control numerous output genes in a circadian manner. In addition, PPARs are integrated in this system (shown in yellow). PPARα and PPARγ regulate the expression of BMAL1 and REV-ERB via binding to PPRE in their promoters. PPARα is also a direct target gene of BMAL1. PPARβ/δ is a target for miR-122 whose transcription is inhibited by REV-ERB. Besides, as the PPAR partner, RXR inhibits the transcriptional activity of BMAL1:CLOCK/NPAS2 complex via binding to CLOCK or NPAS2. All PPARs display circadian expression pattern in given tissues; however, it is still not known if γ or β/δ isoform is directly regulated by Bmal1 or if the integration of PPARs in circadian clock system forms a closed loop.

plays a critical role in connecting circadian biology to heart performance.

3. PPARγ and Circadian Clock

PPARγ is a key regulator of adipogenesis and is well known for serving as a therapeutic target for treating metabolic diseases. Agonists of PPARγ rosiglitazone and pioglitazone have been widely used for many years for treating type 2 diabetes, owing to their effectiveness in promoting insulin sensitivity. Recently, PPARγ was shown to exhibit a remarkable circadian expression pattern in mouse liver, fat, and blood vessels [25, 28]. Global deletion of PPARγ in mice abolished or dampened circadian rhythms at both behavioral and cellular levels [43].

Day-night variations in the blood pressure (BP) and heart rate (HR) are among the best known circadian rhythms of physiology. Vascular conditional deletion of PPARγ in mice dampened diurnal variations of HR and BP via deregulation of BMAL1 [28]. Yang et al. found that global deletion of PPARγ abolished these rhythms even without affecting locomotor activity under regular light/dark conditions [43]. In addition, pioglitazone has been shown to transform BP from a nondipper to a dipper type in type 2 diabetic patients [44]. These findings strongly support an essential role of PPARγ in maintaining circadian rhythms of BP and HR, which may partially explain the beneficial side effects of PPARγ agonists in cardiovascular system.

Moreover, several other key factors related to PPARγ play important roles in circadian rhythm. Notably, REV-ERBα, a target gene of PPARγ [45], is one of the core clock components, although there has not been a direct evidence showing that PPARγ exerts circadian function via REV-ERBα yet. PPARγ coactivator 1α (PGC-1α) is also identified as a circadian factor. PGC-1α is rhythmically expressed in mouse liver and muscle and positively regulates BMAL1, CLOCK, and REV-ERBα [46]. Mice lacking PGC-1α show abnormal

locomotor activity and disrupted diurnal oscillation of body temperature and energy metabolism, which is correlated with aberrant expression pattern of metabolic genes and clock genes [46]. Nocturnin, a clock controlled gene, binds to PPARγ and enhance its transcriptional activity [47]. Deletion of nocturnin abolished PPARγ oscillation in the liver of mice fed on high-fat diet, accompanied by a decrease in expression of many genes related to lipid metabolism [48]. 15-Deoxy-D 12,14-prostaglandin J_2 (15d-PGJ_2), a natural PPARγ ligand, was reported to be an entrainment factor *in vitro* [49], while its circadian function was abolished by PPARγ deletion [43].

4. PPARβ/δ and Circadian Clock

Despite accumulating evidence supporting the role of PPARβ/δ in metabolic control and energy homeostasis [6, 50] and abundant data showing association between metabolism and circadian rhythm [51], little is known concerning the influence of PPARβ/δ in circadian rhythm unlike PPARα and PPARγ, even though mRNA level of PPARβ/δ is cyclic in mouse liver and brown adipose tissue [25]. REV-ERBα and miR-122 may serve as a possible link between PPARβ/δ and circadian clock. miR-122 is a highly abundant, liver-specific microRNA whose transcription is regulated by REV-ERBα. It has previously been shown to regulate lipid metabolism in mouse liver [52]. Gatfield et al. proved PPARβ/δ as a new target for miR-122, suggesting that PPARβ/δ might act as a circadian metabolic regulator in miR-122-mediated metabolic control [53]. Recently, Challet et al. observed oscillations in PPARβ/δ expression in hamster SCN. Administration of PPARβ/δ agonist L-16504 amplified the delay phase of locomotor response induced by a light pulse [54], indicating that PPARβ/δ may play a role in circadian behavior. In another recent paper, Liu et al. revealed a PPARβ/δ-dependent diurnal oscillation of *de novo* lipogenesis in mouse liver [55]. Using hepatocyte specific knockout mice, they found that PPARβ/δ controls temporal expression of hepatic lipogenic genes including acetyl-CoA carboxylase 1 (ACC1), ACC2, FAS, and stearoyl-CoA desaturase-1 (SCD1), thus affecting fatty acid metabolism in the liver.

In addition, RXRα, the partner of all PPARs, interacts with CLOCK protein in a ligand-dependent manner to inhibit CLOCK:BMAL1-dependent transcriptional activation of clock gene expression in vascular cells [56]. However, it is still not known whether its circadian function is dependent on PPARs. If this is the case, PPARβ/δ may be the dominant partner since α and γ isoforms were reported to be positive regulators for BMAL1 [27, 28].

5. Conclusions and Future Directions

Within the family of nuclear receptors, ROR and REV-ERB have been identified as core clock components. Recent findings suggest their closest phylogenetic neighbor PPARs as circadian regulators as well. PPARs have been extensively demonstrated as effective molecular targets for treating metabolic diseases. Circadian oscillations of PPARs and their target genes display a strong association with energy and metabolism homeostasis. The aberration of PPARs-circadian clock system could result in altered expression of metabolic genes, leading to disturbance in energy status. Therefore, the diseases jointly regulated by PPARs and the circadian clock have become an exploratory area. Further investigation into the regulation of PPARs in circadian rhythmic diseases could strengthen our understanding of mechanisms for disorders in energy homeostasis and metabolism and may provide novel therapeutic avenues for the treatment of metabolic ailments.

Things to keep in mind, however, most of the current studies were from mouse models. The extent to which mouse models simulate responses in human is still controversial, especially for circadian research since humans are diurnal. To date, the circadian expression of PPARα in human fibroblasts [31] and PPARγ in human adipose explants [57] has been identified, while how they link energy metabolism and circadian clock in humans remains to be determined.

Conflict of Interests

The authors declare that there is no conflict of interests regarding the publication of this paper.

Acknowledgment

The authors are grateful to Michael Adam and Ashmita Saigal for reading and commenting on this paper.

References

[1] J. Wu, L. Chen, D. Zhang et al., "Peroxisome proliferator-activated receptors and renal diseases," *Frontiers in Bioscience*, vol. 14, no. 3, pp. 995–1009, 2009.

[2] Y. Guan, J. Yang, L. Chen et al., "PPARs and female reproduction: evidence from genetically manipulated mice," *PPAR Research*, vol. 2008, Article ID 723243, 2008.

[3] Y. Guan, "Peroxisome proliferator-activated receptor family and its relationship to renal complications of the metabolic syndrome," *Journal of the American Society of Nephrology*, vol. 15, no. 11, pp. 2801–2815, 2004.

[4] H. Takano and I. Komuro, "Peroxisome proliferator-activated receptor γ and cardiovascular diseases," *Circulation Journal*, vol. 73, no. 2, pp. 214–220, 2009.

[5] A. Y. Y. Cheng and L. A. Leiter, "PPAR-alpha: therapeutic role in diabetes-related cardiovascular disease," *Diabetes, Obesity and Metabolism*, vol. 10, no. 9, pp. 691–698, 2008.

[6] T. Coll, R. Rodríguez-Calvo, E. Barroso et al., "Peroxisome Proliferator-Activated Receptor (PPAR) β/δ: a new potential therapeutic target for the treatment of metabolic syndrome," *Current Molecular Pharmacology*, vol. 2, no. 1, pp. 46–55, 2009.

[7] B. Desvergne and W. Wahli, "Peroxisome proliferator-activated receptors: nuclear control of metabolism," *Endocrine Reviews*, vol. 20, no. 5, pp. 649–688, 1999.

[8] O. Braissant, F. Foufelle, C. Scotto, M. Dauça, and W. Wahli, "Differential expression of Peroxisome Proliferator-Activated Receptors (PPARs): tissue distribution of PPAR-α, -β, and -γ in the adult rat," *Endocrinology*, vol. 137, no. 1, pp. 354–366, 1996.

[9] B. Staels, J. Dallongeville, J. Auwerx, K. Schoonjans, E. Leitersdorf, and J.-C. Fruchart, "Mechanism of action of fibrates on

lipid and lipoprotein metabolism," *Circulation*, vol. 98, no. 19, pp. 2088–2093, 1998.

[10] A. B. Jones, "Peroxisome Proliferator-Activated Receptor (PPAR) modulators: diabetes and beyond," *Medicinal Research Reviews*, vol. 21, no. 6, pp. 540–552, 2001.

[11] M. D. Leibowitz, C. Fiévet, N. Hennuyer et al., "Activation of PPARδ alters lipid metabolism in db/db mice," *FEBS Letters*, vol. 473, no. 3, pp. 333–336, 2000.

[12] S. Z. Duan, M. G. Usher, and R. M. Mortensen, "PPARs: the vasculature, inflammation and hypertension," *Current Opinion in Nephrology and Hypertension*, vol. 18, no. 2, pp. 128–133, 2009.

[13] C. W. Park, Y. Zhang, X. Zhang et al., "PPARα agonist fenofibrate improves diabetic nephropathy in db/db mic," *Kidney International*, vol. 69, no. 9, pp. 1511–1517, 2006.

[14] G. Yang, G. Paschos, A. M. Curtis, E. S. Musiek, S. C. McLoughlin, and G. A. Fitzgerald, "Knitting up the raveled sleave of care," *Science Translational Medicine*, vol. 5, no. 212, Article ID 212rv3, 2013.

[15] B. Karlsson, A. Knutsson, and B. Lindahl, "Is there an association between shift work and having a metabolic syndrome? Results from a population based study of 27,485 people," *Occupational and Environmental Medicine*, vol. 58, no. 11, pp. 747–752, 2001.

[16] J. E. Gangwisch, D. Malaspina, B. Boden-Albala, and S. B. Heymsfield, "Inadequate sleep as a risk factor for obesity: analyses of the NHANES I," *Sleep*, vol. 28, no. 10, pp. 1289–1296, 2005.

[17] J.-P. Chaput, M. Brunet, and A. Tremblay, "Relationship between short sleeping hours and childhood overweight/obesity: results from the "Québec en Forme" project," *International Journal of Obesity*, vol. 30, no. 7, pp. 1080–1085, 2006.

[18] C. Gallou-Kabani, A. Vigé, and C. Junien, "Lifelong circadian and epigenetic drifts in metabolic syndrome," *Epigenetics*, vol. 2, no. 3, pp. 137–146, 2007.

[19] E. Maury, K. M. Ramsey, and J. Bass, "Circadian rhythms and metabolic syndrome: from experimental genetics to human disease," *Circulation Research*, vol. 106, no. 3, pp. 447–462, 2010.

[20] B. Karlsson, "Commentary: metabolic syndrome as a result of shift work exposure?" *International Journal of Epidemiology*, vol. 38, no. 3, pp. 854–855, 2009.

[21] U. Holmbäck, A. Forslund, A. Lowden et al., "Endocrine responses to nocturnal eating—possible implications for night work," *European Journal of Nutrition*, vol. 42, no. 2, pp. 75–83, 2003.

[22] M. Hatori, C. Vollmers, A. Zarrinpar et al., "Time-restricted feeding without reducing caloric intake prevents metabolic diseases in mice fed a high-fat diet," *Cell Metabolism*, vol. 15, no. 6, pp. 848–860, 2012.

[23] G. K. Paschos, S. Ibrahim, W. L. Song et al., "Obesity in mice with adipocyte-specific deletion of clock component Arntl," *Nature Medicine*, vol. 18, no. 12, pp. 1768–1777, 2012.

[24] H. R. Ueda, W. Chen, A. Adachi et al., "A transcription factor response element for gene expression during circadian night," *Nature*, vol. 418, no. 6897, pp. 534–539, 2002.

[25] X. Yang, M. Downes, R. T. Yu et al., "Nuclear receptor expression links the circadian clock to metabolism," *Cell*, vol. 126, no. 4, pp. 801–810, 2006.

[26] I. Inoue, Y. Shinoda, M. Ikeda et al., "CLOCK/BMAL1 is involved in lipid metabolism via transactivation of the Peroxisome Proliferator-Activated Receptor (PPAR) response element," *Journal of Atherosclerosis and Thrombosis*, vol. 12, no. 3, pp. 169–174, 2005.

[27] L. Canaple, J. Rambaud, O. Dkhissi-Benyahya et al., "Reciprocal regulation of brain and muscle Arnt-like protein 1 and peroxisome proliferator-activated receptor α defines a novel positive feedback loop in the rodent liver circadian clock," *Molecular Endocrinology*, vol. 20, no. 8, pp. 1715–1727, 2006.

[28] N. Wang, G. Yang, Z. Jia et al., "Vascular PPARγ controls circadian variation in blood pressure and heart rate through Bmal1," *Cell Metabolism*, vol. 8, no. 6, pp. 482–491, 2008.

[29] T. Lemberger, R. Saladin, M. Vázquez et al., "Expression of the peroxisome proliferator-activated receptor α gene is stimulated by stress and follows a diurnal rhythm," *Journal of Biological Chemistry*, vol. 271, no. 3, pp. 1764–1769, 1996.

[30] H. H. Steineger, H. N. Sorensen, J. D. Tugwood, S. Skrede, O. Spydevold, and K. M. Gautvik, "Dexamethasone and insulin demonstrate marked and opposite regulation of the steady-state mRNA level of the Peroxismal Proliferator-Activated Receptor (PPAR) in hepatic cells. Hormonal modulation of fatty-acid-induced transcription," *European Journal of Biochemistry*, vol. 225, no. 3, pp. 967–974, 1994.

[31] K. Oishi, H. Shirai, and N. Ishida, "CLOCK is involved in the circadian transactivation of peroxisome- proliferator-activated receptor α (PPARα) in mice," *Biochemical Journal*, vol. 386, no. 3, pp. 575–581, 2005.

[32] P. Gervois, S. Chopin-Delannoy, A. Fadel et al., "Fibrates increase human REV-ERBα expression in liver via a novel peroxisome proliferator-activated receptor response element," *Molecular Endocrinology*, vol. 13, no. 3, pp. 400–409, 1999.

[33] I. Schmutz, J. A. Ripperger, S. Baeriswyl-Aebischer, and U. Albrecht, "The mammalian clock component PERIOD2 coordinates circadian output by interaction with nuclear receptors," *Genes and Development*, vol. 24, no. 4, pp. 345–357, 2010.

[34] H. Shirai, K. Oishi, T. Kudo, S. Shibata, and N. Ishida, "PPARα is a potential therapeutic target of drugs to treat circadian rhythm sleep disorders," *Biochemical and Biophysical Research Communications*, vol. 357, no. 3, pp. 679–682, 2007.

[35] K. Oishi, H. Shirai, and N. Ishida, "PPARα is involved in photoentrainment of the circadian clock," *NeuroReport*, vol. 19, no. 4, pp. 487–489, 2008.

[36] G. F. Gibbons, D. Patel, D. Wiggins, and B. L. Knight, "The functional efficiency of lipogenic and cholesterogenic gene expression in normal mice and in mice lacking the Peroxisomal Proliferator-Activated Receptor-alpha (PPAR-α)," *Advances in Enzyme Regulation*, vol. 42, pp. 227–247, 2002.

[37] D. D. Patel, B. L. Knight, D. Wiggins, S. M. Humphreys, and G. F. Gibbons, "Disturbances in the normal regulation of SREBP-sensitive genes in PPARα-deficient mice," *Journal of Lipid Research*, vol. 42, no. 3, pp. 328–337, 2001.

[38] S. Kersten, J. Seydoux, J. M. Peters, F. J. Gonzalez, B. Desvergne, and W. Wahli, "Peroxisome proliferator-activated receptor α mediates the adaptive response to fasting," *Journal of Clinical Investigation*, vol. 103, no. 11, pp. 1489–1498, 1999.

[39] J. Fu, G. Astarita, S. Gaetani et al., "Food intake regulates oleoylethanolamide formation and degradation in the proximal small intestine," *Journal of Biological Chemistry*, vol. 282, no. 2, pp. 1518–1528, 2007.

[40] J. Fu, S. Gaetani, F. Oveisi et al., "Oleylethanolamide regulates feeding and body weight through activation of the nuclear receptor PPAR-α," *Nature*, vol. 425, no. 6953, pp. 90–93, 2003.

[41] P. M. Barger and D. P. Kelly, "PPAR signaling in the control of cardiac energy metabolism," *Trends in Cardiovascular Medicine*, vol. 10, no. 6, pp. 238–245, 2000.

[42] X. Wu, Z. Liu, G. Shi et al., "The circadian clock influences heart performance," *Journal of Biological Rhythms*, vol. 26, no. 5, pp. 402–411, 2011.

[43] G. Yang, Z. Jia, T. Aoyagi, D. McClain, R. M. Mortensen, and T. Yang, "Systemic PPARγ deletion impairs circadian rhythms of behavior and metabolism," *PLoS ONE*, vol. 7, no. 8, Article ID e38117, 2012.

[44] F. Anan, T. Masaki, N. Fukunaga et al., "Pioglitazone shift circadian rhythm of blood pressure from non-dipper to dipper type in type 2 diabetes mellitus," *European Journal of Clinical Investigation*, vol. 37, no. 9, pp. 709–714, 2007.

[45] C. Fontaine, G. Dubois, Y. Duguay et al., "The orphan nuclear receptor Rev-Erbα is a Peroxisome Proliferator-Activated Receptor (PPAR) γ target gene and promotes PPARγ-induced adipocyte differentiation," *Journal of Biological Chemistry*, vol. 278, no. 39, pp. 37672–37680, 2003.

[46] C. Liu, S. Li, T. Liu, J. Borjigin, and J. D. Lin, "Transcriptional coactivator PGC-1α integrates the mammalian clock and energy metabolism," *Nature*, vol. 447, no. 7143, pp. 477–481, 2007.

[47] M. Kawai, C. B. Green, B. Lecka-Czernik et al., "A circadian-regulated gene, Nocturnin, promotes adipogenesis by stimulating PPAR-γ nuclear translocation," *Proceedings of the National Academy of Sciences of the United States of America*, vol. 107, no. 23, pp. 10508–10513, 2010.

[48] C. B. Green, N. Douris, S. Kojima et al., "Loss of Nocturnin, a circadian deadenylase, confers resistance to hepatic steatosis and diet-induced obesity," *Proceedings of the National Academy of Sciences of the United States of America*, vol. 104, no. 23, pp. 9888–9893, 2007.

[49] Y. Nakahata, M. Akashi, D. Trcka, A. Yasuda, and T. Takumi, "The in vitro real-time oscillation monitoring system identifies potential entrainment factors for circadian clocks," *BMC Molecular Biology*, vol. 7, article 5, 2006.

[50] K.-D. Wagner and N. Wagner, "Peroxisome proliferator-activated receptor beta/delta (PPARβ/δ) acts as regulator of metabolism linked to multiple cellular functions," *Pharmacology and Therapeutics*, vol. 125, no. 3, pp. 423–435, 2010.

[51] G. Asher and U. Schibler, "Crosstalk between components of circadian and metabolic cycles in mammals," *Cell Metabolism*, vol. 13, no. 2, pp. 125–137, 2011.

[52] C. Esau, S. Davis, S. F. Murray et al., "miR-122 regulation of lipid metabolism revealed by in vivo antisense targeting," *Cell Metabolism*, vol. 3, no. 2, pp. 87–98, 2006.

[53] D. Gatfield, G. Le Martelot, C. E. Vejnar et al., "Integration of microRNA miR-122 in hepatic circadian gene expression," *Genes and Development*, vol. 23, no. 11, pp. 1313–1326, 2009.

[54] E. Challet, I. Denis, V. Rochet et al., "The role of PPARβ/δ in the regulation of glutamatergic signaling in the hamster suprachiasmatic nucleus," *Cellular and Molecular Life Sciences*, vol. 70, no. 11, pp. 2003–2014, 2013.

[55] S. Liu, J. D. Brown, K. J. Stanya et al., "A diurnal serum lipid integrates hepatic lipogenesis and peripheral fatty acid use," *Nature*, vol. 502, no. 7472, pp. 550–554, 2013.

[56] P. McNamara, S.-B. Seo, R. D. Rudic, A. Sehgal, D. Chakravarti, and G. A. FitzGerald, "Regulation of CLOCK and MOP4 by nuclear hormone receptors in the vasculature: a humoral mechanism to reset a peripheral clock," *Cell*, vol. 105, no. 7, pp. 877–889, 2001.

[57] J. J. Hernandez-Morante, C. Gomez-Santos, F. Milagro et al., "Expression of cortisol metabolism-related genes shows circadian rhythmic patterns in human adipose tissue," *International Journal of Obesity*, vol. 33, no. 4, pp. 473–480, 2009.

Hindawi Publishing Corporation
PPAR Research
Volume 2014, Article ID 818530, 7 pages
http://dx.doi.org/10.1155/2014/818530

Review Article

New Insights into the PPARγ Agonists for the Treatment of Diabetic Nephropathy

Zhanjun Jia,[1,2,3] Ying Sun,[1,2,3] Guangrui Yang,[4] Aihua Zhang,[1,2,3] Songming Huang,[1,2,3] Kristina Marie Heiney,[5] and Yue Zhang[1,2,3]

[1] *Department of Nephrology, Nanjing Children's Hospital, Nanjing Medical University, Nanjing 210008, China*
[2] *Institute of Pediatrics, Nanjing Medical University, Nanjing, China*
[3] *Key Pediatric Laboratory of Nanjing City, Nanjing 210008, China*
[4] *Institute for Translational Medicine and Therapeutics, University of Pennsylvania, Philadelphia, PA 19104, USA*
[5] *Department of Internal Medicine, University of Utah, Salt Lake City, UT 84132, USA*

Correspondence should be addressed to Zhanjun Jia; zhanjun.jia@hsc.utah.edu and Yue Zhang; zyflora2006@hotmail.com

Received 18 November 2013; Accepted 16 December 2013; Published 29 January 2014

Academic Editor: Lihong Chen

Diabetic nephropathy (DN) is a severe complication of diabetes and serves as the leading cause of chronic renal failure. In the past decades, angiotensin-converting enzyme inhibitors (ACEIs)/angiotensin II receptor blockers (ARBs) based first-line therapy can slow but cannot stop the progression of DN, which urgently requests the innovation of therapeutic strategies. Thiazolidinediones (TZDs), the synthetic exogenous ligands of nuclear receptor peroxisome proliferator-activated receptor-γ (PPARγ), had been thought to be a promising candidate for strengthening the therapy of DN. However, the severe adverse effects including fluid retention, cardiovascular complications, and bone loss greatly limited their use in clinic. Recently, numerous novel PPARγ agonists involving the endogenous PPARγ ligands and selective PPARγ modulators (SPPARMs) are emerging as the promising candidates of the next generation of antidiabetic drugs instead of TZDs. Due to the higher selectivity of these novel PPARγ agonists on the regulation of the antidiabetes-associated genes than that of the side effect-associated genes, they present fewer adverse effects than TZDs. The present review was undertaken to address the advancements and the therapeutic potential of these newly developed PPARγ agonists in dealing with diabetic kidney disease. At the same time, the new insights into the therapeutic strategies of DN based on the PPARγ agonists were fully addressed.

1. Introduction

PPARs are nuclear receptors consisting of three PPAR isoforms of PPARα, PPARβ/δ, and PPARγ. In the past decades, a number of studies demonstrated the critical role of PPARs in the regulation of metabolic homeostasis, inflammation, cell differentiation and proliferation, fluid balance, and so on [1–3]. Among three PPARs, PPARγ was best characterized and its high-affinity ligands of TZDs were widely used in clinic for the treatment of type-2 diabetes mellitus (T2DM). PPARγ is expressed in various organs with the most abundant expression in adipose tissue. It heterodimerizes with retinoid X receptor (RXR) and then binds to PPAR responsive element (PPRE) to regulate a number of target genes. TZDs including rosiglitazone, pioglitazone, and troglitazone are synthetic exogenous PPARγ ligands with high efficacy in treating T2DM via enhancing the insulin sensitivity [3, 4]. Besides the potent role of TZDs in regulating hyperglycemia, they also effectively protect the kidneys from diabetic injury independently of its antihyperglycemia action [5–7]. Moreover, TZDs also displayed their capability of protecting the kidneys against other injuries beyond diabetes [8–11]. Although these beneficial effects of TZDs are so attractive and valuable, the severe side effects including fluid retention, cardiovascular complications, hepatotoxicity, and bone fractures greatly limited their use in clinic [12–14]. Interestingly, recent reports related to nitro-oleic acid, an endogenous PPARγ ligand, demonstrated a potent renal-protective role under diabetic and nondiabetic situations possibly via PPARγ dependent and independent mechanisms with no obvious side effects

seen in TZDs [15–20]. More importantly, numerous selective PPARγ agonists, also termed as selective PPARγ modulators (SPPARγMs), are being generated and some of them are under the clinical trials for the treatment of T2DM [12, 21]. The present review was undertaken to introduce and analyze the role of the exogenous and endogenous PPARγ agonists and the SPPARγMs in the protection of DN. Meanwhile, the therapeutic strategies via manipulating the use of various PPARγ agonists will be fully addressed.

2. Role of PPARγ in Diabetic Podocyte Injury and Proteinuria

With the profound increase of obesity, the prevalence of T2DM is rapidly rising worldwide. Among the patients with T2DM, about 10% of them developed DN [22]. In North America and Europe, DN serves as the leading cause of end-stage renal disease (ESRD). Proteinuria in DN patients is not only an established marker of DN progression, but it also plays a causative role in promoting inflammation and tubulointerstitial fibrosis. The occurrence of proteinuria in DN is due to the excessive passage of protein into the urine through the impaired glomerular filtration barrier (GFB) which is formed by endothelial cells, glomerular basement membrane (GBM), and podocytes. Accumulating evidence indicated the extreme importance of podocytopathy in diabetic glomerular damage [23]. The pathological manifestations of podocytopathy in DN include the cellular hypertrophy, foot process effacement, apoptosis, and detachment from the GBM [24, 25]. Glycemic control and pharmacological intervention using the ACEIs and/or ARBs only slow but cannot stop the DN progression. Therefore, to find more effective therapeutic strategies in countering the diabetes-associated renal injury is of vital importance and urgency.

PPARγ is located in all three types of glomerular cells with a prominent expression in podocytes [26, 27]. Several studies including a recent meta-analysis showed that Ala12 variant of PPARγ2 is significantly associated with a reduced risk of albuminuria among patients with type-2 diabetes [28]. These results highly suggested a functional role of PPARγ in glomeruli, particularly in the podocytes. In agreement with this concept, numerous reports including a meta-analysis of 15 original clinical studies involving 2860 patients convincingly demonstrated the significant efficacy of rosiglitazone or pioglitazone on diabetic proteinuria [5].

In addition to the clinical evidence mentioned above, numerous basic studies performed in diabetic animals and in vitro cells also proved the beneficial action of PPARγ in diabetic kidney disease [6, 7, 26, 27, 29]. Although the role of PPARγ in treating diabetic kidney disease was extensively investigated since PPARγ was discovered, the chief mechanism is roughly focused on the inhibition of inflammation and oxidative stress [8] with poorly understood molecular mechanisms.

A number of in vivo and in vitro studies demonstrated that PPARγ benefits all kinds of kidney cells including the glomerular mesangial cells, endothelial cells, podocytes, and tubular epithelial cells under the diabetic condition [30] with more research emphasis on the podocytes [6, 7, 27, 31, 32]. The possible podocyte-protective mechanisms shown by literatures include the reversing of G1-phase cell circle [27], blockade of stretch-induced AT1 upregulation [7], and antiapoptosis effect [31, 32]. Recently, some reports elucidated the dysfunction of mitochondria in podocytes under the hyperglycemic status [33, 34]. It is known that dysfunctional mitochondria will generate excessive reactive oxygen species (ROS) and release the proapoptotic proteins, which subsequently leads to the cell and tissue damage. Thus, we can reasonably speculate that diabetes-associated mitochondria dysfunction in kidney, especially in podocytes, may contribute to the occurrence and the progression of DN. Moreover, Zhu et al. reported that PPARγ activation remarkably improved the mitochondria dysfunction induced by aldosterone in podocytes [35]. These novel findings highly suggested that a mitochondria-protective effect may serve as an important mechanism of PPARγ in opposing the diabetic podocyte injury. However, a direct link between the PPARγ and mitochondria function in podocytes and other kidney cells under the diabetic condition does need a great deal of experimental evidence.

3. Limitations of TZDs in Treatment of DN

Although there is much evidence from clinical trials and basic studies pronounced the protective role of TZDs in DN, the severe side effects greatly restricted their use in patients. Troglitazone had to quit the market owing to the severe hepatotoxicity. Rosiglitazone has been found to be significantly associated with the increased risk of cardiovascular complications including heart failure and myocardial infarction leading to the restriction or withdrawal from the markets. As for the pioglitazone, it has been thought to have a different safety profile with no increase of cardiovascular disease as compared with other TZDs [36]. But, it still conserves the effects of bodyweight gain, bone loss, edema, and fluid retention which may increase the incidence of congestive heart failure [36]. Besides an established role of renal collecting duct PPARγ in TZDs-induced fluid retention [37, 38], PPARγ in the vasculature also played a crucial role in mediating the fluid retaining effect [39, 40]. All these findings delineated a mechanistic picture of PPARγ-mediated fluid retention and also suggested some potential targets to overcome the TZD-induced fluid volume expansion. In addition to the fluid retaining effect, TZDs also cause the cardiomyocytes hypertrophy and coronary artery lesions with elusive mechanisms [41]. In general, TZD-induced cardiomyocytes hypertrophy was thought to possibly occur through the fluid retention-dependent and fluid retention-independent mechanisms [41]. Collectively, fluid retention and the detrimental effect of TZDs on the cardiomyocytes and cardiovascular system have to be avoided or minimized in the development of novel PPARγ agonists or therapeutic strategies.

4. Strategies Based on Minimizing Adverse Effects of PPARγ Agonists

4.1. Adjustment of the Therapeutic Dose of TZDs. Evidence from studies demonstrated the dose-dependent response of TZDs in antagonizing hyperglycemia of T2DM [42, 43]. Accordingly, the side effects including fluid retention and bodyweight gain were also promoted with the dose increasing [42, 43]. Theoretically, it is possible to optimize a lower dose of TZDs with significant protection of DN without severe adverse effects seen in higher dose of TZDs. Certainly this strategy may sacrifice some glucose-lowering efficacy of TZDs. In agreement with this notion, a low dose of rosiglitazone at 1 mg/kg/day for 7 weeks in STZ diabetic rats significantly lowered the proteinuria and attenuated pathological changes in glomeruli in parallel with reduced renal oxidative stress [44]. Unfortunately, the authors in this report did not show the evidence of TZD-related side effects such as bodyweight gain, Hct change, and plasma volume status [44]. To further validate this hypothesis, the extensive animal studies and clinical trials need to be performed in the future.

4.2. Endogenous PPARγ Agonists Nitro-Oleic Acid for the Treatment of DN. Endogenous ligands for PPARγ include unsaturated and oxidized fatty acids, nitrated fatty acids, eicosanoids, and prostaglandins [45]. 15-Deoxy-delta12, 14-prostaglandin J2 (15d-PGJ2), and nitro-oleic acid are well-recognized endogenous PPARγ ligands and received attention from a number of studies [15–19, 46, 47]. Particularly, the effect of nitro-oleic acid on diabetes and diabetic kidney injury was evaluated [17, 47]. Infusion of nitro-oleic acid normalized the hyperglycemia in a type-2 diabetic model of db/db mice without affecting the bodyweight, an important indicator of fluid retention and fat accumulation [47]. A separate study from our group also found that nitro-oleic acid significantly attenuated proteinuria and metabolic syndrome in diabetic Zucker rats without affecting Hct, a widely used index of fluid retention in TZD models [19]. Most recently, our group gave evidence that nitro-oleic acid in combination with losartan, one of the ARBs, significantly ameliorated proteinuria and podocyte injury in diabetic db/db mice possibly via suppressing oxidative stress and inflammation [17]. In contrast, losartan alone failed to display the therapeutic efficacy during two weeks of treatment. All these results highly suggested that endogenous PPARγ agonists may play a similar role as TZDs in protecting DN with no significant side effects shown by TZDs. Although nitro-oleic acid definitely activates PPARγ [47], the detailed mechanism related to the beneficial role of nitro-oleic acid in opposing the diabetic kidney injury remains uncertain due to its nonselective activation of PPAR [48]. Furthermore, additional animal studies and clinical trials are needed to fully evaluate the safety and efficacy of nitro-oleic acid in treating DN, as well as hyperglycemia.

4.3. Selective PPARγ Modulators for the Treatment of DN. TZDs, as full PPARγ agonists, nonselectively regulate the expressions of antidiabetic efficacy-associated and adverse effect-associated genes in similar proportion [49], which leads to the overlap of dose response curves for therapeutic effect and side effect. Therefore, selective PPARγ modulators (SPPARγMs) are being actively pursued as the second generation of PPARγ agonists. Presumably, SPPARγMs preserve greater capability in the regulation of antidiabetic genes than that of adverse-effect-associated genes, which could effectively limit the side effects seen in TZDs, particularly the fluid retention. By now, numerous synthetic SPPARγMs have been generated [21]. Among them, balaglitazone is the prominent one and is currently under the phase III clinical trials in the United States and Europe [50]. Data from the clinical trials showed a robust antidiabetic effect of balaglitazone with less incidence of fluid retention and fat accumulation [50]. The preclinical data of this drug also indicated less fluid retention, less heart hypertrophy, and no signs of bone loss [50]. Besides balaglitazone, INT131 also reached human trials. Data from animals showed no significant fluid retention, bodyweight gain, cardiac hypertrophy, and bone loss with similar glucose-lowering effect as TZDs [49]. Human studies also showed that INT131 at doses from 0.5 to 3 mg per day effectively lowered blood glucose in patients with type-2 diabetes without causing edema [49]. Although these SPPARγMs convincingly demonstrated the antihyperglycemia effect with fewer side effects, their efficacy in treating DN is still unclear. We believe, with better recognition on the importance of SPPARγMs and the research progression of this field, this question will be answered soon.

5. Strategies Based on Increasing the Efficacy of PPARγ Agonists

5.1. Combination of RAS Blockers with PPARγ Agonists. RAS blockers including ACEIs and ARBs served as the cornerstone therapy of DN in the past decades. Although their efficacy in reducing the proteinuria and retarding the DN progression was established, a large number of DN patients with the therapy of RAS blockade and glycemic control still stepped onto the stage of renal failure. This situation raised a serious request for more effective therapies of DN. Due to the established role of PPARγ in protecting DN, TZDs partnering with ACEI and/or ARB served to be a better option for the nephrologists. However, the unacceptable side effects of TZDs unfortunately interrupted such an ideal marriage. Even so, we still believe that with the discovery and the clinical application of novel PPARγ agonists including endogenous PPARγ agonists and SPPARγMs, this marriage between RAS blocker and PPARγ agonist will be rebuilt in the near future. Currently, an exciting example is telmisartan with dual properties of AT1 blocker and selective PPARγ modulator [51, 52]. But, it still needs the evidence from clinical trials and basic studies to certify that telmisartan could play a better role than a specific AT1 blocker alone for the treatment of DN. Moreover, a combination of low dose TZDs with RAS blockers is also worth consideration.

5.2. Dual Activation of PPARγ and PPARα. PPARα is distributed in several tissues including the kidney and its agonists had shown the pivotal roles in regulating lipid metabolism, inflammation, and cardiovascular response [53]. Recent reports demonstrated that PPARα agonists such as fenofibrate can effectively protect DN via reducing renal lipotoxicity and inhibiting renal inflammation and oxidative stress [54]. These findings highly suggested that PPARα may serve as a new therapeutic target of DN. In addition, dual activation of PPARα and PPARγ may be a novel strategy against DN. In line with this concept, an animal study using combined low dose PPARα agonist fenofibrate and low dose PPARγ agonist rosiglitazone more remarkably attenuated the diabetic kidney injury than drug alone [44]. Moreover, the dual PPARα/γ agonist tesaglitazar markedly ameliorated the diabetic renal injury in db/db mice [55] and obese Zucker rats [56]. Based on this notion and some research findings, we can conceive that a combination of PPARα agonist with novel PPARγ agonists or low dose of TZDs could be a suitable strategy for the treatment of DN.

5.3. Blockade of COX-2/PGE2/EP Pathway Partnering with PPARγ Agonists. COX-2 was induced in the podocytes under the diabetic status [57]. Inhibition of COX-2 or interruption of PGE2 receptors EP1/EP4 significantly attenuated diabetic kidney injury [58–61]. Under some nondiabetic conditions, such as the chronic kidney disease model of 5/6 nephrectomy and acute kidney injury model of adriamycin nephropathy, COX-2/PGE2/EP4 pathway also played a detrimental role in podocytes [62]. These results highly suggested a new therapeutic target of COX-2/PGE2/EP pathway in treating DN. Unfortunately, the increased cardiovascular mortality and morbidity and the fluid retaining effect of the COX inhibitors limited their long-term application in clinic [63]. In theory, blockade of COX-2/PGE2/EP pathway in combination with PPARγ agonists will cause greater extracellular fluid volume expansion and more severe cardiovascular complications. However, low dose aspirin has been used for long-term primary or secondary prevention of vascular disease in clinic and the safety has been well evaluated. Although there is no convincing evidence showing the efficacy of low dose COX inhibitors in the therapy of DN, the combination of a lower dose COX inhibitor with SPPARγM or endogenous PPARγ agonist could be a feasible strategy in treating DN. Moreover, it is also worthwhile to investigate whether a low dose of COX inhibitor will strengthen the effect of RAS inhibitors in protecting the diabetic kidney. By reviewing the literatures, we did not find any clinical or animal reports demonstrating this notion.

mPGES-1 is one of three characterized prostaglandin E synthases (mPGES-1, mPGES-2, and cPGES). In the past decade, only mPGES-1 was evidenced as a functional PGE2 synthase in vivo and played important roles under various physiological and pathological conditions [64–71]. Evidence from mPGES-2 and cPGES KO mice strongly argued against their property of PGE2 synthesis [72, 73]. mPGES-1 mediated the injury in some kidney injury models [71, 74]. For example, in a 5/6 nephrectomy mouse model, mPGES-1 deletion significantly reduced proteinuria and attenuated glomerular injury and podocyte damage possibly through the inhibition of inflammation and oxidative stress [71]. However, in a STZ diabetic mouse model, renal mPGES-1 was not regulated by hyperglycemia and deletion of mPGES-1 did not affect renal PGE2 production and glomerular injury. This largely excluded the involvement of mPGES-1 in mediating the renal PGE2 induction and kidney injury in type-1 diabetes, at least in mouse (unpublished data). Oppositely, in a type-2 diabetic model of db/db mouse, mPGES-1 was remarkably elevated in the glomeruli [75]. This discrepancy of mPGES-1 regulation may reflect the difference of the pathogenic mechanism and disease status of DN between the type-1 and type-2 diabetes. More interestingly, one-week rosiglitazone treatment abolished mPGES-1 induction in glomeruli without affecting COX-2 expression in these db/db mice. This result suggested that inhibition of COX-2 in combination with PPARγ agonist may provide additional protection from diabetic kidney disease. In addition, it is also expected that antagonism of specific PGE2 receptors partnering with a selective PPARγ agonist could achieve better outcome in DN treatment than PPARγ agonist alone. However, none of the mPGES-1 inhibitors or EP antagonists is available in clinic now. The investigations in animals or in vitro cells may be the current emphasis to validate the present hypothesis.

6. Perspectives

Except for the known side effects, TZDs have been so fantastic for the treatment of T2DM and diabetic kidney disease. We believe that the withdrawal or restriction of TZDs owing to their severe side effects only temporarily fades the light of PPARγ in treating human diseases. With the development of novel PPARγ agonists with minimal side effects, the PPARγ will gain the researcher's focus again. Actually, PPARγ activation not only ameliorates diabetic kidney disease, but it also protects kidneys from a variety of other acute and chronic insults. In the past decades, only RAS blockers stand on the first line in fighting against chronic kidney diseases (CKDs). With the generation and application of novel PPARγ agonists in the near future, we can conceive that the therapeutic outcome of DN and other CKDs will be significantly advanced.

Conflict of Interests

The authors declare that there is no conflict of interests regarding the publication of this paper.

Acknowledgment

This work was supported by Grants from National Natural Science Foundation of China (nos. 81370802, 81300591, and 81070511).

References

[1] R. M. Evans, G. D. Barish, and Y.-X. Wang, "PPARs and the complex journey to obesity," *Nature Medicine*, vol. 10, no. 4, pp. 355–361, 2004.

[2] G. D. Barish, V. A. Narkar, and R. M. Evans, "PPARδ: a dagger in the heart of the metabolic syndrome," *The Journal of Clinical Investigation*, vol. 116, no. 3, pp. 590–597, 2006.

[3] L. Poulsen, M. Siersbæk, and S. Mandrup, "PPARs: fatty acid sensors controlling metabolism," *Seminars in Cell & Developmental Biology*, vol. 23, no. 6, pp. 631–639, 2012.

[4] P. Tontonoz and B. M. Spiegelman, "Fat and beyond: the diverse biology of PPARγ," *Annual Review of Biochemistry*, vol. 77, pp. 289–312, 2008.

[5] P. A. Sarafidis, P. C. Stafylas, P. I. Georgianos, A. N. Saratzis, and A. N. Lasaridis, "Effect of thiazolidinediones on albuminuria and proteinuria in diabetes: a meta-analysis," *American Journal of Kidney Diseases*, vol. 55, no. 5, pp. 835–847, 2010.

[6] H.-C. Yang, L.-J. Ma, J. Ma, and A. B. Fogo, "Peroxisome proliferator-activated receptor-gamma agonist is protective in podocyte injury-associated sclerosis," *Kidney International*, vol. 69, no. 10, pp. 1756–1764, 2006.

[7] I. Miceli, D. Burt, E. Tarabra, G. Camussi, P. C. Perin, and G. Gruden, "Stretch reduces nephrin expression via an angiotensin II-AT_1-dependent mechanism in human podocytes: effect of rosiglitazone," *American Journal of Physiology*, vol. 298, no. 2, pp. F381–F390, 2010.

[8] J. Yang, Y. Zhou, and Y. Guan, "PPARγ as a therapeutic target in diabetic nephropathy and other renal diseases," *Current Opinion in Nephrology and Hypertension*, vol. 21, no. 1, pp. 97–105, 2012.

[9] J. Lepenies, M. Hewison, P. M. Stewart, and M. Quinkler, "Renal PPARγ mRNA expression increases with impairment of renal function in patients with chronic kidney disease," *Nephrology*, vol. 15, no. 7, pp. 683–691, 2010.

[10] A. Sugawara, A. Uruno, M. Kudo, K. Matsuda, C. W. Yang, and S. Ito, "Effects of PPARγ on hypertension, atherosclerosis, and chronic kidney disease," *Endocrine Journal*, vol. 57, no. 10, pp. 847–852, 2010.

[11] A. B. Fogo, "PPARγ and chronic kidney disease," *Pediatric Nephrology*, vol. 26, no. 3, pp. 347–351, 2011.

[12] M. Ahmadian, J. M. Suh, N. Hah et al., "PPARγ signaling and metabolism: the good, the bad and the future," *Nature Medicine*, vol. 99, no. 5, pp. 557–566, 2013.

[13] J. Kung and R. R. Henry, "Thiazolidinedione safety," *Expert Opinion on Drug Safety*, vol. 11, no. 4, pp. 565–579, 2012.

[14] S. E. Nissen and K. Wolski, "Effect of rosiglitazone on the risk of myocardial infarction and death from cardiovascular causes," *The New England Journal of Medicine*, vol. 356, no. 24, pp. 2457–2471, 2007.

[15] J. Zhang, L. Villacorta, L. Chang et al., "Nitro-oleic acid inhibits angiotensin II-induced hypertension," *Circulation Research*, vol. 107, no. 4, pp. 540–548, 2010.

[16] H. Wang, H. Liu, Z. Jia et al., "Nitro-oleic acid protects against endotoxin-induced endotoxemia and multiorgan injury in mice," *American Journal of Physiology*, vol. 298, no. 3, pp. F754–F762, 2010.

[17] Y. Liu, Z. Jia, S. Liu et al., "Combined losartan and nitro-oleic acid remarkably improves diabetic nephropathy in mice," *American Journal of Physiology*, vol. 305, no. 11, pp. F1555–F1562, 2013.

[18] H. Liu, Z. Jia, S. Soodvilai et al., "Nitro-oleic acid protects the mouse kidney from ischemia and reperfusion injury," *American Journal of Physiology*, vol. 295, no. 4, pp. F942–F949, 2008.

[19] H. Wang, H. Liu, Z. Jia, G. Guan, and T. Yang, "Effects of endogenous PPAR agonist nitro-oleic acid on metabolic syndrome in obese zucker rats," *PPAR Research*, vol. 2010, Article ID 601562, 7 pages, 2010.

[20] E. Kansanen, H.-K. Jyrkkänen, O. L. Volger et al., "Nrf2-dependent and -independent responses to nitro-fatty acids in human endothelial cells: identification of heat shock response as the major pathway activated by nitro-oleic acid," *The Journal of Biological Chemistry*, vol. 284, no. 48, pp. 33233–33241, 2009.

[21] L. S. Doshi, M. K. Brahma, U. A. Bahirat, A. V. Dixit, and K. V. S. Nemmani, "Discovery and development of selective PPARγ modulators as safe and effective antidiabetic agents," *Expert Opinion on Investigational Drugs*, vol. 19, no. 4, pp. 489–512, 2010.

[22] C. Centers for Disease, Prevention, "Incidence of end-stage renal disease among persons with diabetes—United States, 1990–2002," *Morbidity and Mortality Weekly Report*, vol. 54, no. 43, pp. 1097–1100, 2005.

[23] E. J. Weil, K. V. Lemley, C. C. Mason et al., "Podocyte detachment and reduced glomerular capillary endothelial fenestration promote kidney disease in type 2 diabetic nephropathy," *Kidney International*, vol. 82, pp. 1010–1017, 2012.

[24] K. Susztak, A. C. Raff, M. Schiffer, and E. P. Böttinger, "Glucose-induced reactive oxygen species cause apoptosis of podocytes and podocyte depletion at the onset of diabetic nephropathy," *Diabetes*, vol. 55, no. 1, pp. 225–233, 2006.

[25] A. Diez-Sampedro, O. Lenz, and A. Fornoni, "Podocytopathy in diabetes: a metabolic and endocrine disorder," *American Journal of Kidney Diseases*, vol. 58, no. 4, pp. 637–646, 2011.

[26] Y. Guan and M. D. Breyer, "Peroxisome proliferator-activated receptors (PPARs): novel therapeutic targets in renal disease," *Kidney International*, vol. 60, no. 1, pp. 14–30, 2001.

[27] T. Okada, J. Wada, K. Hida et al., "Thiazolidinediones ameliorate diabetic nephropathy via cell cycle-dependent mechanisms," *Diabetes*, vol. 55, no. 6, pp. 1666–1677, 2006.

[28] S. de Cosmo, S. Prudente, O. Lamacchia et al., "PPARγ2 P12A polymorphism and albuminuria in patients with type 2 diabetes: a meta-analysis of case-control studies," *Nephrology Dialysis Transplantation*, vol. 26, no. 12, pp. 4011–4016, 2011.

[29] Y. J. Liang, J. H. Jian, C. Y. Chen, C. Y. Hsu, C. Y. Shih, and J. G. Leu, "L-165,041, troglitazone and their combination treatment to attenuate high glucose-induced receptor for advanced glycation end products (RAGE) expression," *European Journal of Pharmacology*, vol. 715, no. 1–3, pp. 33–38, 2013.

[30] Y. Qian, E. Feldman, S. Pennathur, M. Kretzler, and F. C. Brosius, "From fibrosis to sclerosis: mechanisms of glomerulosclerosis in diabetic nephropathy," *Diabetes*, vol. 57, no. 6, pp. 1439–1445, 2008.

[31] T. Kanjanabuch, L.-J. Ma, J. Chen et al., "PPAR-γ agonist protects podocytes from injury," *Kidney International*, vol. 71, no. 12, pp. 1232–1239, 2007.

[32] G. Miglio, A. C. Rosa, L. Rattazzi et al., "The subtypes of peroxisome proliferator-activated receptors expressed by human podocytes and their role in decreasing podocyte injury," *British Journal of Pharmacology*, vol. 162, no. 1, pp. 111–125, 2011.

[33] W. Wang, Y. Wang, J. Long et al., "Mitochondrial fission triggered by hyperglycemia is mediated by ROCK1 activation in podocytes and endothelial cells," *Cell Metabolism*, vol. 15, no. 2, pp. 186–200, 2012.

[34] N. Stieger, K. Worthmann, B. Teng et al., "Impact of high glucose and transforming growth factor-β on bioenergetic profiles in podocytes," *Metabolism*, vol. 61, no. 8, pp. 1073–1086, 2012.

[35] C. Zhu, S. Huang, Y. Yuan et al., "Mitochondrial dysfunction mediates aldosterone-induced podocyte damage: a therapeutic target of PPARγ," *The American Journal of Pathology*, vol. 178, no. 5, pp. 2020–2031, 2011.

[36] P. Shah and S. Mudaliar, "Pioglitazone: side effect and safety profile," *Expert Opinion on Drug Safety*, vol. 9, no. 2, pp. 347–354, 2010.

[37] H. Zhang, A. Zhang, D. E. Kohan, R. D. Nelson, F. J. Gonzalez, and T. Yang, "Collecting duct-specific deletion of peroxisome proliferator-activated receptor γ blocks thiazolidinedione-induced fluid retention," *Proceedings of the National Academy of Sciences of the United States of America*, vol. 102, no. 26, pp. 9406–9411, 2005.

[38] Y. Guan, C. Hao, D. R. Cha et al., "Thiazolidinediones expand body fluid volume through PPARγ stimulation of ENaC-mediated renal salt absorption," *Nature Medicine*, vol. 11, no. 8, pp. 861–866, 2005.

[39] K. B. Sotiropoulos, A. Clermont, Y. Yasuda et al., "Adipose-specific effect of rosiglitazone on vascular permeability and protein kinase C activation: novel mechanism for PPARγ agonist's effects on edema and weight gain," *The FASEB Journal*, vol. 20, no. 8, pp. 1203–1205, 2006.

[40] T. Yang and S. Soodvilai, "Renal and vascular mechanisms of thiazolidinedione-induced fluid retention," *PPAR Research*, vol. 2008, Article ID 943614, 8 pages, 2008.

[41] E. Robinson and D. J. Grieve, "Significance of peroxisome proliferator-activated receptors in the cardiovascular system in health and disease," *Pharmacology & Therapeutics*, vol. 122, no. 3, pp. 246–263, 2009.

[42] S. Aronoff, S. Rosenblatt, S. Braithwaite, J. W. Egan, A. L. Mathisen, and R. L. Schneider, "Pioglitazone hydrochloride monotherapy improves glycemic control in the treatment of patients with type 2 diabetes: a 6-month randomized placebo-controlled dose-response study," *Diabetes Care*, vol. 23, no. 11, pp. 1605–1611, 2000.

[43] J. J. Nolan, N. P. Jones, R. Patwardhan, and L. F. Deacon, "Rosiglitazone taken once daily provides effective glycaemic control in patients with type 2 diabetes mellitus," *Diabetic Medicine*, vol. 17, no. 4, pp. 287–294, 2000.

[44] M. K. Arora, K. Reddy, and P. Balakumar, "The low dose combination of fenofibrate and rosiglitazone halts the progression of diabetes-induced experimental nephropathy," *European Journal of Pharmacology*, vol. 636, no. 1–3, pp. 137–144, 2010.

[45] B. Cariou, B. Charbonnel, and B. Staels, "Thiazolidinediones and PPARγ agonists: time for a reassessment," *Trends in Endocrinology & Metabolism*, vol. 23, no. 5, pp. 205–215, 2012.

[46] S. Ueki, H. Kato, Y. Kobayashi et al., "Anti- and proinflammatory effects of 15-deoxy-$\Delta^{12,14}$-prostaglandin J_2(15d-PGJ_2) on human eosinophil functions," *International Archives of Allergy and Immunology*, vol. 143, supplement 1, pp. 15–22, 2007.

[47] F. J. Schopfer, M. P. Cole, A. L. Groeger et al., "Covalent peroxisome proliferator-activated receptor γ adduction by nitro-fatty acids: selective ligand activity and anti-diabetic signaling actions," *The Journal of Biological Chemistry*, vol. 285, no. 16, pp. 12321–12333, 2010.

[48] M. C. Menon, P. Y. Chuang, and J. C. He, "Nitro-oleic acid is a novel anti-oxidative therapy for diabetic kidney disease," *American Journal of Physiology*, vol. 305, pp. F1542–F1543, 2013.

[49] T. Yew, S.-A. Toh, and J. S. Millar, "Selective peroxisome proliferator-activated receptor-γ modulation to reduce cardiovascular risk in patients with insulin resistance," *Recent Patents on Cardiovascular Drug Discovery*, vol. 7, no. 1, pp. 33–41, 2012.

[50] R. Agrawal, P. Jain, and S. N. Dikshit, "Balaglitazone: a second generation peroxisome proliferator-activated receptor (PPAR) gamma (γ) agonist," *Mini-Reviews in Medicinal Chemistry*, vol. 12, no. 2, pp. 87–97, 2012.

[51] Y. Lamotte, P. Martres, N. Faucher et al., "Synthesis and biological activities of novel indole derivatives as potent and selective PPARγ modulators," *Bioorganic & Medicinal Chemistry Letters*, vol. 20, no. 4, pp. 1399–1404, 2010.

[52] J. F. Dropinski, T. Akiyama, M. Einstein et al., "Synthesis and biological activities of novel aryl indole-2-carboxylic acid analogs as PPARγ partial agonists," *Bioorganic & Medicinal Chemistry Letters*, vol. 15, no. 22, pp. 5035–5038, 2005.

[53] A. Shah, D. J. Rader, and J. S. Millar, "The effect of PPAR-α agonism on apolipoprotein metabolism in humans," *Atherosclerosis*, vol. 210, no. 1, pp. 35–40, 2010.

[54] P. Balakumar, S. Kadian, and N. Mahadevan, "Are PPAR alpha agonists a rational therapeutic strategy for preventing abnormalities of the diabetic kidney?" *Pharmacological Research*, vol. 65, no. 4, pp. 430–436, 2012.

[55] D. R. Cha, X. Zhang, Y. Zhang et al., "Peroxisome proliferator-activated receptor α/γ dual agonist tesaglitazar attenuates diabetic nephropathy in db/db mice," *Diabetes*, vol. 56, no. 8, pp. 2036–2045, 2007.

[56] J. Liao, Z. Soltani, P. Ebenezer et al., "Tesaglitazar, a dual peroxisome proliferator- activated receptor agonist (PPARα/γ), improves metabolic abnormalities and reduces renal injury in obese zucker rats," *Nephron*, vol. 114, no. 2, pp. e61–e68, 2010.

[57] E. Stitt-Cavanagh, L. MacLeod, and C. Kennedy, "The podocyte in diabetic kidney disease," *The Scientific World Journal*, vol. 9, pp. 1127–1139, 2009.

[58] H.-F. Cheng, C. J. Wang, G. W. Moeckel, M.-Z. Zhang, J. A. McKanna, and R. C. Harris, "Cyclooxygenase-2 inhibitor blocks expression of mediators of renal injury in a model of diabetes and hypertension," *Kidney International*, vol. 62, no. 3, pp. 929–939, 2002.

[59] H. Makino, I. Tanaka, M. Mukoyama et al., "Prevention of diabetic nephropathy in rats by prostaglandin E receptor EP1-selective antagonist," *Journal of the American Society of Nephrology*, vol. 13, no. 7, pp. 1757–1765, 2002.

[60] R. Mohamed, C. Jayakumar, and G. Ramesh, "Chronic administration of EP4-selective agonist exacerbates albuminuria and fibrosis of the kidney in streptozotocin-induced diabetic mice through IL-6," *Laboratory Investigation*, vol. 93, pp. 933–945, 2013.

[61] H. Cheng, X. Fan, G. W. Moeckel, and R. C. Harris, "Podocyte COX-2 exacerbates diabetic nephropathy by increasing podocyte (pro)renin receptor expression," *Journal of the American Society of Nephrology*, vol. 22, no. 7, pp. 1240–1251, 2011.

[62] E. M. Stitt-Cavanagh, W. H. Faour, K. Takami et al., "A maladaptive role for EP4 receptors in podocytes," *Journal of the American Society of Nephrology*, vol. 21, no. 10, pp. 1678–1690, 2010.

[63] A. Rios, H. Vargas-Robles, A. M. Gámez-Méndez, and B. Escalante, "Cyclooxygenase-2 and kidney failure," *Prostaglandins & Other Lipid Mediators*, vol. 98, no. 3-4, pp. 86–90, 2011.

[64] Z. Jia, G. Liu, Y. Sun et al., "mPGES-1-derived PGE_2 mediates dehydration natriuresis," *American Journal of Physiology*, vol. 304, no. 2, pp. F214–F221, 2013.

[65] Z. Jia, G. Liu, M. Downton, Z. Dong, A. Zhang, and T. Yang, "mPGES-1 deletion potentiates urine concentrating capability after water deprivation," *American Journal of Physiology*, vol. 302, no. 8, pp. F1005–F1012, 2012.

[66] Z. Jia, T. Aoyagi, D. E. Kohan, and T. Yang, "mPGES-1 deletion impairs aldosterone escape and enhances sodium appetite," *American Journal of Physiology*, vol. 299, no. 1, pp. F155–F166, 2010.

[67] Z. Jia, T. Aoyagi, and T. Yang, "mPGES-1 protects against DOCA-salt hypertension via inhibition of oxidative stress or stimulation of NO/cGMP," *Hypertension*, vol. 55, no. 2, pp. 539–546, 2010.

[68] Z. Jia, H. Wang, and T. Yang, "Mice lacking mPGES-1 are resistant to lithium-induced polyuria," *American Journal of Physiology*, vol. 297, no. 6, pp. F1689–F1696, 2009.

[69] S. Soodvilai, Z. Jia, M.-H. Wang, Z. Dong, and T. Yang, "mPGES-1 deletion impairs diuretic response to acute water loading," *American Journal of Physiology*, vol. 296, no. 5, pp. F1129–F1135, 2009.

[70] S. Soodvilai, Z. Jia, and T. Yang, "Hydrogen peroxide stimulates chloride secretion in primary inner medullary collecting duct cells via mPGES-1-derived PGE_2," *American Journal of Physiology*, vol. 293, no. 5, pp. F1571–F1576, 2007.

[71] Z. Jia, H. Wang, and T. Yang, "Microsomal prostaglandin e synthase 1 deletion retards renal disease progression but exacerbates anemia in mice with renal mass reduction," *Hypertension*, vol. 59, no. 1, pp. 122–128, 2012.

[72] L. A. Jania, S. Chandrasekharan, M. G. Backlund et al., "Microsomal prostaglandin E synthase-2 is not essential for *in vivo* prostaglandin E_2 biosynthesis," *Prostaglandins & Other Lipid Mediators*, vol. 88, no. 3-4, pp. 73–81, 2009.

[73] A. K. Lovgren, M. Kovarova, and B. H. Koller, "cPGES/p23 is required for glucocorticoid receptor function and embryonic growth but not prostaglandin E_2 synthesis," *Molecular and Cellular Biology*, vol. 27, no. 12, pp. 4416–4430, 2007.

[74] Z. Jia, N. Wang, T. Aoyagi, H. Wang, H. Liu, and T. Yang, "Amelioration of cisplatin nephrotoxicity by genetic or pharmacologic blockade of prostaglandin synthesis," *Kidney International*, vol. 79, no. 1, pp. 77–88, 2011.

[75] Y. Sun, Z. Jia, G. Liu et al., "PPARγ agonist rosiglitazone suppresses renal mPGES-1/PGE2 pathway in db/db mice," *PPAR Research*, vol. 2013, Article ID 612971, 9 pages, 2013.

Hindawi Publishing Corporation
PPAR Research
Volume 2014, Article ID 124583, 10 pages
http://dx.doi.org/10.1155/2014/124583

Research Article

The Proatherogenic Effect of Chronic Nitric Oxide Synthesis Inhibition in ApoE-Null Mice Is Dependent on the Presence of PPARα

Michal Vechoropoulos, Maya Ish-Shalom, Sigal Shaklai, Jessica Sack, Naftali Stern, and Karen M. Tordjman

The Institute of Endocrinology, Metabolism, and Hypertension, Tel Aviv-Sourasky Medical Center, The Sackler Faculty of Medicine, Tel Aviv University, 6 Weizmann Street, 64239 Tel Aviv, Israel

Correspondence should be addressed to Karen M. Tordjman; karent@tlvmc.gov.il

Received 24 August 2013; Revised 14 October 2013; Accepted 18 October 2013; Published 22 January 2014

Academic Editor: Lihong Chen

Inhibition of endothelial nitric oxide synthase (eNOS) accelerates atherosclerosis in ApoE-null mice by impairing the balance between angiotensin II (AII) and NO. Our previous data suggested a role for PPARα in the deleterious effect of the renin-angiotensin system (RAS). We tested the hypothesis that ApoE-null mice lacking PPARα (DKO mice) would be resistant to the proatherogenic effect of NOS inhibition. DKO mice fed a Western diet were immune to the 23% worsening in aortic sinus plaque area seen in the ApoE-null animals under 12 weeks of NOS inhibition with a subpressor dose of L-NAME, $P = 0.002$. This was accompanied by a doubling of reactive oxygen species (ROS-) generating aortic NADPH oxidase activity (a target of AII, which paralleled Nox1 expression) and by a 10-fold excess of the proatherogenic iNOS, $P < 0.01$. L-NAME also caused a doubling of aortic renin and angiotensinogen mRNA level in the ApoE-null mice but not in the DKO, and it upregulated eNOS in the DKO mice only. These data suggest that, in the ApoE-null mouse, PPARα contributes to the proatherogenic effect of unopposed RAS/AII action induced by L-NAME, an effect which is associated with Nox1 and iNOS induction, and is independent of blood pressure and serum lipids.

1. Introduction

Expressed in all the cellular components of the vascular wall, and present in the atherosclerotic plaque, the precise role of the peroxisome proliferator-activated receptor alpha (PPARα) in atherogenesis is still controversial. Its known effect on lipoprotein metabolism, and mostly surrogate endpoints derived from animal studies, helped shape the view that its activation confers protection against atherosclerosis (for review [1]). Large clinical trials designed to assess the potential of fibrates to reduce the rate of cardiovascular endpoints have, however, reached mixed results, suggesting that benefit may be restricted to subsets of subjects with defined lipoprotein abnormalities [2–4]. We previously reported that ApoE-null mice lacking PPARα were resistant to diet-induced atherosclerosis, despite exhibiting the worsened lipid profile expected from the absence of PPARα. In addition, the double knockout mice had also a somewhat lower blood pressure [5]. Although by itself this reduction could not explain the protection from atherosclerosis, it suggested that PPARα could affect a system central to both atherogenesis and blood pressure regulation. In this respect, a natural candidate is the renin-angiotensin system (RAS). We subsequently showed that ablation of PPARα totally abolished hypertension and greatly reduced diet-induced atherosclerosis in the Tsukuba hypertensive mouse, a model of angiotensin II (AII-) mediated hypertension and atherosclerosis due to the transgenic expression of the human renin and angiotensinogen genes. In this model, absence of PPARα markedly reduced the level of circulating kidney-derived human renin (the rate-limiting step of the RAS), and also that of human renin secreted in the medium by aortic smooth muscle cell primary cultures established form these mice, suggesting that some of the vascular protection could stem from downregulation of the tissue RAS in the vessel wall [6].

A delicate balance between AII and nitric oxide (NO) in vascular health has been well recognized [7]. AII elevates

blood pressure, reduces the generation of NO, increases the production of reactive oxygen species (ROS) mostly through nicotinamide adenine dinucleotide phosphate (NADPH) oxidase, and thus promotes inflammation and atherosclerosis. In contrast, endothelium-derived NO lowers blood pressure, reduces the accumulation of ROS, suppresses inflammation, and ultimately limits atherosclerosis. Thus any event that might downplay the NO side of this balance incurs the potential of promoting atherosclerosis. Indeed, it has been demonstrated that genetic or pharmacologic ablation of NO synthase (NOS) accelerates atherosclerosis in the ApoE-null mouse [8, 9].

We hypothesized that as PPARα appears to be required for the full deleterious effect of the RAS, the double ApoE/PPARα knockout (DKO) mouse should be resistant to the worsening of atherosclerosis induced by chronic inhibition of endothelial NOS (eNOS) activity by a subpressor dose of N_ω-nitro-L-arginine methyl ester hydrochloride (L-NAME). In the current report we show this to be the case, and we also point at two main culprits in the PPARα-dependent proatherogenic effect of eNOS inhibition, namely, Nox1 and iNOS.

2. Methods

2.1. Animals and Study Design. ApoE-null mice maintained at the Tel Aviv-Sourasky Medical Center animal facility were crossbred with PPARα-null mice; both lines were on the C57Bl/6 genetic background following extensive backcrossing. Identified by genotyping (http://jaxmice.jax.org/pub-gi/protocols/protocols.sh?objtype=protocol&protocol_id=221), F2 doubly transgenic founders were then used to create the DKO line. In these experiments ApoE-null and DKO mice were used under the same protocol.

At the age of 4 weeks, half the animals were given a subpressor dose of L-NAME (5 mg/L), an inhibitor of NOS, in the drinking water (Sigma-Aldrich Cat number N5751). This dose was based on that given to rats, which was shown to be devoid of pressor effects, while it still reduced both plasma and urinary NO production [10, 11]. There were thus 4 experimental groups, each comprising approximately 20 mice. At the age of 8 weeks, noninvasive basal blood pressure was obtained as described [12], and animals were switched to a high fat Western diet (Teklad diet 88317, Harlan, Madison, WI) for 8 weeks. L-NAME administration was continued throughout the experiment.

At the end of the experiment, blood pressure was recorded again. After a 4 h fast, under light isoflurane anesthesia, blood samples were obtained from the retro-orbital plexus for biochemical determinations. Animals were sacrificed with a lethal dose of isoflurane. All experimental protocols were carried out after obtaining the authorization of the institutional committee for experiments in laboratory animals and conformed to the NIH Guide for the Care and Use of Laboratory Animals [13].

2.2. Biochemical Determinations and Fast Protein Liquid Chromatography (FPLC) Analysis of Lipoproteins. Serum biochemistry was assessed on an Advia 1650 autoanalyzer (Siemens AG, Germany). In addition, the various lipoprotein fractions were also analyzed by FPLC. For this procedure 4 samples from each animal group, each sample representing pooled plasma from 2 mice and diluted 1 : 1 v/v in buffer, were first filtered through a 0.45 μ filter to remove chylomicrons. Samples were loaded on a superpose-6 column (GE Pharmacia) and separated by size exclusion into 41 fractions. VLDL particles were typically collected between tubes 15–19, LDL between tubes 21–27, and HDL between tubes 29–37. Following separation, the cholesterol concentration of each fraction was determined in a colorimetric reaction (cholesterol reagent, Roche) on a microplate and read on an ELISA reader (Cobas, Roche) at 495 nm.

2.3. Heart and Aorta Processing and Atherosclerosis Analysis. The aortas were snap-frozen for RNA isolation and for NADPH oxidase activity determination. The hearts were sectioned through the ventricles; the upper third including the aortic root was embedded in OCT and frozen until analysis.

For assessment of atherosclerosis, 10 μm cryostat sections of the hearts encompassing the area of the aortic sinus were collected and stained with Oil-Red-O. Quantification of the plaques was performed using a digital imaging processing program (NIS element Br 3.0 imaging system) (Nikon Instruments Europe B.V., The Netherlands), as described [12].

2.4. NADPH Oxidase Activity Assessment. NADPH oxidase activity was measured in aortas in an in-house lucigenin-enhanced chemoluminescent assay as follows. Aortas were thoroughly cleaned from adjacent fat and connective tissue, isolated in ice-cold Krebs-Hepes buffer, pH 7.4, and snap-frozen in liquid N_2 until assayed at which time they were thawed in ice-cold KHB and kept on ice. Under binocular magnification, aortas were meticulously cleaned from all adjacent tissues and cut into 3–5 mm rings. They were subsequently incubated at 37°C for 45 min in prewarmed KHB. Each ring was then placed in an optical plate well in 175 μL of KHB containing freshly made NADPH (Sigma-Aldrich Cat. number N6505) to yield a final reaction concentration of 100 μM. The reaction started after the automatic injection of 25 μL of lucigenin (Sigma-Aldrich Cat number M8010) to give a final concentration of 5 μM. Luminescence was measured every 5 seconds for 1 minute on a LUMIstar Galaxy luminometer (BMG Labtech, Offenburg, Germany). After the subtraction of background (recorded in the absence of tissue), the average luminescence for each sample was adjusted for the dried weight of the ring, and the mean NADPH oxidase activity of each aorta (6–8 rings) was expressed as relative luminescence units$\cdot mg^{-1}\cdot min^{-1}$. Under the experimental conditions, the luminescence was specific for NADPH oxidase as the fluorescence in the absence of added substrate (NADPH) was negligible.

2.5. Aortic Gene Expression Studies. After RNA isolation (TRIzol, Invitrogen, Life Technology, Carlsbad, CA) and reverse transcriptase synthesis of cDNA, the level of

Table 1: Animals weights and systolic blood pressure at baseline and following treatment and biochemical measurements at the end of the study. The number of mice in each subgroup is shown in parentheses.

Parameter	ApoE-null males $n = 26$	ApoE-null females $n = 23$	DKO males $n = 25$	DKO females $n = 19$	P
Baseline weight (g)	23.6 ± 0.6	19.0 ± 0.6	26.3 ± 0.7	21.4 ± 0.7	<0.01 (males) 0.01 (females)
End weight control (g)	26.2 ± 0.8 (13)	21.6 ± 0.7 (9)	36.3 ± 1.6 (15)	29.0 ± 1.4 (10)	<0.0001*
End weight L-NAME (g)	27.7 ± 1.1 (13)	22.1 ± 0.5 (14)	32.8 ± 1.6 (10)	26.4 ± 0.6 (9)	<0.0001*
Baseline blood pressure† (mm Hg)	106.6 ± 1.7		101.0 ± 2.1		NS†
End blood pressure control (mm Hg)	104.8 ± 2.9		104.1 ± 4.2		NS
End blood pressure L-NAME (mm Hg)	101.7 ± 1.7		102.9 ± 2.5		NS†
Cholesterol control (mg/dL)‡	737 ± 93§		1451 ± 147		0.001
Cholesterol L-NAME (mg/dL)	1021 ± 63		1026 ± 102		NS
Triglycerides control (mg/dL)	86.1 ± 6.4§		288.7 ± 47.9		<0.0001
Triglycerides L-NAME (mg/dL)	132.4 ± 14.5		260.5 ± 36.5		<0.0005

*For gender-specific comparisons.
†Blood pressure data are presented for males and females together as there were no differences between sexes. There were no differences between lines, treatment groups, or the time point at which blood pressure was measured.
‡Biochemical data are presented for males and females together as there were no differences between sexes in neither line.
§$P < 0.05$ for comparison between ApoE-null control and ApoE-null with L-NAME.

expression of several relevant genes was assessed on a StepOne Real-Time System (Applied Biosystems, Life Technology).

The following TaqMan gene expression assays on demand were used: renin: MM02342887_MH; angiotensinogen: AGT-MM00599662_M1; angiotensin converting enzyme 1: ACE1-MM00802048_M1; angiotensin II type 1 receptor: AT1-R-AGTR1a MM00616371_M1; endothelial nitric oxide synthase: eNOS-MM00435217_M1; inducible NOS: iNOS-MM01309897-M1, with HPRT as the endogenous gene MM00446968_M1. In addition, aortic expression of monocyte chemotactic protein 1 (MCP1), and that of the NADPH oxidase genes Nox1, Nox2, and Nox4, was assessed semiquantitatively. The level of aortic expression of the following genes was determined by semiquantitative PCR in the linear range of the reactions, using beta-actin as the housekeeping, and the following forward and reverse primers:

MCP1: 5′-CATTCACCAGCAAGATCC-3′;
5′-CTCATTTGGTTCCGATCCAG-3′;
Nox1: 5′-ATATTTTGGAATTGCAGATGAACA-3′;
5′-ATATTGAGGAAGAGACGGTAG-3′;
Nox2: 5′-CTTGGGTCAGCACTGG-3′;
5′-TTCCTGTCCAGTTGTCTTCG-3′;
Nox4: 5′-TTGTCTTCTACATGCTGCTG-3′;
5′-AGGCACAAAGGTCCGHAAAT-3′;
Beta actin: 5′-GACTACCTCATGAAGATCCTG-ACC-3′;
5′-TGATCTTCATGGTGCTAGGAGCC-3′.

All reactions were carried out with a 2 mM $MgCl_2$ final concentration (except for Nox1 that required 4 mM), using the Promega GoTaq Green Master Mix (Promega Corp. Madison, WI). PCR products were size-separated by electrophoresis in an ethidium bromide-containing 2% agarose gel. The band fluorescence intensity was captured on the 202D Bio-Imaging System (Dinco, Rhenium, Jerusalem, Israel) and analyzed with TINA software (Raytest, Straubenhardt, Germany).

2.6. Statistical Analysis. Data are expressed as mean ± SE. Groups were compared by parametric ANOVA followed by posttests. A repeated measure ANOVA was used for parameters obtained at baseline and at the end of the experiment. When comparison between the 4 groups was deemed unnecessary, Student's t-test was used. Correlations between parameters were established using linear regression or Spearman rank correlation. Statistical significance was assumed for $P < 0.05$.

3. Results

3.1. Animals' Weight, Blood Pressure, Serum Biochemistry, and FPLC of Lipoproteins. Deliberately given at a subpressor dose, L-NAME had indeed no effect on animals' blood pressure. All animals were normotensive both at baseline and after 8 weeks of high fat feeding, independently of treatment and despite increased adiposity in the DKO animals already detected at baseline (Table 1). As expected from the role of PPARα in lipoprotein metabolism, cholesterol levels were twice as high, and triglycerides were 3 times higher in the DKO mice than in the ApoE-null mice following the high fat feeding period. However, L-NAME increased cholesterol by another 39% and triglycerides by more than 50% in the ApoE-null mice, while it was without any effect in the DKO. Such a rise essentially brought the cholesterol to equal levels in both lines (Table 1).

FPLC analysis followed by cholesterol determination in the various fractions subsequently confirmed that the elevation caused by L-NAME was essentially limited to very low density lipoproteins (VLDL). Low density lipoprotein (LDL) cholesterol, however, unaffected by L-NAME remained significantly higher in the DKO (Figure 1).

3.2. DKO Mice Have Less Atherosclerosis and Are Immune to the Proatherogenic Effect of L-NAME. Confirming our earlier observations [5], the DKO control mice developed less atherosclerosis at the aortic sinus than their ApoE-null counterparts despite having a worse lipoprotein profile. Indeed, after 8 weeks on the Western diet, the atherosclerotic plaque encompassed 44.1% of the sinus area in the ApoE-null mice, yet only 33.8% in the DKO, a 23% difference, $P = 0.01$, (Figures 2(a), 2(c), and 2(e)). The DKO mice were also immune to the proatherogenic effect of blocking NO generation with L-NAME, as the plaque covered 34.4% of the sinus in the treated animals (Figures 2(d) and 2(e)). In contrast, L-NAME treatment increased the extent of the plaque in the ApoE-null mice by another 23% compared to control, to cover 54.3% of the sinus area (Figures 2(b) and 2(e); $P < 0.05$ compared to control), thereby creating a plaque area that was 37% larger than that measured in the treated DKO ($P = 0.002$).

3.3. Aortic NADPH Oxidase Activity Is Induced by L-NAME Only in ApoE-Null Mice and Correlates with NOX-1 Expression and with Atherosclerosis. NADPH oxidase, the main ROS generating system, is a major player in the initiation and development of atherosclerosis. We assessed its activity in the entire aorta. NADPH oxidase activity was similar in control, high fat-fed animals in both lines. However, inhibition of NO generation by L-NAME doubled the activity in the ApoE-null mice ($P < 0.05$ versus control) but was without any effect in the DKO (Figure 3(a)). An insight into the relevance of this system was the finding that the extent of atherosclerosis was also associated with the degree of NADPH oxidase activity ($r = 0.48$, $P = 0.03$).

As several isoforms of NADPH oxidase are expressed in the vasculature, we questioned which form might contribute to the activity measured. This was addressed in part by examining the expression of Nox1, Nox2, and Nox4 in the aorta. While the level of Nox1 mRNA in the control was similar in the ApoE-null mice and the DKO, much like the activity level, L-NAME treatment induced an 80% increase in the expression of Nox1 in the ApoE-null mice, whereas it tended to suppress it in the DKO ($P = 0.07$ versus control), leaving it at a mere 1/3 of that measured in the ApoE-null animals (Figure 3(b)). Although Nox2 was not augmented by L-NAME in the ApoE-null mice, the level observed under treatment in the DKO aortas was about half that seen in the ApoE-null animals ($P = 0.02$). Nox4 expression on the other hand was identical in both lines and was not affected by L-NAME treatment (not shown). In fact, the significant positive correlation found between NADPH oxidase activity and the level of expression of Nox1 mRNA in the aorta (Figure 3(c)) suggests this isoform of NADPH oxidase, a well-recognized AII target, is driving the increase in activity measured under L-NAME in the ApoE-null mice.

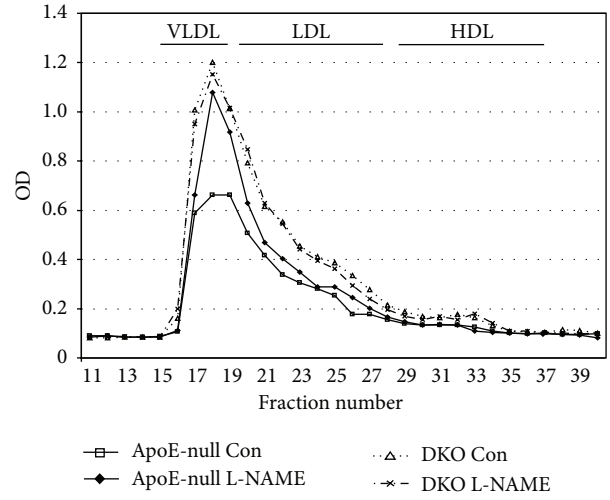

Figure 1: Lipoprotein FPLC analysis. Each curve represents the average of 4 samples, pooled from the sera of 2 mice each (error bars omitted for clarity). L-NAME increased VLDL cholesterol in the ApoE-null mice to the level seen in the DKO. DKO mice were not affected and maintained significantly higher LDL under all conditions ($P < 0.01$ for area under the curve, AUC).

3.4. Aortic Angiotensinogen and Renin Are Induced by L-NAME in Apo-E Null Mice but Not in the Absence of PPARα (DKO Mice). We had previously reported that the attenuation of atherosclerosis in the DKO was accompanied by a sustained reduction in the aortic expression of MCP1, compared to that seen in the ApoE-null mice, and that this effect was dependent on the presence and the activation of PPARα. A potent proinflammatory chemokine, MCP1, is induced by AII and has been implicated in the development of atherosclerosis in the ApoE-null mouse [14]. We therefore questioned whether it was involved in the observed differential effect of L-NAME on atherosclerosis. As a whole, MCP-1 expression was greatly reduced in the DKO mice, but it was not affected by L-NAME-induced NOS inhibition. Like MCP1, the aortic expression of the ACE-1 mRNA was considerably lower in the DKO but unaffected by L-NAME in either line. In contrast, tissue expression of renin and angiotensinogen more than doubled with L-NAME treatment in ApoE-null mice with the wild type PPARα gene but not in the DKO mice (Table 2). The absence of PPARα was then linked to lesser expression of aortic ACE and with the absence of aortic renin and angiotensinogen induction by L-NAME. Taken together these changes would favor more tissue AII generated under all experimental conditions in the ApoE-null mice aortas.

3.5. Aortic iNOS Robustly Correlates with Atherosclerosis. Contrarily to eNOS whose net effect is to supply NO for vasodilation, antithrombotic, and antiatherogenic purposes, iNOS, not normally significantly active in the vascular wall, is

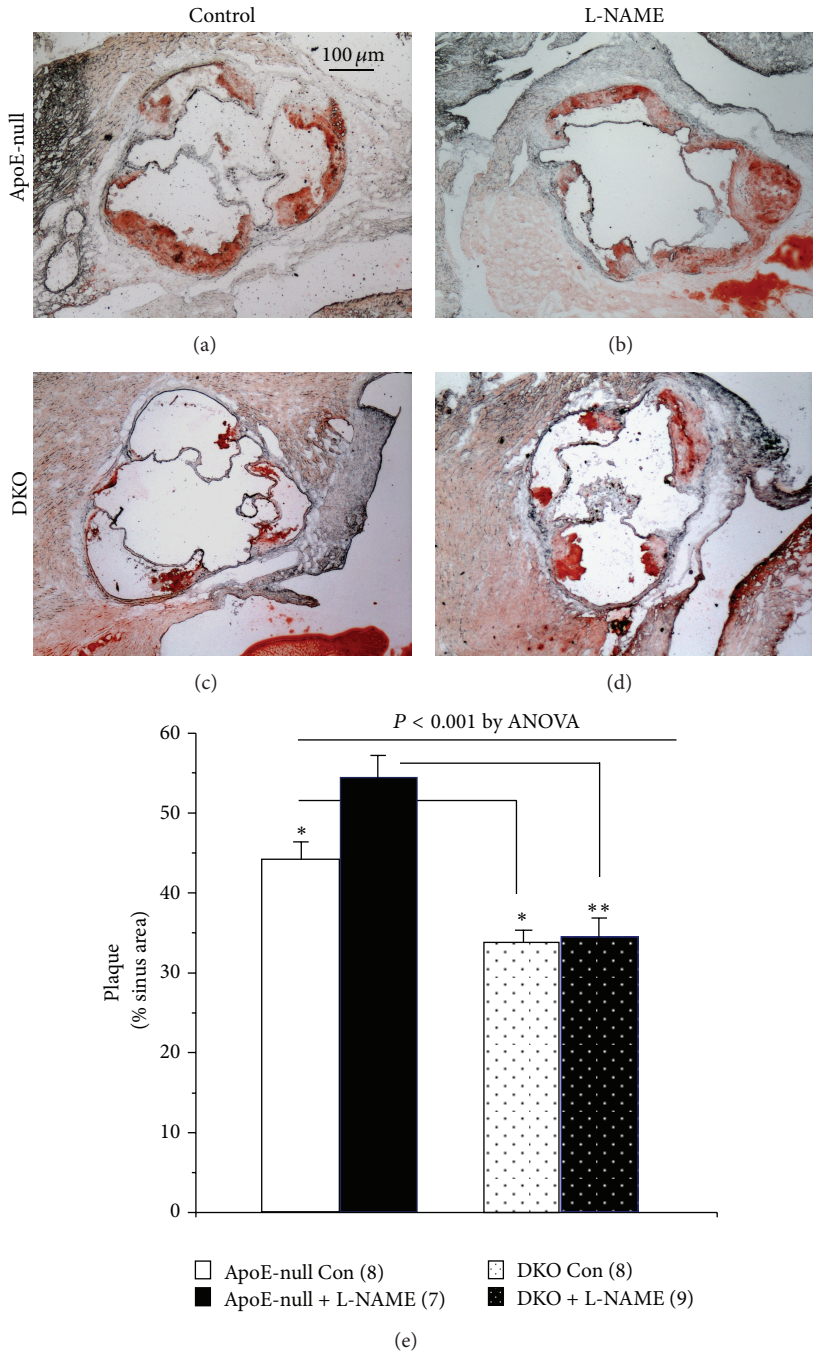

Figure 2: Atherosclerosis at the aortic sinus. Representative photographs of the oil-red-O-stained lesions ((a)–(d)), and after quantification (e), mice number in parentheses. Atherosclerosis was 23% lower in the DKO control mice (c) versus the ApoE-null (a), $^{*}P < 0.05$. L-NAME increased the extent of the plaque by 23% in the ApoE-null mice, ((a), (b), and (e)), $^{*}P < 0.05$, but had no effect in the DKO ((c), (d), and (e)), resulting in a 37% greater plaque area in the treated ApoE-null mice versus the treated DKO animals, $^{**}P < 0.005$.

induced by inflammatory cytokines and ROS. The abundant NO production that it then generates contributes to the formation of peroxynitrite, increasing the oxidative stress and rendering eNOS dysfunctional by uncoupling its activity, ultimately promoting inflammation and atherosclerosis. In view of the heightened expression of MCP1, and the induction of NADPH oxidase activity in the ApoE-null mice, conditions conducive to the induction of iNOS, we assessed its expression in the mice aorta and expected to see a greater level in the ApoE-null mice. In control ApoE-null mice the level of iNOS mRNA was 4 times higher than that in the untreated DKO mice. L-NAME treatment further increased iNOS 2.7-fold in the ApoE-null mice, while in contrast it had no effect on iNOS in the DKO mice. This resulted in ~10 fold higher expression of aortic iNOS in L-NAME-treated ApoE null mice compared to L-NAME-treated DKO (Figure 4(a)).

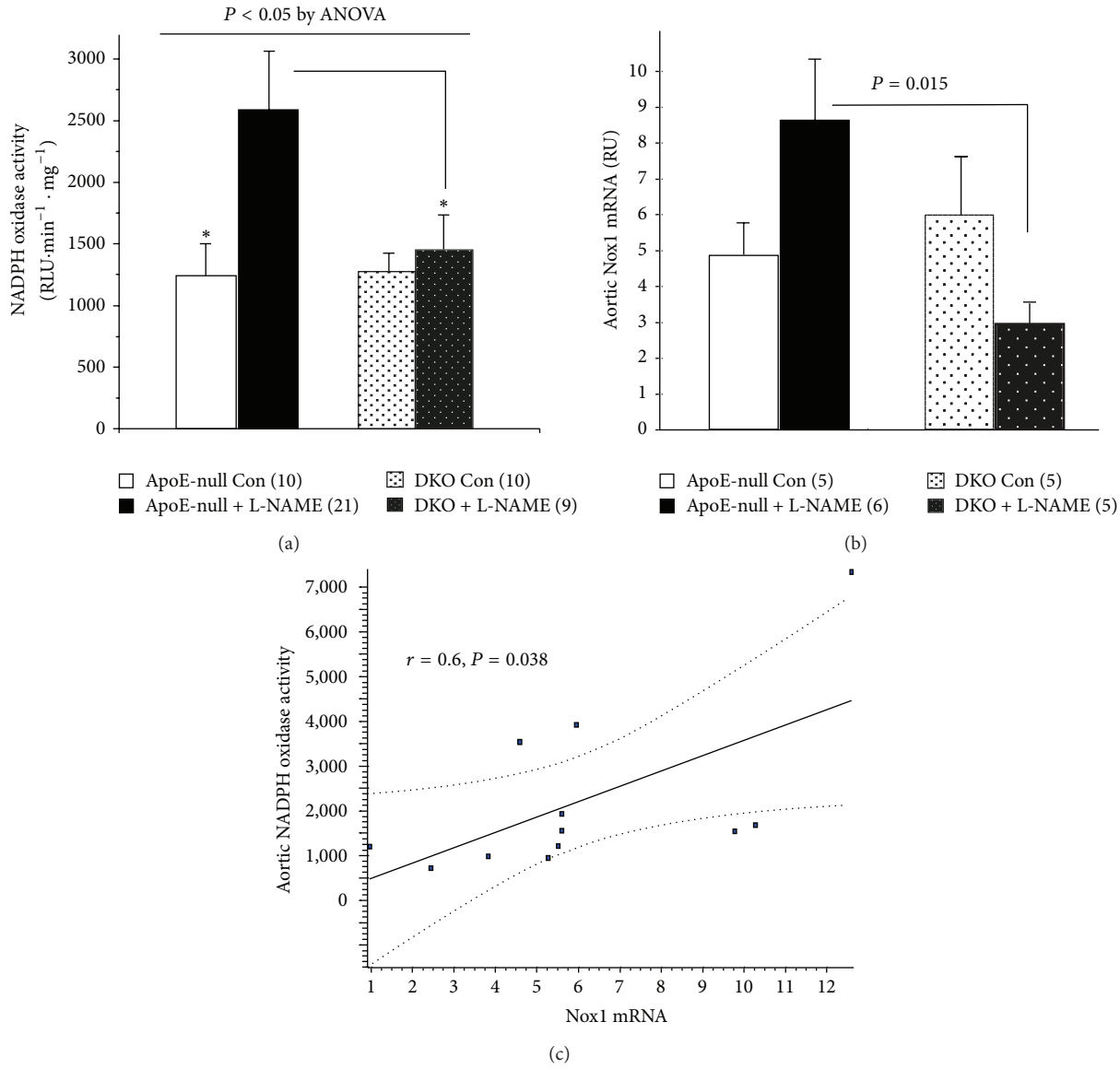

Figure 3: Aortic NADPH oxidase correlates with Nox1. (a) DKO mice are immune to the significant ($^*P < 0.05$) induction of NDAPH oxidase activity induced by L-NAME in the ApoE-null mice (mice number). (b) Relative expression of Nox1 mRNA (adjusted for actin) in mice aortas (mice numbers), which parallels NADPH oxidase activity, and is significantly correlated to it in a subset of mice in which both measurements were performed (c).

Table 2: Aortic MCP1 and RAS components mRNA levels. Each group included 7–9 animals; while there were no differences between sexes, the breakdown by gender for each group is given in parentheses. Data are given as mean ± (SE). Data are expressed relative to the level in the ApoE-null control animals; thus, the Dunnett's posttest was chosen to follow the ANOVA.

Gene	ApoE-null control (4 M/4 F)	ApoE-null L-NAME (3 M/4 F)	DKO control (5 M/4 F)	DKO L-NAME (3 M/4 F)	P ANOVA
MCP1	1.0 (0.05)	1.02 (0.06)	0.6* (0.08)	0.5† (0.13)	0.001
ACE1	1.0 (0.33)	0.55 (0.09)	0.27† (0.09)	0.23† (0.04)	0.005
Renin	1.0 (0.51)	2.57‡ (0.68)	2.0 (0.85)	1.68 (1.08)	NS
Angiotensinogen	1.0 (0.52)	2.25‡ (0.53)	1.26 (0.24)	1.0 (0.52)	NS
AT1-R	1.0 (0.24)	1.79 (0.78)	1.71 (0.42)	1.59 (0.34)	NS

*$P < 0.05$ versus control ApoE-null mice.
†$P < 0.01$ versus control ApoE-null mice.
‡$P < 0.05$ versus control ApoE-null mice by Student's t-test.

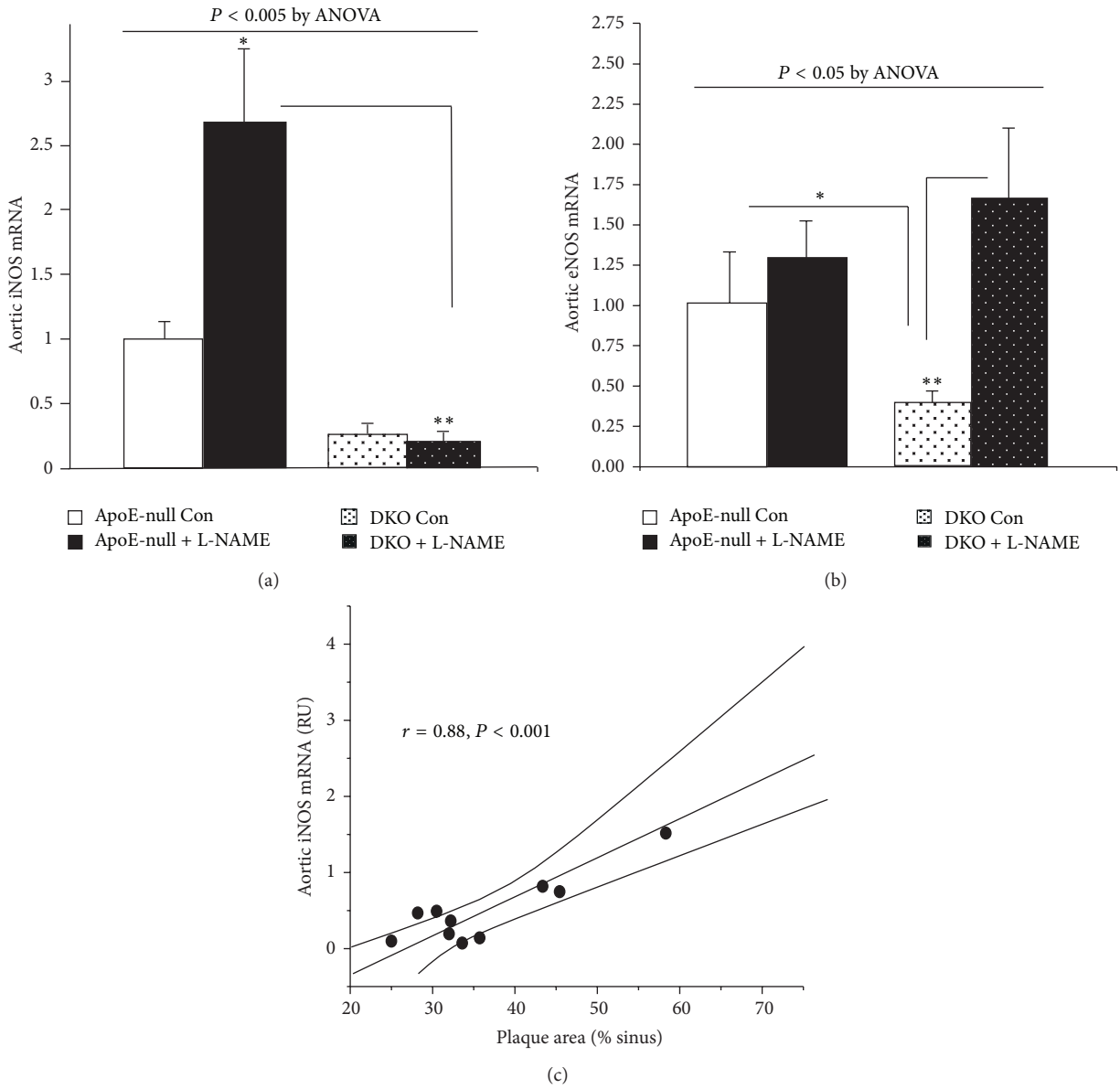

Figure 4: Aortic iNOS is induced by L-NAME in ApoE-null mice and correlates with atherosclerosis. Effects are expressed relative to the control ApoE-null mice. (a) iNOS expression by real-time PCR indicates a 4-fold excess in control ApoE-null versus DKO ($^{*}P < 0.05$) and a tenfold difference after L-NAME ($^{**}P < 0.01$), number of mice used in the experiment: 9 apoE-null control: 7 apoE-null L-NAME, 8 DKO control, and 8 DKO L-NAME. (b) eNOS is significantly increased by L-NAME in the DKO but not in the ApoE-null mice, $n = 5$ animals in each group. (c) Significant positive correlation between the extent of the plaque and iNOS expression.

Further support for the pathophysiologic significance of this observation comes from the strong correlation between the extent of atherosclerosis and the level of aortic iNOS, $r = 0.88$, $P < 0.001$ (Figure 4(c)). Control ApoE-null mice had a higher degree of expression of aortic eNOS than the DKO mice; however, this failed to increase under L-NAME treatment, while it more than tripled in the DKO (Figure 4(b)).

Finally, in a multiple regression analysis that included the variables shown to be correlated to the extent of the plaque by univariate analysis (MCP-1, NADPH oxidase activity, and the level of iNOS mRNA), NADPH oxidase activity along with iNOS alone predicted 86% of the atherosclerosis under the study conditions, $P < 0.01$. No other variable studied had any significant impact in predicting the extent of atherosclerosis. Notably, in this paradigm, the extent of atherosclerosis was unrelated to the severity of the hyperlipidemia.

4. Discussion

The salient finding of the current study is that absence of PPARα gene prevents the aggravation of diet-induced atherosclerosis elicited by L-NAME in the ApoE-null mouse *in vivo*, independently of blood pressure or serum lipid

alterations. These results extend and reinforce our previous reports that the absence of PPARα is protective of atherosclerosis driven by ApoE-null/high fat diet status [5] as well as by overexpression of the RAS in the Tsukuba hypertensive mouse [6]. That the absence of PPARα also prevents L-NAME-induced atherosclerosis on the genetic background of ApoE-KO, reemphasizes the role of this gene in the development of atherosclerosis driven by several different triggers.

An important aspect of our study is that we employed 20 times lower than that reported in various rodent models of atherosclerosis in which this agent was delivered in the drinking water as was done in the current study [8]. None of these studies presented hard data regarding blood pressure; at the most, they stated that treatment had no effect. Thus it is hard to exclude that the accelerated atherosclerosis reported under L-NAME was not also due to an unappreciated increase in blood pressure and shear stress. In contrast, as per our design, the dose chosen for L-NAME (approximately 1.5 $mg \cdot kg^{-1} \cdot d^{-1}$) resulted in no elevation of blood pressure in either strain, while it has been shown to effectively reduce NO production [10, 11]. Thus, by preventing L-NAME-induced hypertension and maintaining identical blood pressure throughout the study in all animal groups, we have excluded the possibility that our findings might be explained by higher blood pressure and/or shear stress.

Complementary to the exclusion of the role of L-NAME-induced hypertension in our model are the observed changes in serum lipids, which likewise cannot explain the aggravation of atherosclerosis in L-NAME treated mice. L-NAME was previously reported to elevate circulating lipids [15–17] due to increased triglyceride synthesis through induction of hepatic phosphatidate phosphohydrolase (an enzyme essential in triglyceride synthesis) and decreased oxidation due to suppression of carnitine palmitoyltransferase I (CPT-1), and elevation of cholesterol secondary to lower bile acid synthesis due to suppression of hepatic cholesterol 7 alpha-hydroxylase (CYP7A1), the latter two genes being known targets for PPARα [18, 19]. Yet, in the present study, DKO mice had, as expected, higher circulating lipid levels, and while L-NAME did induce an increase in lipid levels in the ApoE-null mice, it merely brought circulating lipids to the same level seen in L-NAME-treated DKO mice. Hence, the protection from the L-NAME-related acceleration of atherosclerosis seen in the DKO cannot be ascribed to circulating lipids, which calls for the examination of other possibilities.

NADPH oxidase, the main superoxide ROS generator in the vasculature, is a target of AII. Its activation causes a burst of ROS generation that ultimately brings about endothelial dysfunction, uncouples eNOS, thereby limiting NO availability, which then initiates more superoxide and reactive nitrogen species production. The level of NADPH oxidase activity in the control mice of both lines after 8 weeks on the Western diet was identical. However, upon concomitant L-NAME treatment, the level of activity doubled in the ApoE-null mice but barely changed in the DKO. As other potential stimuli of NADPH oxidase activation such as hyperglycemia, LDL cholesterol, and shear stress can be excluded to account for this difference, it is conceivable that upregulation of NADPH oxidase under low dose L-NAME treatment is dependent on the presence of PPARα and could reflect unopposed AII action.

Nox1, Nox4, and Nox2 are expressed in the vasculature. Nox1 is constitutively expressed at low levels in the endothelium and at higher levels in vascular smooth muscle cells (VSMC). It is induced in both cell types in culture by AII [20, 21]. Moreover, and most relevantly, genetic ablation of Nox1 was shown to greatly reduce the extent of diet-induced atherosclerosis in ApoE-null mice [22]. Both Nox2 and Nox4 are felt to be implicated in cardiovascular pathology. Constitutively active, Nox4 is also upregulated by AII, nonetheless it has recently received attention for its protective vascular properties [23]. Nox2 is associated with phagocytic respiratory burst activity, and expressed in endothelial cells. However studies looking at its role in atherosclerosis by specifically ablating it in ApoE-null mice failed to show any benefit [24]. Our finding that the NADPH oxidase activity brought about by L-NAME paralleled the induction of Nox1 suggests that this isoform is responsible for the activity we measured, and that it is dependent on the presence of PPARα. Further, since NADPH oxidase is an established target for AII action, the concomitant alterations in several components of the aortic RAS observed in the Apoe-null mice are consistent with the notion that this system plays at least an ancillary role in the induction of NADPH oxidase in L-NAME treated ApoE-null mice, while this mechanism is not operative in the absence of PPARα. Aortic ACE mRNA is much less expressed in DKO than in Apo-E mice, with or without L-NAME treatment. Furthermore, aortic renin and angiotensinogen mRNA expression are induced by L-NAME in the ApoE-null mice but not in the DKO mice, which parallels the absence of induction of aortic NADPH oxidase activity in this setting. In spite of the fact that aortic MCP1 mRNA expression significantly correlated with the degree of atherosclerosis, there was no further induction under L-NAME treatment in the ApoE-null mice. Such a result could have been expected given that it is also a target for AII. Although we cannot offer an explanation for this discrepancy, and perhaps different findings would have emerged had we measured the protein level, the fact that it was expressed at significantly lower levels in the DKO is reproducible [5] and needs to be emphasized.

In contrast to eNOS, which is widely expressed in the endothelium and is the main form of NOS in the normal vasculature, iNOS is barely detectable in normal vascular cells. Known to be induced by AII, iNOS produces large amounts of both NO and O_2^-, which by reacting together generate peroxynitrite. The latter further oxidizes LDL and uncouples eNOS. Thus iNOS is felt to exert a central role in the atherogenic process and is indeed abundant in atherosclerotic plaques [25, 26]. Moreover, genetic ablation of iNOS protected ApoE-null mice from atherosclerosis [27]. Consistent with the large difference in iNOS mRNA expression we observed between ApoE-null and DKO mice, amplification of mesangial iNOS expression by PPARα agonists has been reported [28]. As L-NAME displays some specificity for eNOS [29], the low dose employed in the present study could have been particularly detrimental insofar as it inhibited

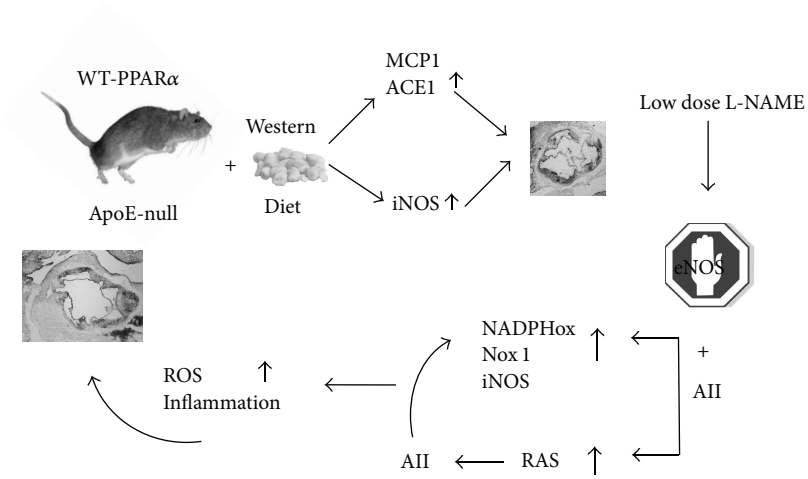

Figure 5: Proposed mechanism for the collusion of PPARα and AII in the ApoE-null mouse with wild type (WT) PPARα gene. The preferential eNOS activity inhibition by low dose L-NAME is suggested to alter the balance between AII and endothelium-derived NO, allowing amplification of the proatherogenic effect of unopposed AII action.

endothelial NO production, while leaving iNOS activity unaffected.

Taken together, with the limitation that the expression data are based solely on mRNA levels, the data suggest that the presence of PPARα is permissive for the expression of iNOS in the aorta of high fat-fed ApoE-null mice. This ensuing increase in oxidative burden could possibly underlie the difference in the extent of atherosclerosis we observed between the ApoE-null and DKO control animals.

In summary, the findings suggest that, in the high fat-fed ApoE-null mouse, reduction of endothelial-derived NO unleashes PPARα-dependent unopposed prooxidative and proatherogenic effects of AII, mediated both by NADPH oxidase through its Nox1 isoform, and by further induction of iNOS. We generated further evidence that not only is PPARα central in the detrimental action of unopposed AII, but also that its presence may drive greater aortic RAS synthetic activity in response to decreased NO (a diagram summarizing the proposed mechanisms is given in Figure 5). We thus propose that, in the ApoE-null mice, absence of PPARα mitigates the proatherogenic effect of reduced endothelium-derived NO supply.

Conflict of Interests

The authors declare that there is no conflict of interests regarding the publication of this paper.

Acknowledgments

This study was funded by a Grant no. 3_3093 from the Ministry of Health Chief Scientist to Karen M. Tordjman and by a research grant for young investigators from the Israeli Society for the Research and Treatment of Atherosclerosis to Maya Ish-Salom. The authors wish to thank Ms. Hanna Levkovitz for her invaluable help with the FPLC.

References

[1] J.-C. Fruchart, "Peroxisome proliferator-activated receptor-alpha (PPARα): at the crossroads of obesity, diabetes and cardiovascular disease," *Atherosclerosis*, vol. 205, no. 1, pp. 1–8, 2009.

[2] S. Behar, D. Brunner, E. Kaplinsky, L. Mandelzweig, and M. Benderly, "Secondary prevention by raising HDL cholesterol and reducing triglycerides in patients with coronary artery disease: the bezafibrate infarction prevention (BIP) study," *Circulation*, vol. 102, no. 1, pp. 21–27, 2000.

[3] H. B. Rubins, S. J. Robins, D. Collins et al., "Gemfibrozil for the secondary prevention of coronary heart disease in men with low levels of high-density lipoprotein cholesterol: veterans Affairs High-Density Lipoprotein Cholesterol Intervention Trial Study Group," *The New England Journal of Medicine*, vol. 341, no. 6, pp. 410–418, 1999.

[4] H. N. Ginsberg, M. B. Elam, L. C. Lovato et al., "Effects of combination lipid therapy in type 2 diabetes mellitus," *The New England Journal of Medicine*, vol. 362, no. 17, pp. 1563–1574, 2010.

[5] K. Tordjman, C. Bernal-Mizrachi, L. Zemany et al., "PPARα deficiency reduces insulin resistance and atherosclerosis in apoE-null mice," *Journal of Clinical Investigation*, vol. 107, no. 8, pp. 1025–1034, 2001.

[6] K. M. Tordjman, C. F. Semenkovich, T. Coleman et al., "Absence of peroxisome proliferator-activated receptor-α abolishes hypertension and attenuates atherosclerosis in the Tsukuba hypertensive mouse," *Hypertension*, vol. 50, no. 5, pp. 945–951, 2007.

[7] K. P. Patel and H. D. Schultz, "Angiotensin peptides and nitric oxide in cardiovascular disease," *Antioxidants and Redox Signaling*, vol. 19, no. 10, 2013.

[8] K. Kauser, V. da Cunha, R. Fitch, C. Mallari, and G. M. Rubanyi, "Role of endogenous nitric oxide in progression of atherosclerosis in apolipoprotein E-deficient mice," *The American Journal of Physiology*, vol. 278, no. 5, pp. H1679–H1685, 2000.

[9] P. J. Kuhlencordt, R. Gyurko, F. Han et al., "Accelerated atherosclerosis, aortic aneurysm formation, and ischemic heart disease in apolipoprotein ApoE/eNOS double-knockout mice," *Circulation*, vol. 104, no. 4, pp. 448–454, 2001.

[10] D. H. Sigmon, E. Gonzalez-Feldman, M. A. Cavasin, D. L. Potter, and W. H. Beierwaltes, "Role of nitric oxide in the renal hemodynamic response to unilateral nephrectomy," *Journal of the American Society of Nephrology*, vol. 15, no. 6, pp. 1413–1420, 2004.

[11] I. Rodríguez-Gómez, J. Sainz, R. Wangensteen et al., "Increased pressor sensitivity to chronic nitric oxide deficiency in hyperthyroid rats," *Hypertension*, vol. 42, no. 2, pp. 220–225, 2003.

[12] M. Ish-Shalom, J. Sack, M. Vechoropoulos et al., "Low-dose calcitriol decreases aortic renin, blood pressure, and atherosclerosis in ApoE-null mice," *Journal of Atherosclerosis and Thrombosis*, vol. 19, pp. 422–434, 2012.

[13] Committee for the Update of the Guide for the Care and Use of Laboratory Animals, *Guide For the Care and Use of Laboratory Animals*, The National Academies Press, Washington, DC, USA, 8th edition, 2011.

[14] C. Tikellis, R. J. Pickering, D. Tsorotes et al., "Activation of the Renin-Angiotensin system mediates the effects of dietary salt intake on atherogenesis in the apolipoprotein E knockout mouse," *Hypertension*, vol. 60, pp. 98–105, 2012.

[15] A. Khedara, Y. Kawai, J. Kayashita, and N. Kato, "Feeding rats the nitric oxide synthase inhibitor, L-N(ω)nitroarginine, elevates serum triglyceride and cholesterol and lowers hepatic fatty acid oxidation," *Journal of Nutrition*, vol. 126, no. 10, pp. 2563–2567, 1996.

[16] T. Goto, S. Ohnomi, A. Khedara, N. Kato, H. Ogawa, and T. Yanagita, "Feeding the nitric oxide synthase inhibitor L-N(ω)nitroarginine elevates serum very low density lipoprotein and hepatic triglyceride synthesis in rats," *Journal of Nutritional Biochemistry*, vol. 10, no. 5, pp. 274–278, 1999.

[17] A. Khedara, T. Goto, J. Kayashita, and N. Kato, "Hypercholesterolemic effect in rats of a dietary addition of the nitric oxide synthase inhibitor, L-NωNitroarginine, by less synthesis of bile acids," *Bioscience, Biotechnology and Biochemistry*, vol. 62, no. 4, pp. 773–777, 1998.

[18] S. K. Cheema and L. B. Agellon, "The murine and human cholesterol 7α-hydroxylase gene promoters are differentially responsive to regulation by fatty acids mediated via peroxisome proliferator-activated receptor α," *Journal of Biological Chemistry*, vol. 275, no. 17, pp. 12530–12536, 2000.

[19] S. Song, R. R. Attia, S. Connaughton et al., "Peroxisome proliferator activated receptor α (PPARα) and PPAR gamma coactivator (PGC-1α) induce carnitine palmitoyltransferase IA (CPT-1A) via independent gene elements," *Molecular and Cellular Endocrinology*, vol. 325, no. 1-2, pp. 54–63, 2010.

[20] F. Tabet, E. L. Schiffrin, G. E. Callera et al., "Redox-sensitive signaling by angiotensin II involves oxidative inactivation and blunted phosphorylation of protein tyrosine phosphatase SHP-2 in vascular smooth muscle cells from SHR," *Circulation Research*, vol. 103, no. 2, pp. 149–158, 2008.

[21] A. Dikalova, R. Clempus, B. Lassègue et al., "Nox1 overexpression potentiates angiotensin II-induced hypertension and vascular smooth muscle hypertrophy in transgenic mice," *Circulation*, vol. 112, no. 17, pp. 2668–2676, 2005.

[22] A. L. Sheehan, S. Carrell, B. Johnson, B. Stanic, B. Banfi, and F. J. Miller, "Role for Nox1 NADPH oxidase in atherosclerosis," *Atherosclerosis*, vol. 216, no. 2, pp. 321–326, 2011.

[23] K. Schröder, M. Zhang, S. Benkhoff et al., "Nox4 is a protective reactive oxygen species generating vascular NADPH oxidase," *Circulation Research*, vol. 110, pp. 1217–1225, 2012.

[24] E. A. Kirk, M. C. Dinauer, H. Rosen, A. Chait, J. W. Heinecke, and R. C. LeBoeuf, "Impaired superoxide production due to a deficiency in phagocyte NADPH oxidase fails to inhibit atherosclerosis in mice," *Arteriosclerosis, Thrombosis, and Vascular Biology*, vol. 20, no. 6, pp. 1529–1535, 2000.

[25] P. Ponnuswamy, E. Ostermeier, A. Schröttle et al., "Oxidative stress and compartment of gene expression determine proatherosclerotic effects of inducible nitric oxide synthase," *The American Journal of Pathology*, vol. 174, no. 6, pp. 2400–2410, 2009.

[26] M. Ohishi, G. J. Dusting, P. A. Fennessy, F. A. O. Mendelsohn, X. C. Li, and J. L. Zhuo, "Increased expression and co-localization of ACE, angiotensin II AT1 receptors and inducible nitric oxide synthase in atherosclerotic human coronary arteries," *International Journal of Physiology, Pathophysiology and Pharmacology*, vol. 2, no. 2, pp. 111–124, 2010.

[27] P. J. Kuhlencordt, J. Chen, F. Han, J. Astern, and P. L. Huang, "Genetic deficiency of inducible nitric oxide synthase reduces atherosclerosis and lowers plasma lipid peroxides in apolipoprotein E-knockout mice," *Circulation*, vol. 103, no. 25, pp. 3099–3104, 2001.

[28] E. Cernuda-Morollón, F. Rodríguez-Pascual, P. Klatt, S. Lamas, and D. Pérez-Sala, "PPAR agonists amplify iNOS expression while inhibiting NF-κB: implications for mesangial cell activation by cytokines," *Journal of the American Society of Nephrology*, vol. 13, no. 9, pp. 2223–2231, 2002.

[29] G. J. Southan and C. Szabó, "Selective pharmacological inhibition of distinct nitric oxide synthase isoforms," *Biochemical Pharmacology*, vol. 51, no. 4, pp. 383–394, 1996.

Hindawi Publishing Corporation
PPAR Research
Volume 2014, Article ID 541394, 9 pages
http://dx.doi.org/10.1155/2014/541394

Research Article

HMGB1 Is Involved in the Protective Effect of the PPARα Agonist Fenofibrate against Cardiac Hypertrophy

Zhankui Jia,[1] Rui Xue,[1] Gangqiong Liu,[2] Ling Li,[2] Jinjian Yang,[1] Guofu Pi,[3] Shengli Ma,[3] and Quancheng Kan[4]

[1] *Department of Urology, The First Affiliated Hospital of Zhengzhou University, No. 1 Jian She Dong Avenue, Zhengzhou 450002, China*
[2] *Department of Cardiology, The First Affiliated Hospital of Zhengzhou University, No. 1 Jian She Dong Avenue, Zhengzhou 450002, China*
[3] *Department of Orthopedics, The First Affiliated Hospital of Zhengzhou University, No. 1 Jian She Dong Avenue, Zhengzhou 450002, China*
[4] *Department of Pharmacology, The First Affiliated Hospital of Zhengzhou University, No. 1 Jian She Dong Avenue, Zhengzhou 450002, China*

Correspondence should be addressed to Quancheng Kan; maxuankun@126.com

Received 19 October 2013; Revised 13 December 2013; Accepted 13 December 2013; Published 9 January 2014

Academic Editor: Zhanjun Jia

High mobility group box 1 (HMGB1) is a ubiquitous nuclear DNA-binding protein whose function is dependent on its cellular location. Extracellular HMGB1 is regarded as a delayed mediator of proinflammatory cytokines for initiating and amplifying inflammatory responses, whereas nuclear HMGB1 has been found to prevent cardiac hypertrophy and heart failure. Because fenofibrate, a peroxisome proliferator-activated receptor α (PPARα) agonist, has shown both protective effects against cardiac hypertrophy and inhibitory effects against inflammation, the potential modulation of HMGB1 expression and secretion by fenofibrate is of great interest. We herein provide evidence that fenofibrate modulates basal and LPS-stimulated HMGB1 expression and localization in addition to secretion of HMGB1 in cardiomyocytes. In addition, administration of fenofibrate to mice prevented the development of cardiac hypertrophy induced by thoracic transverse aortic constriction (TAC) while increasing levels of nuclear HMGB1. Altogether, these data suggest that fenofibrate may inhibit the development of cardiac hypertrophy by regulating HMGB1 expression, which provides a new potential strategy to treat cardiac hypertrophy.

1. Introduction

High mobility group box 1 (HMGB1), a nuclear DNA-binding protein, is expressed in diverse cell types, including cardiomyocytes [1, 2]. HMGB1 exhibits diverse functions according to its cellular location. In the extracellular compartment, it plays an important role in inflammatory responses when actively secreted from stressed cells [3]. However, in addition to its extracellular functions, intracellular HMGB1 participates in a number of fundamental cellular processes such as transcription, replication, and DNA repair [4, 5]. HMGB1 has been demonstrated to play a pivotal role in cardiovascular disease in different studies [6]. Additionally, maintenance of stable nuclear HMGB1 levels has emerged as a potential treatment for cardiac hypertrophy because HMGB1 overexpression in the nucleus can prevent hypertrophy and heart failure by inhibiting DNA damage [2].

Peroxisome proliferator-activated receptors (PPARs) are ligand-dependent transcription factors belonging to the nuclear receptor superfamily [7]. There are three known PPAR isoforms, α, β/δ, and γ, which exhibit tissue-specific distribution and legend-specific effects [8, 9]. In particular, PPARα is abundant in metabolically active tissues, including the liver, brown fat, kidney, skeletal muscle, and heart [10]. In addition to their metabolic roles in the heart, PPARα and its agonist fenofibrate have received great attention because of their effects related to cardiac inflammation and hypertrophy [11, 12]. In cardiomyocytes, coadministration with fenofibrate inhibits the hypertrophic response induced by endothelin-1 by reducing cardiomyocyte surface area and

decreasing protein synthesis [13]. Fenofibrate also reduces the Ang-II induced expression of TGF-β1, collagen deposition, and macrophage infiltration during the process of myocardial inflammation [14]. Considering that HMGB1 is highly expressed in cardiomyocytes and promotes both cardiac inflammation and cardiac hypertrophy, we hypothesize that HMGB1 is possibly regulated by fenofibrate. Therefore, we investigated whether activation of PPARα with fenofibrate, a PPARα-specific agonist, modulates HMGB1 expression and localization in cardiomyocytes. Furthermore, we provide insights into a possible mechanism of how PPARα suppresses the progression of cardiac hypertrophy, with HMGB1 involvement. This study reveals a novel role of fenofibrate in modulating HMGB1 expression and provides a new potential mechanism for fenofibrate in treating cardiac hypertrophy.

2. Materials and Methods

2.1. Reagents. Fenofibrate (catalog: F6020) and LPS (catalog: L3755) were purchased from Sigma-Aldrich (St. Louis, MO). All of the cell culture media and supplements were from Sigma. Antibodies against HMGB1 (catalog: 3935) were from Cell Signaling Technology (Danvers, MA). The anti-PPARα antibody (catalog: ab8934) and anti-histone H3 antibody (catalog: ab1791) were obtained from Abcam (Hong Kong). The anti-actin antibody (catalog: A2668) was obtained from Sigma. Primers for quantitative real-time reverse transcriptase-PCR were designed using GenBank sequences.

2.2. Cell Culture. Primary cultures of neonatal rat cardiomyocytes were performed as described previously [15, 16]. In brief, hearts were collected from 1- to 2-day-old neonatal rats promptly after euthanasia by decapitation. The ventricular tissue parts were subjected to multiple rounds of enzymatic digestion with collagenase II (Worthington). The digested samples were then centrifuged at 800 g for 5 min at 4°C and the cells were collected. Nonmyocytes were removed by two rounds of preplating on culture dishes. The enriched cardiomyocytes were cultured in 4 mL of growth medium (Dulbecco's modified Eagle medium supplemented with 10% fetal bovine serum and 10 μM cytosine 1-β-d-arabinofuranoside). Addition of cytosine 1-β-d-arabinofuranoside inhibits the growth of contaminating nonmyocytes. More than 90% of the cells were cardiomyocytes (positive for α-actinin). Cardiomyocytes were washed with PBS the next day to remove unbound cells and were used for experiments at 3 d after the cells stabilized.

2.3. Hypertrophic Myocardium Model. Cardiac hypertrophy was induced in mice by thoracic transverse aortic constriction (TAC), a well-known surgical technique that can lead to pressure overload. The TAC model has been previously used to examine the role of HMGB1 [2, 17]. Healthy 10-week-old male mice weighing 24–26 g were randomly divided into the model group and sham group. Thoracic TAC was performed as described by Hu et al. [18]. Briefly, mice were anesthetized by intraperitoneal injection with a mixture of ketamine (80 mg/kg) and xylazine (8 mg/kg), and the aortic arch was exposed under the thymus, without thoracotomy, in spontaneously breathing mice. A 5–0 silk thread was passed under the aorta between the origin of the right innominate and left common carotid arteries and snared around the aorta, and a bent 27-gauge needle was placed alongside the aortic arch. After ligation, the needle was quickly removed, the skin was closed, and the mice were allowed to recover under infrared light until they were fully awake. The sham operation was identical, except that the thread was not ligated.

Table 1: Primers for real-time PCR.

Genes	Primers
Rat HMGB1	Forward: 5′-AGCAATCTGAACTTCTGTCC-3′ Reverse: 5′-GTTCTTGTGATAGCCTTCTC-3′
Rat PPARα	Forward: 5′-CCCTCTCTCCAGCTTCCAGCCC-3′ Reverse: 5′-CCACAAGCGTCTTCTCAGCCATG-3′
Mouse ANP	Forward: 5′-CAGCATGGGCTCCTTCTCCA-3′ Reverse: 5′-TCCGCTCTGGGCTCCAATCCT-3′
Mouse BNP	Forward: 5′-CTGAAGGTGCTGCCCCAGATG-3′ Reverse: 5′-GACGGATCCGATCCGGTC-3′
Mouse β-MHC	Forward: 5′-CTACAGGCCTGGGCTTACCT-3′ Reverse: 5′-TCTCCTTCTCAGACTTCCGC-3′
Rat β-actin	Forward: 5′-TCATGAAGTGTGACGTTGCATCCGT-3′ Reverse: 5′-CCTAGAAGCATTTGCGGTGCCGATG-3′
Mouse GAPDH	Forward: 5′-AACTTTGGCATTGTGGAAGG-3′ Reverse: 5′-TGTGAGGGAGATGCTCAGTG-3′

2.4. Echocardiography. Echocardiography was used to determine cardiac parameters in live mice, including interventricular wall thickness (IVS), left-ventricular end-diastolic dimension (LVEDD), and left-ventricular end-systolic dimension (LVESD). Echocardiography was performed on mice sedated with isoflurane vaporized in oxygen. A Vevo 770 high-resolution ECHO system equipped with a 35 MHz transducer was used to obtain images. All of the mice underwent echocardiography at 4 weeks after the TAC or sham surgery.

2.5. RNA Extraction and Real-Time PCR. Total RNA from cardiomyocytes and hearts was isolated using Trizol reagent (Life Technologies). Total RNA was reverse-transcribed to cDNA using the TaqMan Reverse Transcription Reagent Kit (Applied Biosystems) according to the manufacturer's protocol. Real-time PCR was performed using an iCycler device with the SYBR Green I probe (Bio-Rad, Hercules, CA). Each sample was analyzed in triplicate and mRNA levels were normalized against the level of GAPDH mRNA. Rat HMGB1 and PPARα mRNA levels, in addition to mouse ANP, BNP, and β-MHC mRNA levels, were determined by quantitative real-time RT-PCR. The primer sequences are in Table 1. PCR products were validated by electrophoresis on 2% agarose.

2.6. Western Blot Analysis. Cytoplasmic and nuclear proteins of neonatal rat and adult mouse ventricles were extracted

using nuclear and cytoplasmic extraction reagents (Pierce, Rockford, IL) according to the manufacturer's instructions. The protein concentration of the myocardial samples was determined using a protein concentration assay (Bio-Rad Laboratories, Hercules, CA). The extracted proteins were boiled in protein buffer for 5 min, separated by 12% SDS-PAGE, and transferred to a nitrocellulose membrane. The membrane was incubated at room temperature for 1 h in TBS-T (Tris-buffered saline containing 0.1% Tween 20) containing 5% skimmed milk to block nonspecific binding sites. The membrane was then incubated overnight at 4°C with the primary antibodies. The membrane was washed for 5 min with TBS-T buffer three times and then incubated with a horseradish peroxide-conjugated secondary antibody at room temperature for 1 h. Finally, the membrane was developed using ECL reagent (Vigorous Biotechnology, Beijing, China) and exposed to Kodak XBT-1 film.

2.7. ELISA Analysis for HMGB1 in Medium. ELISA analysis was performed as described previously [19]. The HMGB1 level in cardiomyocyte supernatants was measured using a commercially available ELISA Kit from Shino-Test Corporation (Tokyo, Japan) according to the manufacturer's instructions. Absorbance was measured at 450 nm on an ELISA reader (Bio-Rad Laboratories).

2.8. Statistical Analysis. SPSS software was used to analyze the data. All of the real-time PCR and ELISA data are presented as the mean ± standard error of the mean (SEM). All of the experiments were repeated a minimum of three times. Differences between groups were evaluated using a one-way ANOVA analysis of variance with post hoc Bonferroni tests. $P < 0.05$ was considered statistically significant.

3. Results

3.1. Fenofibrate Inhibits the Basal and LPS-Induced Expression of HMGB1 in Cardiomyocytes. It has been reported that both HMGB1 and PPARα are constitutively expressed in cardiomyocytes [2]; therefore, we examined whether activation of PPARα affects HMGB1 expression in primary cultures of neonatal rat cardiomyocytes. Fenofibrate induced a time-dependent reduction in HMGB1 expression at the mRNA level and protein level (Figures 1(a) and 1(b)), and this downregulation of HMGB1 was concentration dependent (Figures 1(c) and 1(d)). In addition, secretion of HMGB1 was also inhibited by fenofibrate (Figure 1(g)).

Considering that expression of HMGB1 may be increased in disease states, in addition to evaluating the influence of fenofibrate on HMGB1 expression at the basal level, we also investigated its effect on upregulation of HMGB1 by LPS. As shown in Figures 1(e) and 1(f), HMGB1 expression increased with LPS treatment. However, pretreatment with fenofibrate attenuated the LPS-induced upregulation of HMGB1. The HMGB1 level in the supernatant was also determined by ELISA and found to change in parallel with HMGB1 expression (Figure 1(g)).

3.2. Activation of PPAR by Fenofibrate Modulates the Localization of HMGB1. It is well known that HMGB1 is normally located in the nucleus as a chromatin-associated protein and that its function is dependent on its cellular location. However, it is still unknown whether fenofibrate modulates the nuclear-cytoplasmic translocation of HMGB1. Here, we detected the protein level of HMGB1 in the nucleus and cytoplasm of cardiomyocytes with or without fenofibrate treatment. As shown in Figure 2, HMGB1 was predominantly expressed in the nucleus of cardiomyocytes in the DMSO control group, and fenofibrate treatment decreased the protein level of HMGB1 in the nucleus compared to that for the DMSO control. However, LPS stimulation resulted in a dramatic increase in HMGB1 in both the nucleus and cytoplasm of cardiomyocytes, which was also inhibited by fenofibrate. Therefore, fenofibrate modulates HMGB1 expression and may also modulate its nuclear and cytoplasmic localization.

3.3. Expression and Location of HMGB1 in the Hearts of Mice with or without Cardiac Hypertrophy. After demonstrating the effect of PPARα on HMGB1 expression and localization in cardiomyocytes, we next investigated whether this effect could influence the progression of cardiac hypertrophy. A mouse model of cardiac hypertrophy induced by TAC was used to investigate the expression of both HMGB1 and PPARα in the hearts of the model mice. Control mice were subjected to sham surgery. At 4 weeks after operation, both TAC mice and sham mice were sacrificed, and their hearts were rapidly excised for experiments. We found that the increase in the weight of the heart was significantly higher in TAC mice than in sham mice (Figure 3(a)), which means that the cardiac hypertrophy model was successfully constructed. We next examined the expression of HMGB1 and PPARα in the hearts of the TAC group and sham group, and the results showed that PPARα expression was higher in the sham group than in the TAC group. In contrast, HMGB1 expression was higher in TAC group (Figure 3(b)). In addition, we also determined the localization of HMGB1 in cardiomyocytes in both TAC and sham mice. Compared with the findings for sham-operated mice, the expression of nuclear HMGB1 in the TAC group was lower, whereas the expression of cytoplasmic HMGB1 was higher (Figure 3(c)), suggesting that the location of HMGB1 in cardiomyocytes may be associated with the progression of cardiac hypertrophy.

3.4. Fenofibrate Prevents the Development of Cardiac Hypertrophy Possibly by Modulating HMGB1 Localization. The *in vitro* experiments clearly demonstrated that fenofibrate modulates HMGB1 expression and localization in cardiomyocytes. Additionally, nuclear HMGB1 in cardiomyocytes was also found to be upregulated in TAC mice. To determine whether fenofibrate also regulates HMGB1 *in vivo*, mice that underwent the TAC operation were randomly divided into two groups: one group received fenofibrate (50 mg/kg via gavage) daily for 4 weeks after the operation and the other group was administered saline. Sham-operated mice were used as normal controls and received saline rather than

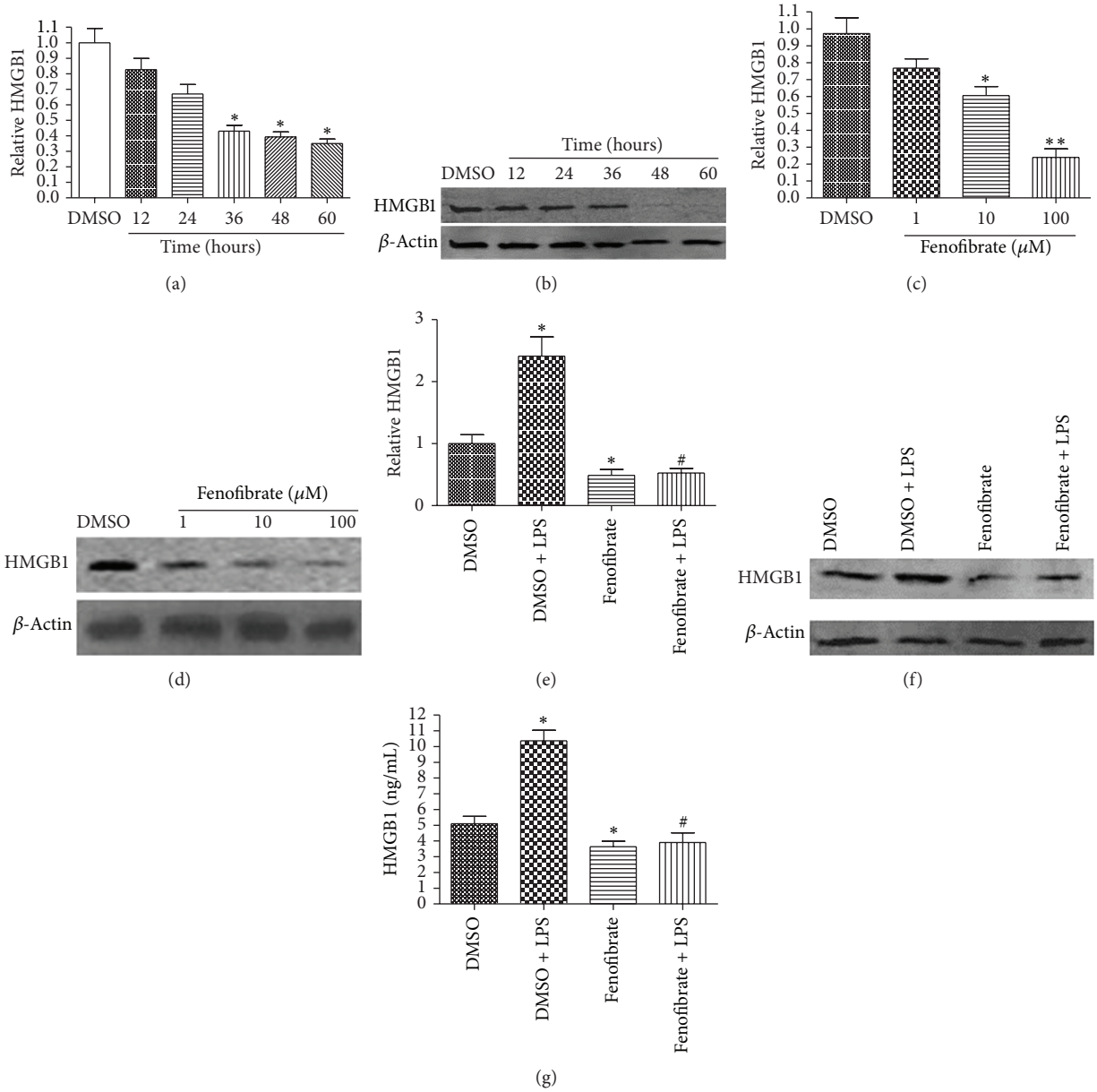

Figure 1: Fenofibrate inhibits the basal and LPS-induced expression of HMGB1. (a) and (b) Fenofibrate induces time-dependent inhibition of the expression of HMGB1 in primary cardiomyocytes at the mRNA level (a) and protein level (b). Cells were treated with 10 μM fenofibrate for 12, 24, 36, 48, and 60 h before being used for experiments. (c) and (d) Fenofibrate-induced concentration-dependent inhibition of the expression of HMGB1 in primary cardiomyocytes at the mRNA level (c) and protein level (d). Cells were treated with 1, 10, and 100 μM fenofibrate for 36 h before experiments. (e) and (f) Fenofibrate inhibited basal and LPS-induced HMGB1 expression in cardiomyocytes as determined by real-time PCR (e) and western blot (f). Cells were treated with the DMSO vehicle or the same dose of fenofibrate at a final concentration of 10 μM for 36 h; LPS (50 ng/mL) was then added and incubated for 10 h. (g) Fenofibrate inhibits basal and LPS-induced secretion of HMGB1 in cardiomyocytes; similar treatments were performed as described for (e) and (f), and the HMGB1 level was analyzed by ELISA. All the data are representative of at least three independent experiments, and the data in (a), (c), (e), and (g) are presented as the mean ± SEM. $^{*}P < 0.05$ versus DMSO vehicle and $^{\#}P < 0.05$ versus LPS alone.

fenofibrate. Fenofibrate treatment increased the protein level of HMGB1 in the nucleus to a greater extent in the TAC group (Figure 4(a)).

We therefore subsequently determined whether fenofibrate-mediated promotion of HMGB1 translocation from the nucleus to the cytoplasm plays a role in the development of cardiac hypertrophy. Cardiac function at 4 weeks after the TAC or sham operation was evaluated by examining the mRNA expression of fetal cardiac genes. As shown in Figure 4(b), ANP, BNP, and β-MHC were significantly upregulated in the TAC group compared with the sham surgery group, and this upregulation was significantly attenuated

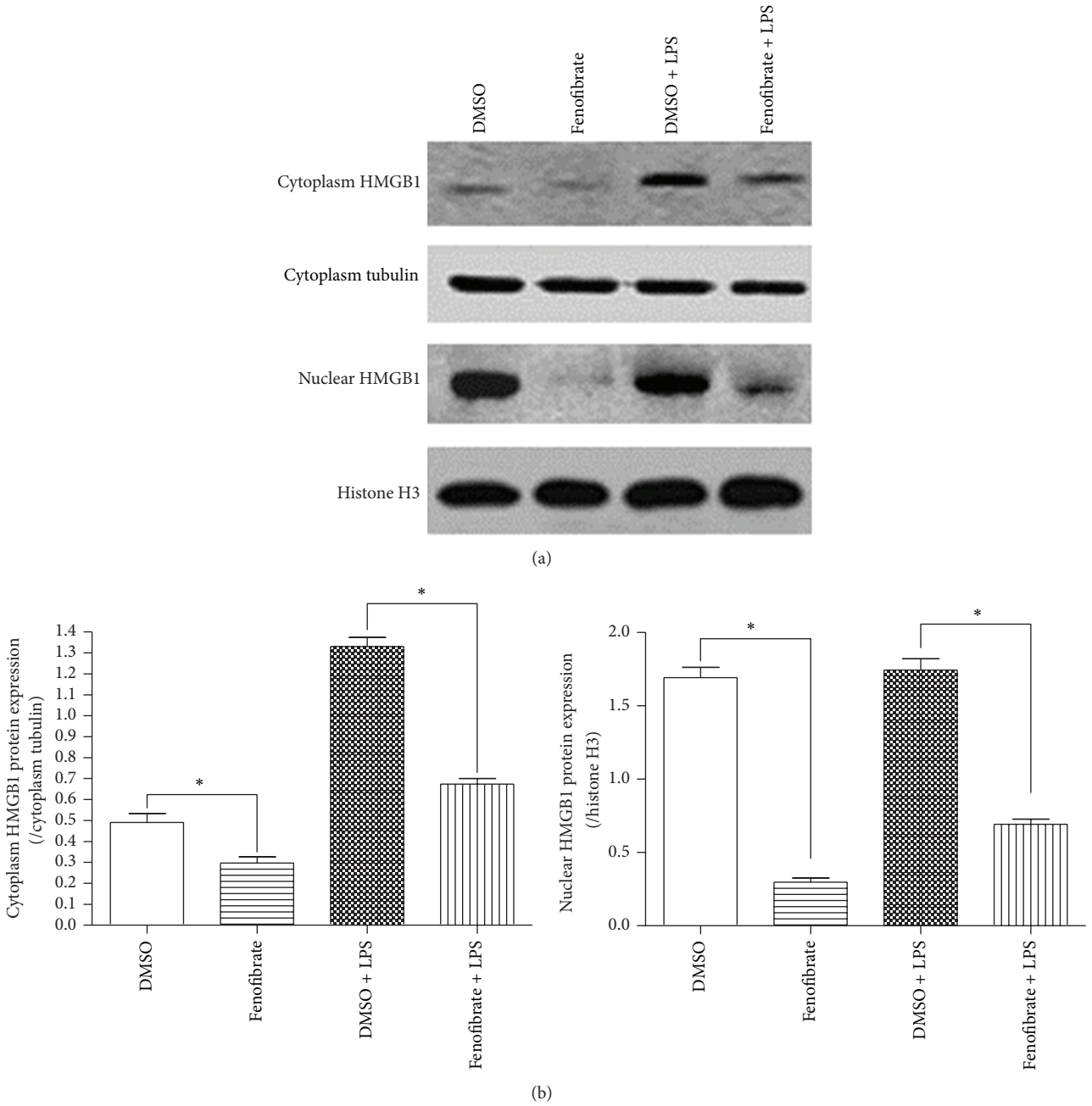

Figure 2: Fenofibrate modulates the localization of HMGB1 in cardiomyocytes. Cells were treated with 10 μM fenofibrate or DMSO for 36 h and then with or without LPS stimulation (50 ng/mL) for 10 h. (a) Cells were analyzed by western blot to determine the effect of fenofibrate on the distribution of HMGB1 between the nucleus and cytoplasm. Histone H3 and cytoplasmic tubulin were used as loading controls for nuclear protein and cytoplasm protein, respectively. Data are representative of three independent experiments. (b) Densitometry results for western blot, $^{*}P < 0.05$ as indicated comparisons; all data are expressed as means ± SEM, $n = 3$.

when mice were treated with fenofibrate after the operation. Moreover, systolic dysfunction and left-ventricular dilatation after TAC were attenuated by fenofibrate treatment (Figure 4(c)). These findings demonstrate that fenofibrate inhibits cardiac hypertrophy and regulates HMGB1 translocation; therefore, we hypothesized that fenofibrate-mediated regulation of HMGB1 localization may also play a role in inhibiting the development of cardiac hypertrophy.

4. Discussion

In the present study, we found that activation of PPARα by fenofibrate downregulates HMGB1 in cardiomyocytes and modulates their localization between the nucleus and cytoplasm. These effects of fenofibrate may also play a role in the development of cardiac hypertrophy. To our knowledge, this is the first study demonstrating that fenofibrate

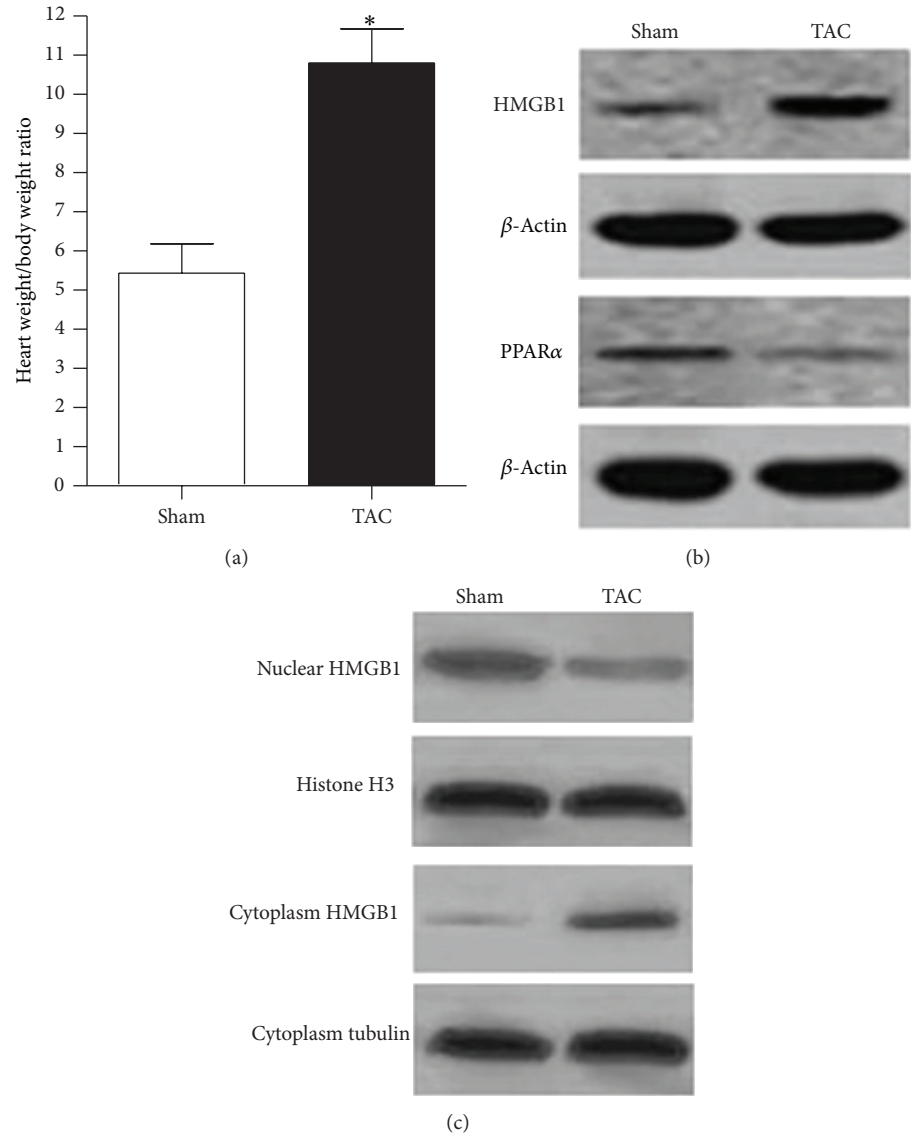

Figure 3: Decreased expression of PPARα and increased expression of HMGB1 in hypertrophic hearts induced by TAC. (a) Heart weight : body weight in TAC and sham-operated mice at 4 weeks after the operation. (b) Decrease in PPARα and increase in HMGB1 at the protein level in cardiomyocytes after the TAC operation; western blot was performed to analyze the expression of PPARα and HMGB1, and β-actin was used as the loading control. (c) Translocation of HMGB1 from the nucleus to the cytoplasm after the TAC operation; histone H3 and cytoplasmic tubulin were used as loading controls for nuclear protein and cytoplasm protein, respectively. All of the data are representative of at least three independent experiments. The data in (a) are presented as the mean ± SEM for five mice from each group. $^{*}P < 0.05$ versus sham-operated mice.

prevents cardiac hypertrophy development by inhibiting nuclear HMGB1 expression.

Thus far, several approaches have been used to target HMGB1, including the use of anti-HMGB1 antibodies, peptide antagonists, soluble receptors, and inhibitory molecules such as ethyl pyruvate and thrombomodulin [6, 20, 21]. In the present study, we found that activation of PPARα by fenofibrate is also effective in inhibiting HMGB1 expression in cardiomyocytes at both basal and LPS-enhanced levels. To date, no study has addressed the role of PPARα in regulating HMGB1 expression. However, a recent report demonstrated that PPARγ-dependent inhibition of HMGB1 may play a role in inhibiting inflammatory reactions in postischemic injury [22]. Additionally, a previous investigation also showed that the PPARγ agonist troglitazone inhibited HMGB1 expression in endothelial cells [19]. Because the physiological functions of PPARα and PPARγ are crossed in many diseases, fenofibrate is a logical candidate to block LPS-induced inflammation by inhibiting HMGB1 expression.

In addition to the finding that fenofibrate inhibited the expression of HMGB1, we also found that fenofibrate may modulate HMGB1 localization in the nucleus and cytoplasm. Previous studies have reported that posttranslational modification by acetylation of lysine residues in cultured cells modifies the binding of HMGB1 to DNA and the extranuclear

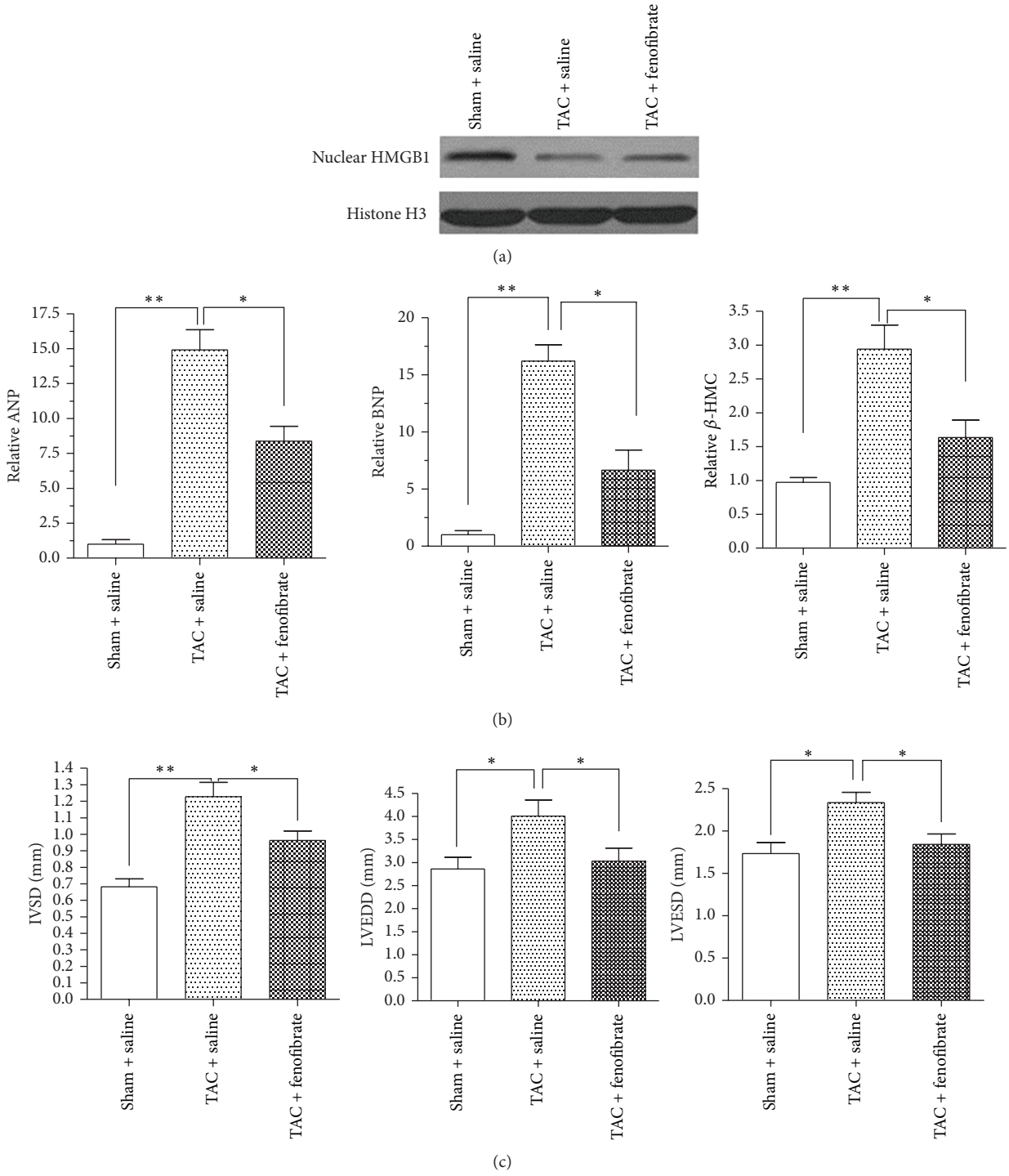

Figure 4: Fenofibrate suppresses the development of cardiac hypertrophy and increases the expression of nuclear HMGB1 in the heart. (a) Mice were treated with saline or the same dose of fenofibrate (50 mg/kg via gavage) after operation for 4 weeks; nuclear HMGB1 levels in the hearts of the mice were analyzed by western blot, and histone H3 was used as the loading control. (b) Mice were treated as described above, and ANP, BNP, and β-MHC gene expressions in mice were quantitatively analyzed by real-time PCR. All of the data are representative of at least three independent experiments, and the data in (b) are the mean ± SEM from five mice for each group. $^{*}P < 0.05$ and $^{**}P < 0.01$ as indicated in the comparisons. (c) Data showing echocardiographic measurements in mice treated as described above. IVS: interventricular wall thickness; LVEDD: left-ventricular end-diastolic dimension; LVESD: left-ventricular end-systolic dimension. Data are the mean ± SEM from three mice for each group. $^{*}P < 0.05$ and $^{**}P < 0.01$, as indicated in the comparisons.

localization of HMGB1 [23, 24]. Hyperacetylation of HMGB1 induced by lipopolysaccharide and hydrogen peroxide triggers its translocation into the cytoplasm [24–26]. A recent report also showed that, in cardiomyocytes, ET-1 and AngII promoted HMGB1 acetylation and subsequently suppressed the development of cardiac hypertrophy [2]. In this study, we demonstrated that fenofibrate maintained the level of nuclear HMGB1, which may affect the acetylation or phosphorylation of HMGB1. However, more evidence should be provided to determine the molecular mechanism underlying HMGB1 localization upon fenofibrate-induced PPARα activation.

Several cell- and rodent-based studies have demonstrated PPARα-dependent cardioprotection in the context of cardiac hypertrophy. Fenofibrate was found to inhibit endothelin-induced Akt and glycogen synthase kinase-3-β phosphorylation, thereby inhibiting the development of cardiomyocyte hypertrophy [27]. Nuclear translocation of the prohypertrophic transcription factor—nuclear factor of activated T cells (NFAT)—has been shown to be inhibited by fenofibrate [12, 27]. However, these results cannot fully explain the mechanism underlying the effect of fenofibrate in cardiac hypertrophy, and more evidence is required for this process. We showed that facilitation of PPARα expression by fenofibrate was accompanied by reduction in HMGB1 expression. In addition, we found that nuclear HMGB1 levels decreased in the mice with cardiac hypertrophy and that fenofibrate treatment reversed this decrease and inhibited the development of this disease. Previous studies have shown that nuclear HMGB1 may play a role in preventing DNA damage in the brain and neurons [28, 29]. Recent experiments conducted by Funayama et al. [2] have demonstrated that maintaining the nuclear HMGB1 level may prevent DNA damage in cardiomyocytes, thus decreasing the severity of cardiac hypertrophy. Taken together, these results further support our hypothesis that activation of PPAR by fenofibrate might prevent the development of cardiac hypertrophy by modulating HMGB1 expression and localization.

There are several limitations to this study. In the present study, we showed that upregulation of nuclear HMGB1 by fenofibrate in cardiomyocytes and the heart prevents cardiac dysfunction after TAC operation; however, we did not find a direct link between increased nuclear HMGB1 levels and cardiac hypertrophy *in vivo*. To confirm such a relationship, it may be necessary to evaluate cardiac function in cardiac-specific HMGB1 knockout mice in a future study. However, we demonstrated that fenofibrate could prevent the development of cardiac hypertrophy by modulating HMGB1 expression and localization, which also provides a novel approach to the investigation of the pathogenesis of cardiac hypertrophy.

Conflict of Interests

The authors declare that they have no conflict of interests.

Authors' Contribution

Zhankui Jia and Rui Xue contributed equally to this paper.

Acknowledgments

This study was supported by Grants from the Natural Science Foundation of China (U1304804) and the Youth Innovation Fund of the First Affiliated Hospital of Zhengzhou University.

References

[1] U. Andersson, H. Wang, K. Palmblad et al., "High mobility group 1 protein (HMG-1) stimulates proinflammatory cytokine synthesis in human monocytes," *Journal of Experimental Medicine*, vol. 192, no. 4, pp. 565–570, 2000.

[2] A. Funayama, T. Shishido, S. Netsu et al., "Cardiac nuclear high mobility group box 1 prevents the development of cardiac hypertrophy and heart failure," *Cardiovascular Research*, vol. 99, no. 4, pp. 657–664, 2013.

[3] U. Andersson and K. J. Tracey, "HMGB1 is a therapeutic target for sterile inflammation and infection," *Annual Review of Immunology*, vol. 29, pp. 139–162, 2011.

[4] K. Nightingale, S. Dimitrov, R. Reeves, and A. P. Wolffe, "Evidence for a shared structural role for HMG1 and linker histones B4 and H1 in organizing chromatin," *The EMBO Journal*, vol. 15, no. 3, pp. 548–561, 1996.

[5] S. S. Lange, D. L. Mitchell, and K. M. Vasquez, "High mobility group protein B1 enhances DNA repair and chromatin modification after DNA damage," *Proceedings of the National Academy of Sciences of the United States of America*, vol. 105, no. 30, pp. 10320–10325, 2008.

[6] W. Li, A. E. Sama, and H. Wang, "Role of HMGB1 in cardiovascular diseases," *Current Opinion in Pharmacology*, vol. 6, no. 2, pp. 130–135, 2006.

[7] K. C. Lee and W. L. Kraus, "Nuclear receptors, coactivators and chromatin: new approaches, new insights," *Trends in Endocrinology and Metabolism*, vol. 12, no. 5, pp. 191–197, 2001.

[8] E. D. Rosen and B. M. Spiegelman, "PPARγ: a nuclear regulator of metabolism, differentiation, and cell growth," *Journal of Biological Chemistry*, vol. 276, no. 41, pp. 37731–37734, 2001.

[9] J. Vamecq and N. Latruffe, "Medical significance of peroxisome proliferator-activated receptors," *The Lancet*, vol. 354, no. 9173, pp. 141–148, 1999.

[10] W. Wahli, O. Braissant, and B. Desvergne, "Peroxisome proliferator activated receptors: transcriptional regulators of adipogenesis, lipid metabolism and more," *Chemistry and Biology*, vol. 2, no. 5, pp. 261–266, 1995.

[11] S. Ichihara, K. Obata, Y. Yamada et al., "Attenuation of cardiac dysfunction by a PPAR-α agonist is associated with down-regulation of redox-regulated transcription factors," *Journal of Molecular and Cellular Cardiology*, vol. 41, no. 2, pp. 318–329, 2006.

[12] J. D. Molkentin, J.-R. Lu, C. L. Antos et al., "A calcineurin-dependent transcriptional pathway for cardiac hypertrophy," *Cell*, vol. 93, no. 2, pp. 215–228, 1998.

[13] F. Liang, F. Wang, S. Zhang, and D. G. Gardner, "Peroxisome proliferator activated receptor (PPAR)α agonists inhibit hypertrophy of neonatal rat cardiac myocytes," *Endocrinology*, vol. 144, no. 9, pp. 4187–4194, 2003.

[14] Q. N. Diep, K. Benkirane, F. Amiri, J. S. Cohn, D. Endemann, and E. L. Schiffrin, "PPARα activator fenofibrate inhibits myocardial inflammation and fibrosis in angiotensin II-infused rats," *Journal of Molecular and Cellular Cardiology*, vol. 36, no. 2, pp. 295–304, 2004.

[15] T. Shishido, C.-H. Woo, B. Ding et al., "Effects of MEK5/ERK5 association on small ubiquitin-related modification of ERK5: implications for diabetic ventricular dysfunction after myocardial infarction," *Circulation Research*, vol. 102, no. 11, pp. 1416–1425, 2008.

[16] N.-T. Le, Y. Takei, T. Shishido et al., "P90RSK targets the ERK5-CHIP ubiquitin E3 ligase activity in diabetic hearts and promotes cardiac apoptosis and dysfunction," *Circulation Research*, vol. 110, no. 4, pp. 536–550, 2012.

[17] S. Franklin, H. Chen, S. Mitchell-Jordan, S. Ren, Y. Wang, and T. M. Vondriska, "Quantitative analysis of the chromatin proteome in disease reveals remodeling principles and identifies high mobility group protein B2 as a regulator of hypertrophic growth," *Molecular & Cellular Proteomics*, vol. 11, no. 6, Article ID M111.014258, 2012.

[18] P. Hu, D. Zhang, L. Swenson, G. Chakrabarti, E. D. Abel, and S. E. Litwin, "Minimally invasive aortic banding in mice: effects of altered cardiomyocyte insulin signaling during pressure overload," *American Journal of Physiology*, vol. 285, no. 3, pp. H1261–H1269, 2003.

[19] M. Gao, Z. Hu, Y. Zheng et al., "Peroxisome proliferator-activated receptor γ agonist troglitazone inhibits high mobility group box 1 expression in endothelial cells via suppressing transcriptional activity of nuclear factor κb and activator protein 1," *Shock*, vol. 36, no. 3, pp. 228–234, 2011.

[20] H. Yang, M. Ochani, J. Li et al., "Reversing established sepsis with antagonists of endogenous high-mobility group box 1," *Proceedings of the National Academy of Sciences of the United States of America*, vol. 101, no. 1, pp. 296–301, 2004.

[21] J. E. Ellerman, C. K. Brown, M. De Vera et al., "Masquerader: high mobility group box-1 and cancer," *Clinical Cancer Research*, vol. 13, no. 10, pp. 2836–2848, 2007.

[22] T. Haraguchi, K. Takasaki, T. Naito et al., "Cerebroprotective action of telmisartan by inhibition of macrophages/microglia expressing HMGB1 via a peroxisome proliferator-activated receptor γ-dependent mechanism," *Neuroscience Letters*, vol. 464, no. 3, pp. 151–155, 2009.

[23] J. Evankovich, S. W. Cho, R. Zhang et al., "High mobility group box 1 release from hepatocytes during ischemia and reperfusion injury is mediated by decreased histone deacetylase activity," *Journal of Biological Chemistry*, vol. 285, no. 51, pp. 39888–39897, 2010.

[24] T. Bonaldi, F. Talamo, P. Scaffidi et al., "Monocytic cells hyperacetylate chromatin protein HMGB1 to redirect it towards secretion," *The EMBO Journal*, vol. 22, no. 20, pp. 5551–5560, 2003.

[25] H. Y. Ju and J.-S. Shin, "Nucleocytoplasmic shuttling of HMGB1 is regulated by phosphorylation that redirects it toward secretion," *Journal of Immunology*, vol. 177, no. 11, pp. 7889–7897, 2006.

[26] I. Ugrinova, I. G. Pashev, and E. A. Pasheva, "Nucleosome binding properties and co-remodeling activities of native and in vivo acetylated HMGB-1 and HMGB-2 proteins," *Biochemistry*, vol. 48, no. 27, pp. 6502–6507, 2009.

[27] R. Li, W. Zheng, R. Pi et al., "Activation of peroxisome proliferator-activated receptor-α prevents glycogen synthase 3β phosphorylation and inhibits cardiac hypertrophy," *FEBS Letters*, vol. 581, no. 17, pp. 3311–3316, 2007.

[28] Y. Enokido, A. Yoshitake, H. Ito, and H. Okazawa, "Age-dependent change of HMGB1 and DNA double-strand break accumulation in mouse brain," *Biochemical and Biophysical Research Communications*, vol. 376, no. 1, pp. 128–133, 2008.

[29] M.-L. Qi, K. Tagawa, Y. Enokido et al., "Proteome analysis of soluble nuclear proteins reveals that HMGB1/2 suppress genotoxic stress in polyglutamine diseases," *Nature Cell Biology*, vol. 9, no. 4, pp. 402–414, 2007.

Hindawi Publishing Corporation
PPAR Research
Volume 2013, Article ID 612971, 9 pages
http://dx.doi.org/10.1155/2013/612971

Research Article

PPARγ Agonist Rosiglitazone Suppresses Renal mPGES-1/PGE2 Pathway in db/db Mice

Ying Sun,[1,2] Zhanjun Jia,[2] Gang Liu,[2] Li Zhou,[2] Mi Liu,[2] Baoxue Yang,[1] and Tianxin Yang[2,3]

[1] *Department of Pharmacology, School of Basic Medical Sciences, Peking University, 38 Xueyuan Road, Haidian District, Beijing 100191, China*
[2] *Department of Internal Medicine, University of Utah and Veterans Affairs Medical Center, Salt Lake City, UT, USA*
[3] *Division of Nephrology and Hypertension, University of Utah and Veterans Affairs Medical Center, 30N 1900E, RM 4C224, Salt Lake City, UT 84132, USA*

Correspondence should be addressed to Baoxue Yang; baoxue@bjmu.edu.cn and Tianxin Yang; tianxin.yang@hsc.utah.edu

Received 10 October 2013; Revised 30 November 2013; Accepted 2 December 2013

Academic Editor: Guangrui Yang

Evidence had shown the detrimental effect of prostaglandin (PG) E2 in diabetic nephropathy (DN) of STZ-induced type-1 diabetes but its role in the development of DN of type-2 diabetes remains uncertain. The present study was undertaken to investigate the regulation of PGE2 synthetic pathway and the interaction between peroxisome proliferator-activated receptor (PPAR)γ and PGE2 synthesis in the kidneys of db/db mice. Strikingly, urinary PGE2 was remarkably elevated in db/db mice paralleled with the increased protein expressions of COX-2 and mPGES-1. In contrast, the protein expressions of COX-1, mPGES-2, cPGES, and 15-hydroxyprostaglandin dehydrogenase (15-PGDH) were not altered. Following 1-week rosiglitazone (Rosi) therapy, urinary PGE2, but not other prostanoids, was reduced by 57% in parallel with significant reduction of mPGES-1 protein and EP4 mRNA expressions. By immunohistochemistry, mPGES-1 was significantly induced in the glomeruli of db/db mice, which was almost entirely abolished by Rosi. In line with the reduction of glomerular mPGES-1, the glomerular injury score showed a tendency of improvement after 1 week of Rosi therapy. Collectively, the present study demonstrated an inhibitory effect of PPARγ activation on renal mPGES-1/PGE2/EP4 pathway in type-2 diabetes and suggested that mPGES-1 may potentially serve as a therapeutic target for treating type-2 diabetes-associated DN.

1. Introduction

The abnormality of renal prostaglandins in diabetic kidney was thought to be an important factor in mediating the glomerular injury, tubular interstitial fibrosis, and fluid imbalance [1–4]. Among five prostanoids of PGE2, PGD2, PGI2, PGF2α, and thromboxane (TX) A2, PGI2 and TXA2 are important players in regulation of renal hemodynamics [5–7]; PGE2 serves as an important regulator of glomerular integrity, SS hemodynamics, and tubular fluid reabsorption [8–10], while the PGD2 and PGF2α in kidney are less studied and their functions are poorly understood.

The renal PGE2 receptor (EP1-EP4) expression profile is altered in type-1 diabetic mice [11]. Makino et al. demonstrated that EP1-selective antagonist prevented the progression of nephropathy in streptozotocin (STZ) diabetic rats [12]. Most recently, Mohamed et al. reported that EP4 agonist exacerbated kidney injury in STZ-induced type-1 diabetes in mice [13]. These reports strongly suggested a detrimental role of PGE2 in kidney of STZ-induced type-1 diabetes via EP1 and/or EP4 receptors. However, no prior studies examine the role of PGE synthase in the kidney injury of type-2 diabetes. In clinic, type-2 diabetes is more common than type-1 diabetes and the kidney injury of type-2 diabetes possesses more complex pathogenic mechanism than that in type-1 diabetes. For animal studies of type-2 diabetes, the leptin receptor mutant db/db mice are widely used [14, 15]. Our recent publication demonstrated the induction of renal COX-2 and PGE2 in db/db mice [16], but the entire renal profile of prostaglandins, particularly the PGE2-related synthases, remains uncertain in this mouse model.

PPARγ agonists including rosiglitazone and piglitazone are very effective agents in treatment of type-2 diabetes. Besides their insulin sensitizing effect, PPARγ agonists also protect the organs from various injuries via anti-inflammation, antioxidative stress, and antiapoptosis [17, 18]. Although numerous lines of evidence demonstrated the beneficial effect of PPARγ activation on the diabetic kidney injury [19–22], the role of PPARγ in the regulation of renal prostaglandins in diabetic kidney is still unknown. In the present study, we investigated (1) the regulation of renal COX-2/mPGES-1/PGE2/EP pathway in obese-diabetic db/db mice and (2) the effect of PPARγ agonist Rosi on such a regulation.

2. Methods

2.1. Animals and Treatments. Obese-diabetic Lepr$^{db/db}$ (db/db, B6.BKS(D)-leprdb/J), Lepr$^{db/m}$ (db/m, lean control), and C57/BL6 male mice were purchased from the Jacson Laboratories (Bar Harbor, ME). In all studies, 7- to 8-month-old male mice were used. The mice were divided into three groups: db/m control (lean, $n = 4$), db/db without Rosi (db/db, $n = 5$), and db/db with Rosi (db/db + Rosi, $n = 5$). The Rosi was administered to db/db mice in jelly diet (80 mg/kg food) for 1 week as described previously [23]. The db/m control and db/db control mice were given the same jelly diet without Rosi. The Rosi maleate (Cat no. BRL49653C) was provided by GlaxoSmithKline (Harlow, UK). All mice were maintained under a 12:12-h light-dark cycle (lights on at 6:00 a.m. and lights off at 6:00 p.m.). All protocols employing mice were conducted in accordance with the principles and guidance of the University of Utah Institutional Animal Care and Use Committee.

2.2. Immunoblotting. The whole kidney was lysed and protein concentration was determined by Coomassie reagent. Protein (60 μg) from whole kidney lysates was denatured in boiling water for 10 min, separated by SDS-polyacrylamide gel electrophoresis, and transferred onto nitrocellulose membranes. The blots were blocked overnight with 5% nonfat dry milk in Tris-buffered saline (TBS), followed by incubation for 1 h with rabbit anti-COX-1 (Cayman Chemicals, Cat no. 160108), anti-COX-2 (Cayman Chemicals, Cat no. 160106), anti-mPGES-1 (Cayman Chemicals, Cat no. 160140), anti-mPGES-2 (Cayman Chemicals, Cat no. 160145), anti-cPGES (Cayman Chemicals, Cat no. 160150), anti-15-PGDH (Cayman Chemicals, Cat no. 160615), anti-PPARγ (Santa Cruz, CAT no. SC-7273), and anti β-actin (Sigma Aldrich, Cat no. A1978) at a dilution of 1 : 1000. After being washed with TBS, blots were incubated with a goat anti-horseradish peroxidase-conjugated secondary antibody (1 : 1000 dilution) and visualized with ECL kits (Amersham, Piscataway, NJ, USA).

2.3. Immunohistochemistry and Histology. Kidneys from the db/m and db/db mice were fixed with 4% paraformaldehyde and embedded in paraffin. Kidney sections of 4 μm thickness were prepared for the staining. The immunohistochemistry of mPGES-1 was performed using an EnVison TM Mini Kit (Doko, Carpinteria, CA) according to the manufacturer's instruction. The mPGES-1 antibody was purchased from Cayman Chemical (Cat no. 160140) and was applied to the immunohistochemical staining by 1 : 200 dilutions. mPGES-1 specific blocking peptide (Cayman Chemicals, Cat no. 360140) was used to test the specificity of the mPGES-1 antibody signal.

The histology was evaluated by Periodic Acid Schiff (PAS) staining. Semiquantitative scoring of glomerular sclerosis in PAS stained slides was performed using a five-grade method described previously [16, 24]: 0, normal glomerulus; 1, sclerosis <25%; 2, sclerosis between 25 and 50%; 3, sclerosis between 50 and 75%; and 4, sclerosis >75% of glomerular surface. Semiquantitative mesangial area was measured by using computer software Image J (NIH, Bethesda, MD).

2.4. qRT-PCR. Total RNA isolation and reverse transcription were performed as previously described [25]. Oligonucleotides were designed using Primer3 software (available at http://frodo.wi.mit.edu/primer3/). The sequences of primers are as follows: EP1 5′-cagtgaagtgcgggtggag-3′(sense) and 5′-tattggggagcctgggtgt-3′(anti-sense) NM_013641; EP4 5′-cttactcatcgccacctct-3′(sense) and 5′-tggggttcacagaagcaatc-3′(anti-sense) NM_008965; GAPDH 5′-gtcttcactaccatggag-aagg-3′(sense) and 5′-tcatggatgaccttggccag-3′(anti-sense) M32599. Amplification was performed using the SYBR Green Master Mix (Applied Biosystems, Warrington, UK) and the Prism 7500 Real-Time PCR Detection System (Applied Biosystems, Foster City, CA, USA). Cycling conditions were 95°C for 10 min, followed by 40 repeats of 95°C for 15 s, and 60°C for 1 min. The melting curve was examined and the results were analyzed by delta-delta CT method. GAPDH was used as a reference gene.

2.5. Enzyme Immunoassay. Urine samples were centrifuged for 5 minutes at 10000 rpm. Concentrations of PGE2 (Cayman Chemicals, Cat no. 514010), PGD2 (Cayman Chemicals, Cat no. 512031), 6-keto-PGF1α (Cayman Chemicals, Cat no. 515211), and TXB2 (Cayman Chemicals, Cat no. 519031) were determined by enzyme immunoassay according to manufacturer's instructions. For the PGE2 assay, the sensitivity or minimal detection limit was 7.8 pg/mL; intra-assay CV was 4.2% and interassay CV 12.4%. For the PGD2 assay, the sensitivity or minimal detection limit was 19.5 pg/mL; intraassay CV was 11% and interassay CV 6.1%. For the TXB2 assay, the sensitivity or minimal detection limit was 7.8 pg/mL; intra-assay CV was 16.3% and interassay CV 26.6%. For the 6-keto PGF1α assay, the sensitivity or minimal detection limit was 1.6 pg/mL; intra-assay CV was 6.7% and interassay CV 18.1%.

2.6. Statistical Analysis. All values are presented as mean ± SE. Statistical analysis was performed using ANOVA. Differences were considered to be significant when $P < 0.05$.

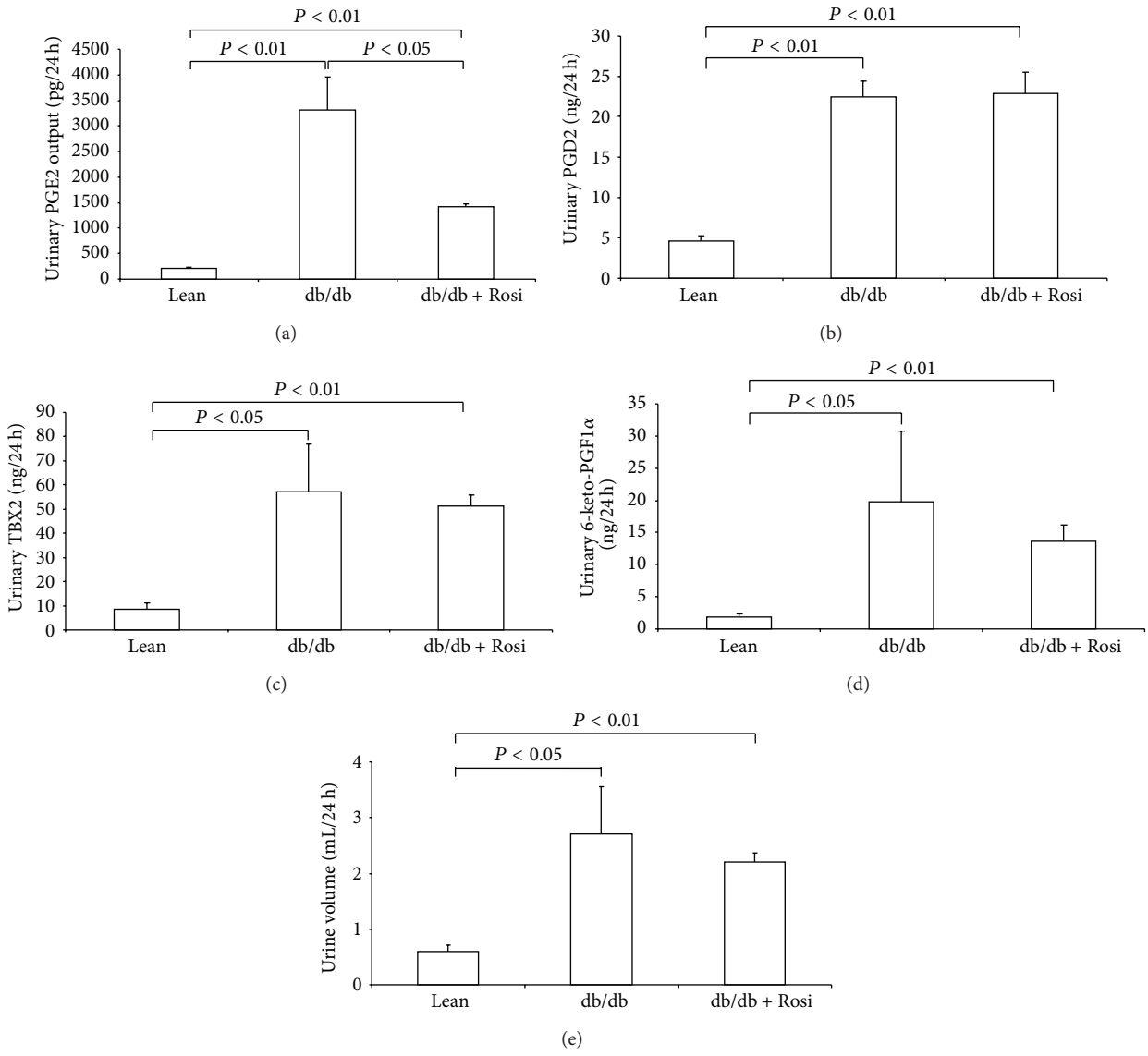

Figure 1: Effect of Rosi treatment on the urinary output of prostanoids and urine volume in db/db mice. (a) Urinary PGE2 output. (b) Urinary PGD2 output. (c) Urinary TXB2 output. (d) Urinary 6-keto-PGF1α output. (e) Urinary volume. N = 4-5 in each group. Data are mean ± SE.

3. Results

3.1. Effect of Rosi Treatment on Urinary Prostanoids Output in db/db Mice. The urinary PGE2 output in db/db mice was markedly elevated compared with the age matched lean mice (Figure 1(a)), and such an increase was significantly blunted by Rosi treatment (Figure 1(a)). In addition, the baseline blood glucose level in this obese-diabetic db/db mouse strain was higher than lean controls (db/db: 160.1 ± 18.7 mg/dL versus lean: 100.0 ± 7.3 mg/dL, $P < 0.05$). One-week Rosi treatment entirely normalized the blood glucose (104.6 ± 8.1 mg/dL). The urinary PGD2 (Figure 1(b)), TXB2 (stable metabolite of TXA2) (Figure 1(c)), and 6-keto-PGF1α (stable metabolite of PGI2) (Figure 1(d)) were all remarkably increased in the db/db mice, which was unaffected by Rosi administration. The urine volume was not affected following 1-week Rosi therapy (Figure 1(e)).

3.2. Effect of Rosi on the Protein Expressions of Prostaglandin E Synthases in db/db Mice. By Western blotting, the renal mPGES-1 protein was markedly elevated in db/db mice by more than 4-fold, and such an induction was remarkably blunted by Rosi (Figures 2(a) and 2(b)). By immunohistochemistry, mPGES-1 protein was significantly induced in the glomeruli, which was entirely abolished by Rosi treatment (Figures 3(a) and 3(b)). Whereas, the protein expressions of COX-1, mPGES-2, cPGES, and 15-PGDH (Figures 4(a) and 4(b)) were not altered by leptin receptor mutation or Rosi treatment. COX-2 protein expression was significantly

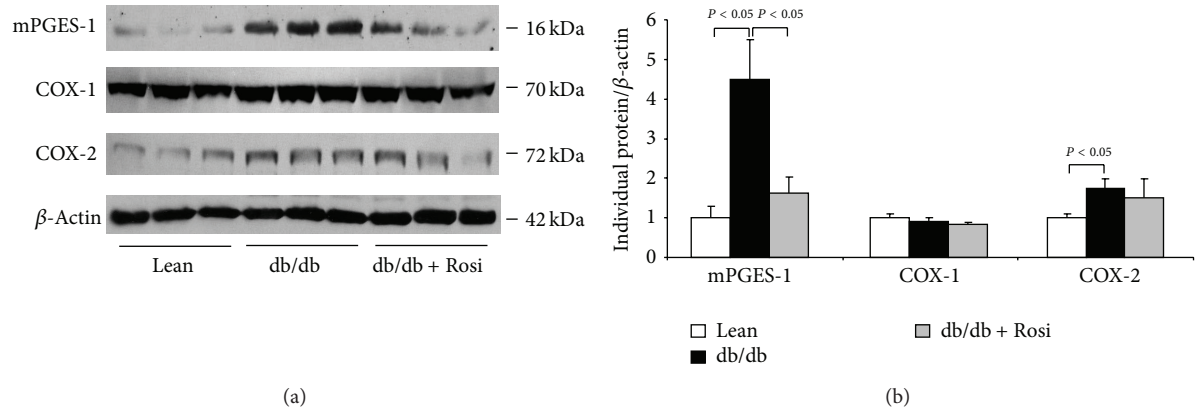

(a) (b)

Figure 2: Effect of Rosi treatment on the protein expressions of mPGES-1, COX-1, and COX-2 in the kidneys of db/db mice. (a) Western blots of mPGES-1, COX-1, COX-2, and β-actin. (b) Densitometry of western blots. N = 4-5 in each group. Data are mean ± SE.

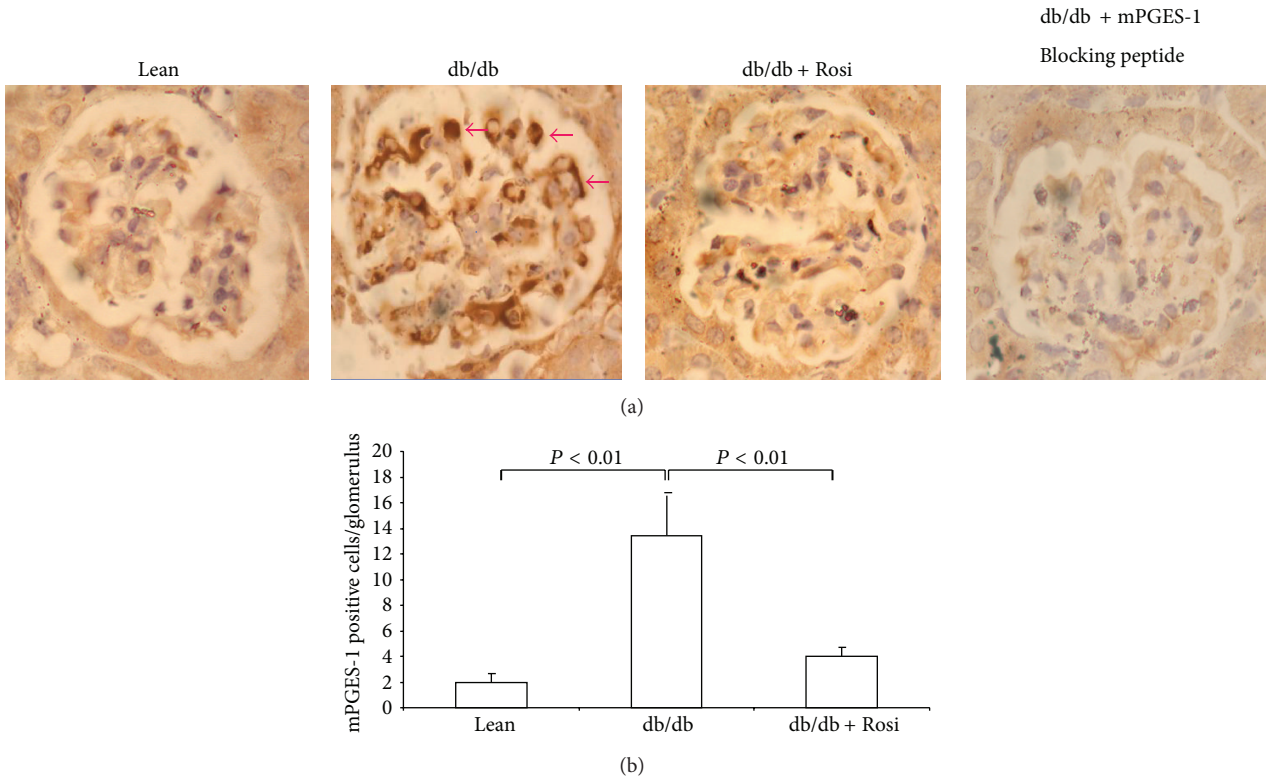

Figure 3: Effect of Rosi treatment on glomerular mPGES-1 expression in db/db mice. (a) Immunohistochemstry of mPGES-1. (b) Quantification of mPGES-1 positive cells in the glomeruli. N = 4-5 in each group. Data are mean ± SE.

higher in the kidney of db/db mice compared with lean mice. However, such an induction of COX-2 protein was not attenuated by Rosi treatment (Figures 2(a) and 2(b)).

3.3. Effect of Rosi on the mRNA Expressions of EP1 and EP4 in the Kidneys of db/db Mice. Rosi treatment led to significant downregulation of EP4 mRNA expression (Figure 5(b)) in line with the striking reduction of urinary PGE2 and renal mPGES-1 protein. However, EP1 mRNA was not influenced by leptin receptor mutation or Rosi treatment (Figure 5(a)).

3.4. Effect of Rosi on the Protein Expression of PPARγ in the Kidneys of db/db Mice. By Western blotting, renal PPARγ protein was 2.6-fold higher in db/db mice compared to lean controls and Rosi treatment further increased its expression (Figures 6(a) and 6(b)).

3.5. Effect of Rosi Treatment on Glomerular Injury in db/db Mice. By PAS staining, we found that the mesangial matrix accumulation was strikingly increased in the db/db mice.

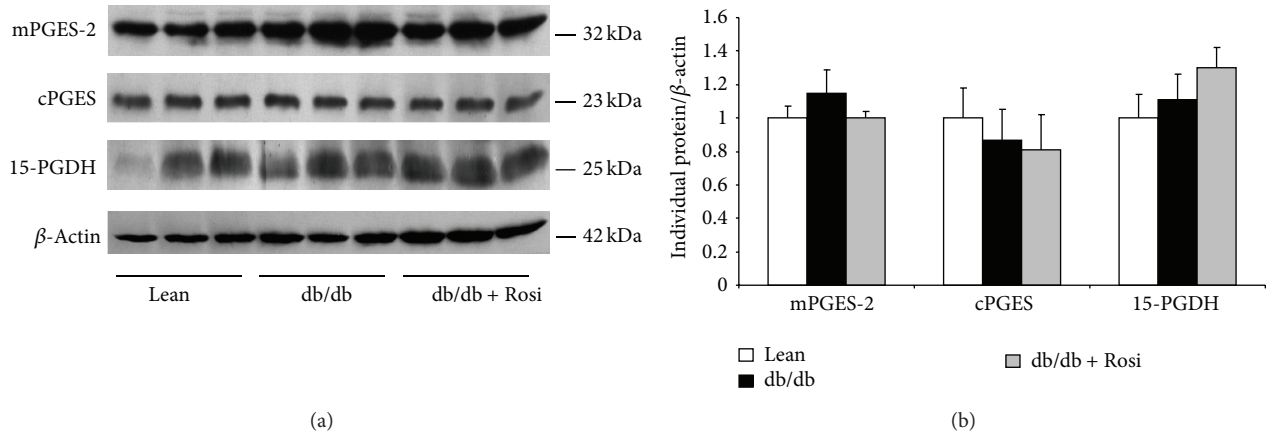

Figure 4: Effect of Rosi treatment on the protein expressions of mPGES-2, cPGES, and 15-PGDH in kidneys of db/db mice. (a) Western blots of mPGES-2, cPGES, 15-PGDH, and β-actin. (b) Densitometry of western blots. N = 4-5 in each group. Data are mean ± SE.

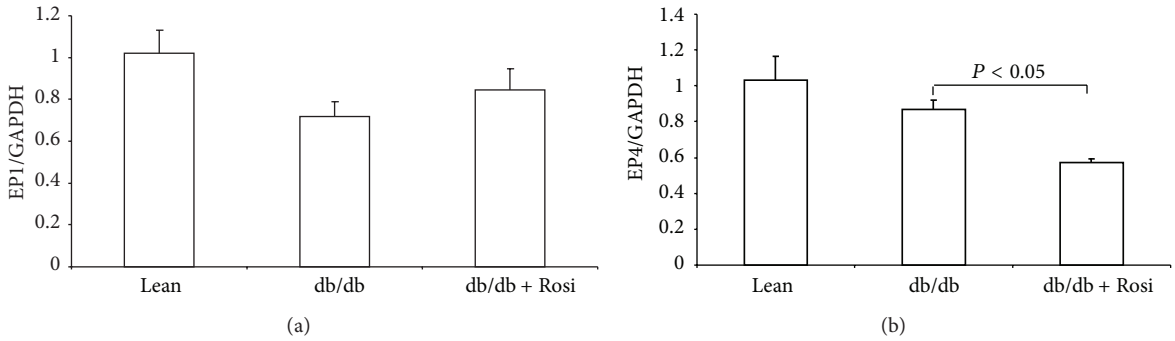

Figure 5: Expressions of EP1 and EP4 mRNA in kidneys of db/db mice following Rosi treatment. (a) qRT-PCR of EP1. (b) qRT-PCR of EP4. N = 4-5 in each group. Data are mean ± SE.

Rosi treatment for 1 week resulted in a trend improvement of glomerular injury ($P = 0.07$) (Figures 7(a) and 7(b)).

4. Discussion

Type-2 diabetes is in epidemic with rapid increase of obesity worldwide [26]. For patients with type-2 diabetes, DN is a common and severe complication leading to the renal failure and death [19]. Although extensive studies on DN have been performed in past decades, the pathogenic mechanism of this disease is still poorly understood. In the animal studies, leptin receptor mutant db/db mouse is a widely used diabetes model presenting hyperglycemia, hyperlipidemia, obesity, and desensitization of insulin signaling pathway. The kidney injury in db/db mice was well established and the potential pathogenic factors may include the hyperglycemia, lipid disorders, inflammation, and hemodynamic disorders [27, 28].

It has been shown that the renal PGE2 level is elevated in STZ type-1 diabetic animals. Recently, evidence demonstrated a detrimental role of PGE2 in the development of DN in type-1 diabetes via EP1 and/or EP4 receptors [12, 13]. However, whether the renal PGE2 in db/db mice plays a role in diabetic kidney injury is still unknown. Considering the more complicated metabolic disorders in db/db mice, the potential mechanism leading to the kidney injury in this mouse model may significantly differ from STZ-diabetic mice. Therefore, it is worthwhile to examine the regulation of renal PGE2 and its synthetic pathway in db/db mice.

In the present study, we found a remarkable elevation of urinary PGE2 in db/db mice. Meanwhile, the renal mPGES-1 protein was also markedly upregulated in glomeruli, which may contribute to increased renal PGE2 production in these mice. In contrast, renal mPGES-1 expression was not altered in type-1 diabetic mouse model induced by STZ, and the systemic deletion of mPGES-1 played no role in renal PGE2 induction, diabetes onset, and the kidney injury in STZ diabetes (data not shown). This discrepancy of mPGES-1 regulation between two models is possibly due to the different pathogenic mechanism of kidney injury.

Unlike mPGES-1, both mPGES-2 and cPGES were not significantly affected in the kidneys of db/db mice. COX-1 and COX-2 are the upstream enzymes of PGE2 synthases providing the substrate of PGH2 to produce PGE2 and other prostanoids. In agreement with findings from Zucker rats [29], we found that COX-2, but not COX-1, was higher in the kidneys of db/db mice. To further elucidate the potential effect of prostaglandin E2 degradation on the renal PGE2 production, we examined 15-PGDH, an enzyme responsible

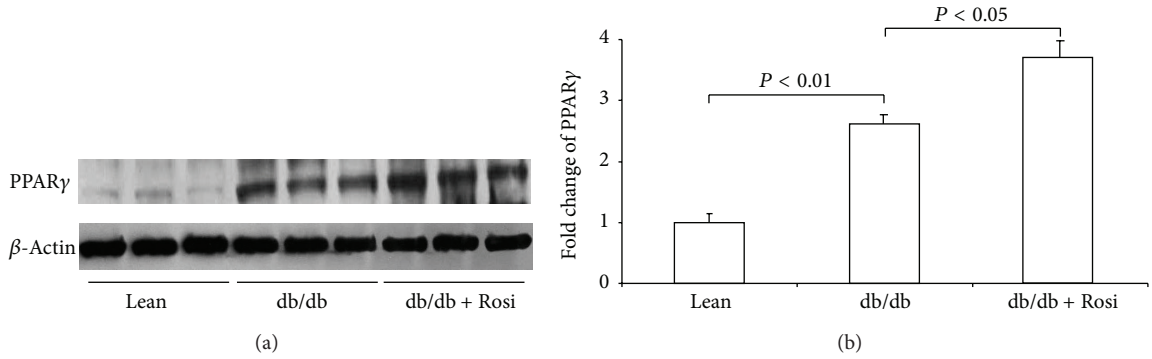

Figure 6: Protein expression of PPARγ in kidneys of db/db mice after Rosi treatment. (a) Western blot of PPARγ and β-actin. (b) Densitometry of western blots. N = 4-5 for each group. Data are mean ± SE.

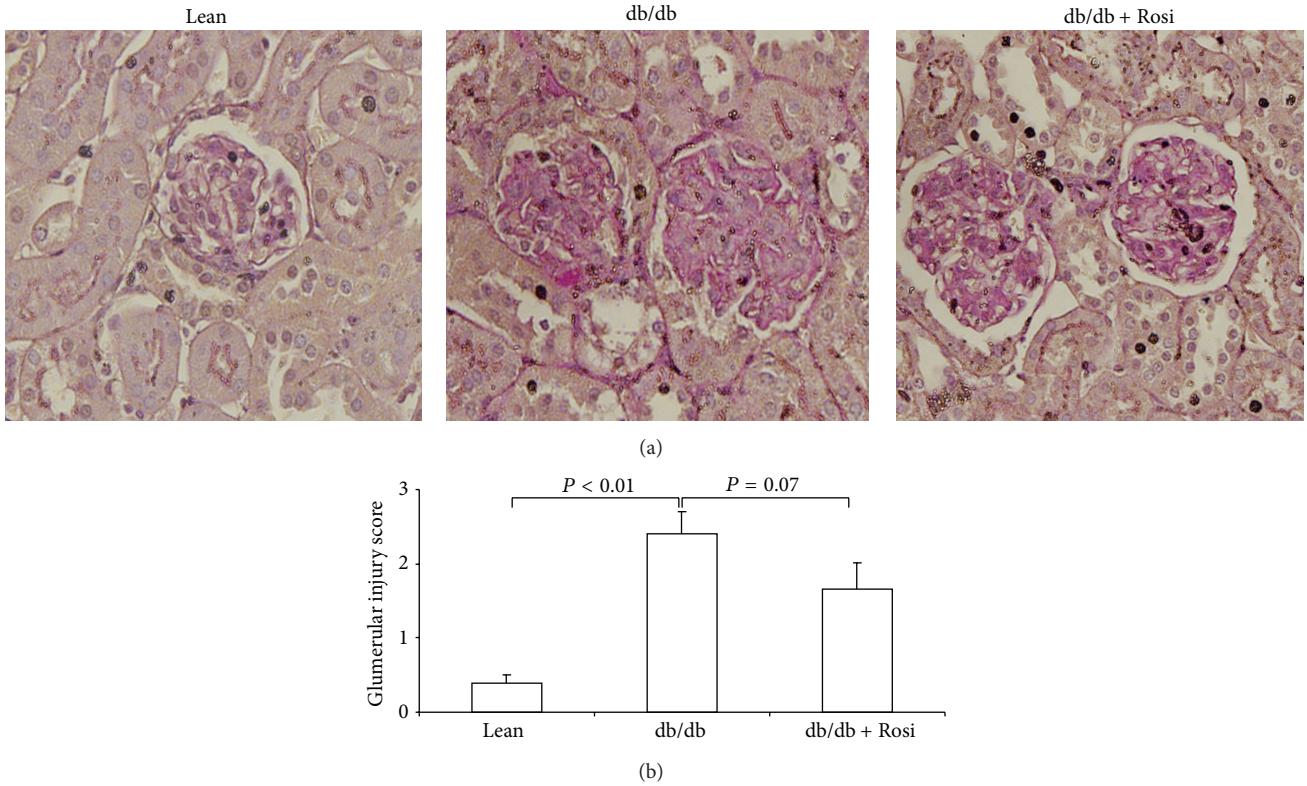

Figure 7: Evaluation of glomerular injury by PAS staining in db/db mice following Rosi treatment. (a) PAS staining. (b) Glomerular injury score. N = 4-5 for each group. Data are mean ± SE.

for the prostaglandins degradation, and found no change in the kidneys of db/db mice.

PPARγ agonists including Rosi and piglitazone are potent agents in treatment of type-2 diabetes mainly via sensitizing the insulin signaling [19, 30–32]. Accumulating evidence demonstrated the beneficial role of PPARγ activation in protecting the diabetic kidney [19–22]. Similarly, our result also showed a trend improvement of glomerular injury following a short period Rosi therapy (7 days). However, the interaction between PPARγ and renal PGE2 production in diabetic kidney is still unidentified. In the present study, we observed that PPARγ agonist Rosi robustly attenuated renal mPGES-1 induction in db/db mice without affecting COX-2 expression. This reduced mPGES-1 protein expression after Rosi treatment could account for the decreased urinary PGE2 excretion. The unaltered high COX-2 expression may contribute to the remained higher urinary PGE2 level in Rosi-treated db/db mice contrasting with the lean controls. The mechanism relating to the Rosi effect on the downregulation of mPGES-1/PGE2 pathway could be complicated. First, this effect might be related to the glycemic control by Rosi. As shown by previous reports, Rosi markedly decreased the blood glucose level in db/db mice [23, 33–35]. Our result also showed that a moderate hyperglycemia in this

obese-diabetic db/db mouse strain was almost normalized following 1-week Rosi therapy. Although this antihyperglycemic effect has to be considered for the downregulation of renal mPGES-1/PGE2/pathway, a separate study from our group strongly disagrees with this possibility. In that study, renal mPGES-1 expression was not regulated in STZ-diabetic mouse and mPGES-1 deletion did not affect renal PGE2 induction during 6 weeks of diabetes. Secondly, it is known that COX-2/mPGES-1/PGE2 signaling is highly inducible by various inflammatory stimuli. Moreover, the enhanced inflammatory response in the kidneys of db/db mice was confirmed by numerous studies [16, 36, 37]. Therefore, inflammation does serve as a candidate in stimulating the renal mPGES-1/PGE2 pathway in db/db mice, and the anti-inflammatory property of Rosi might be responsible for the suppression of this pathway. Thirdly, we can not rule out the direct effect of leptin receptor mutation on the renal mPGES-1/PGE2 induction and the potential interaction between leptin receptor and PPARγ in modulation of mPGES-1/PGE2 pathway. At last, the urine flow may also need to be considered. PGE2 exerts diuretic effect leading to the increase of urine flow [38–44]. Oppositely, the urine flow can stimulate renal tubular PGE2 production [45]. However, 1-week Rosi treatment did not affect the urine volume in db/db mice, which largely excluded this possibility.

It had been reported that EP1 and EP4 receptors were involved in the glomerular injury in STZ-diabetic mice [12, 13]. By qRT-PCR, Rosi treatment led to a moderate but significant reduction of EP4 in contrast to the unaltered EP1. In addition, we also examined the urinary excretion of PGD2, 6-keto-PGF1α, and TXB2. Unlike PGE2, none of them was influenced by Rosi therapy. These results indicated a selective action of Rosi on renal prostanoids production.

In summary, employing the db/db mice, we found that renal mPGES-1/PGE2 pathway was robustly induced and such an induction was markedly suppressed by PPARγ agonist Rosi. These results highly suggested an interaction between PPARγ and mPGES-1/PGE2/EP4 pathway in the kidneys of db/db mice. The downregulation of mPGES-1/PGE2/EP4 pathway possibly contributes to the protective effect of PPARγ on type-2 diabetes-associated DN. To further validate this hypothesis, blockade of mPGES-1 or EP4 in leptin receptor mutant animals by pharmacological strategies or genetic disruption will be of very importance in the future.

Conflict of Interests

All the authors declare no competing interests, including relevant financial interests, activities, relationships, and affiliations.

Acknowledgments

This work was supported by the VA Merit Review (T. Yang), the National Institutes of Health Grant no. DK079162 (T. Yang), and a Scientist Develop Grant (11SDG7480006) to Z. Jia. T. Yang is an Established Investigator from the American Heart Association and Research Career Scientist in the Department of Veterans Affairs.

References

[1] P. A. Craven and F. R. DeRubertis, "Role for local prostaglandin and thromboxane production in the regulation of glomerular filtration rate in the rat with streptozocin-induced diabetes," *Journal of Laboratory and Clinical Medicine*, vol. 113, no. 6, pp. 674–681, 1989.

[2] F. R. DeRubertis and P. A. Craven, "Eicosanoids in the pathogenesis of the functional and structural alterations of the kidney in diabetes," *The American Journal of Kidney Diseases*, vol. 22, no. 5, pp. 727–735, 1993.

[3] R. Ishibashi, I. Tanaka, M. Kotani et al., "Roles of prostaglandin E receptors in mesangial cells under high-glucose conditions," *Kidney International*, vol. 56, no. 2, pp. 589–600, 1999.

[4] M. Schambelan, S. Blake, J. Sraer, M. Bens, M. P. Nivez, and F. Wahbe, "Increased prostaglandin production by glomeruli isolated from rats with streptozotocin-induced diabetes mellitus," *Journal of Clinical Investigation*, vol. 75, no. 2, pp. 404–412, 1985.

[5] H. Schramek, E. Coroneos, and M. J. Dunn, "Interactions of the vasoconstrictor peptides, angiotensin II and endothelin-1, with vasodilatory prostaglandins," *Seminars in Nephrology*, vol. 15, no. 3, pp. 195–204, 1995.

[6] B. M. Chapnick, P. W. Paustian, E. Klainer, P. D. Joiner, A. L. Hyman, and P. J. Kadowitz, "Influence of prostaglandins E, A and F on vasoconstrictor responses to norepinephrine, renal nerve stimulation and angiotensin in the feline kidney," *Journal of Pharmacology and Experimental Therapeutics*, vol. 196, no. 1, pp. 44–52, 1976.

[7] F. Catella-Lawson, B. Mcadam, B. W. Morrison et al., "Effects of specific inhibition of cyclooxygenase-2 on sodium balance, hemodynamics, and vasoactive eicosanoids," *Journal of Pharmacology and Experimental Therapeutics*, vol. 289, no. 2, pp. 735–741, 1999.

[8] M. D. Breyer and R. M. Breyer, "Prostaglandin E receptors and the kidney," *The American Journal of Physiology—Renal Physiology*, vol. 279, no. 1, pp. F12–F23, 2000.

[9] E. P. Silldorff, S. Yang, and T. L. Pallone, "Prostaglandin E2 abrogates endothelin-induced vasoconstriction in renal outer medullary descending vasa recta of the rat," *Journal of Clinical Investigation*, vol. 95, no. 6, pp. 2734–2740, 1995.

[10] N. Kvirkvelia, M. McMenamin, K. Chaudhary, M. Bartoli, and M. P. Madaio, "Prostaglandin E2 promotes cellular recovery from established nephrotoxic serum nephritis in mice, pro-survival, and regenerative effects on glomerular cells," *The American Journal of Physiology—Renal Physiology*, vol. 304, no. 5, pp. F463–F470, 2013.

[11] R. Nasrallah, H. Xiong, and R. L. Hébert, "Renal prostaglandin E2 receptor (EP) expression profile is altered in streptozotocin and B6-Ins2Akita type I diabetic mice," *The American Journal of Physiology—Renal Physiology*, vol. 292, no. 1, pp. F278–F284, 2007.

[12] H. Makino, I. Tanaka, M. Mukoyama et al., "Prevention of diabetic nephropathy in rats by prostaglandin E receptor EP1-selective antagonist," *Journal of the American Society of Nephrology*, vol. 13, no. 7, pp. 1757–1765, 2002.

[13] R. Mohamed, C. Jayakumar, and G. Ramesh, "Chronic administration of EP4-selective agonist exacerbates albuminuria and

fibrosis of the kidney in streptozotocin-induced diabetic mice through IL-6," *Laboratory Investigation*, vol. 93, pp. 933–945, 2013.

[14] H. Chen, O. Charlat, L. A. Tartaglia et al., "Evidence that the diabetes gene encodes the leptin receptor: identification of a mutation in the leptin receptor gene in db/db mice," *Cell*, vol. 84, no. 3, pp. 491–495, 1996.

[15] G. H. Lee, R. Proenca, J. M. Montez et al., "Abnormal splicing of the leptin receptor in diabetic mice," *Nature*, vol. 379, no. 6566, pp. 632–635, 1996.

[16] Y. Liu, Z. Jia, S. Liu et al., "Combined losartan and nitro-oleic acid remarkably improves diabetic nephropathy in mice," *The American Journal of Physiology—Renal Physiology*, vol. 305, no. 11, pp. F1555–F1562, 2013.

[17] Y. Guan, "Peroxisome proliferator-activated receptor family and its relationship to renal complications of the metabolic syndrome," *Journal of the American Society of Nephrology*, vol. 15, no. 11, pp. 2801–2815, 2004.

[18] Y. Guan, J. Yang, L. Chen et al., "PPARs and female reproduction: evidence from genetically manipulated mice," *PPAR Research*, vol. 2008, Article ID 723243, 8 pages, 2008.

[19] F. Zheng and Y. Guan, "Thiazolidinediones: a novel class of drugs for the prevention of diabetic nephropathy?" *Kidney International*, vol. 72, no. 11, pp. 1301–1303, 2007.

[20] Y. Miyazaki, E. Cersosimo, C. Triplitt, and R. A. DeFronzo, "Rosiglitazone decreases albuminuria in type 2 diabetic patients," *Kidney International*, vol. 72, no. 11, pp. 1367–1373, 2007.

[21] F. Pistrosch, K. Herbrig, B. Kindel, J. Passauer, S. Fischer, and P. Gross, "Rosiglitazone improves glomerular hyperfiltration, renal endothelial dysfunction, and microalbuminuria of incipient diabetic nephropathy in patients," *Diabetes*, vol. 54, no. 7, pp. 2206–2211, 2005.

[22] J. Yang, D. Zhang, J. Li, X. Zhang, F. Fan, and Y. Guan, "Role of PPARγ in renoprotection in type 2 diabetes: molecular mechanisms and therapeutic potential," *Clinical Science*, vol. 116, no. 1, pp. 17–26, 2009.

[23] L. Zhou, G. Liu, Z. Jia et al., "Increased susceptibility of db/db mice to rosiglitazone-induced plasma volume expansion: role of dysregulation of renal water transporters," *The American Journal of Physiology—Renal Physiology*, vol. 305, no. 10, pp. F1491–F1497, 2013.

[24] Z. Jia, H. Wang, and T. Yang, "Microsomal prostaglandin e synthase 1 deletion retards renal disease progression but exacerbates anemia in mice with renal mass reduction," *Hypertension*, vol. 59, no. 1, pp. 122–128, 2012.

[25] A. Paliege, D. Mizel, C. Medina et al., "Inhibition of nNOS expression in the macula densa by COX-2-derived prostaglandin E2," *The American Journal of Physiology—Renal Physiology*, vol. 287, no. 1, pp. F152–F159, 2004.

[26] E. Kassi, P. Pervanidou, G. Kaltsas, and G. Chrousos, "Metabolic syndrome: definitions and controversies," *BMC Medicine*, vol. 9, article 48, 2011.

[27] V. Ninichuk, A. G. Khandoga, S. Segerer et al., "The role of interstitial macrophages in nephropathy of type 2 diabetic db/db mice," *The American Journal of Pathology*, vol. 170, no. 4, pp. 1267–1276, 2007.

[28] V. Ninichuk, O. Kulkarni, S. Clauss, and H. Anders, "Tubular atrophy, interstitial fibrosis, and inflammation in type 2 diabetic db/db mice. An accelerated model of advanced diabetic nephropathy," *European Journal of Medical Research*, vol. 12, no. 8, pp. 351–355, 2007.

[29] A. Dey, R. S. Williams, D. M. Pollock et al., "Altered kidney CYP2C and cyclooxygenase-2 levels are associated with obesity-related albuminuria," *Obesity Research*, vol. 12, no. 8, pp. 1278–1289, 2004.

[30] H. Yki-Jarvinen, "ADOPT: lessons from comparison of glycemic durability of rosiglitazone, metformin, or glyburide monotherapy," *Current Diabetes Reports*, vol. 7, no. 3, pp. 173–174, 2007.

[31] C. Sosnowski and E. Janeczko-Sosnowska, "Commentary to the article: Kahn SE, Haffner SM, Heise MA, et al. ADOPT Study Group. Glycemic durability of rosiglitazone, metformin, or glyburide monotherapy. N Engl J Med 2006; 355: 2427–43," *Kardiologia Polska*, vol. 65, no. 2, pp. 214–217, 2007.

[32] S. E. Kahn, S. M. Haffner, M. A. Heise et al., "Glycemic durability of rosiglitazone, metformin, or glyburide monotherapy," *The New England Journal of Medicine*, vol. 355, no. 23, pp. 2427–2443, 2006.

[33] H. Ye, H. J. Zhang, A. Xu, and R. L. Hoo, "Resistin production from adipose tissue is decreased in db/db obese mice, and is reversed by rosiglitazone," *PLoS ONE*, vol. 8, no. 6, Article ID e65543, 2013.

[34] H. Chodavarapu, N. Grobe, H. K. Somineni, E. S. Salem, M. Madhu, and K. M. Elased, "Rosiglitazone treatment of type 2 diabetic db/db mice attenuates urinary albumin and angiotensin converting enzyme 2 excretion," *PLoS ONE*, vol. 8, no. 4, Article ID e62833, 2013.

[35] J. Tonelli, W. Li, P. Kishore et al., "Mechanisms of early insulin-sensitizing effects of thiazolidinediones in type 2 diabetes," *Diabetes*, vol. 53, pp. 1621–1629, 2004.

[36] E. Galkina and K. Ley, "Leukocyte recruitment and vascular injury in diabetic nephropathy," *Journal of the American Society of Nephrology*, vol. 17, no. 2, pp. 368–377, 2006.

[37] T. Furuta, T. Saito, T. Ootaka et al., "The role of macrophages in diabetic glomerulosclerosis," *The American Journal of Kidney Diseases*, vol. 21, no. 5, pp. 480–485, 1993.

[38] R. G. Parnova, "Molecular mechanisms of action of prostaglandin E2 in the regulation of water osmotic permeability," *Membrane and Cell Biology*, vol. 13, no. 2, pp. 287–301, 2000.

[39] Z. Jia, G. Liu, Y. Sun et al., "mPGES-1-derived PGE2 mediates dehydration natriuresis," *The American Journal of Physiology—Renal Physiology*, vol. 304, no. 2, pp. F214–F221, 2013.

[40] Z. Jia, G. Liu, M. Downton, Z. Dong, A. Zhang, and T. Yang, "mPGES-1 deletion potentiates urine concentrating capability after water deprivation," *The American Journal of Physiology—Renal Physiology*, vol. 302, no. 8, pp. F1005–F1012, 2012.

[41] Z. Jia, T. Aoyagi, D. E. Kohan, and T. Yang, "mPGES-1 deletion impairs aldosterone escape and enhances sodium appetite," *The American Journal of Physiology—Renal Physiology*, vol. 299, no. 1, pp. F155–F166, 2010.

[42] Z. Jia, T. Aoyagi, and T. Yang, "MPGES-1 protects against DOCA-salt hypertension via inhibition of oxidative stress or stimulation of NO/cGMP," *Hypertension*, vol. 55, no. 2, pp. 539–546, 2010.

[43] Z. Jia, H. Wang, and T. Yang, "Mice lacking mPGES-1 are resistant to lithium-induced polyuria," *The American Journal of Physiology—Renal Physiology*, vol. 297, no. 6, pp. F1689–F1696, 2009.

[44] S. Soodvilai, Z. Jia, M. H. Wang, Z. Dong, and T. Yang, "mPGES-1 deletion impairs diuretic response to acute water loading," *The American Journal of Physiology—Renal Physiology*, vol. 296, no. 5, pp. F1129–F1135, 2009.

[45] D. Flores, Y. Liu, W. Liu, L. M. Satlin, and R. Rohatgi, "Flow-induced prostaglandin E2 release regulates Na and K transport in the collecting duct," *The American Journal of Physiology—Renal Physiology*, vol. 303, no. 5, pp. F632–F638, 2012.

Hindawi Publishing Corporation
PPAR Research
Volume 2013, Article ID 927915, 8 pages
http://dx.doi.org/10.1155/2013/927915

Research Article

Correlation between PPAR Gene Polymorphisms and Primary Nephrotic Syndrome in Children

Jiaping Jin,[1] Guixia Ding,[1] Huaying Bao,[1] Ying Chen,[1] Yuan Han,[1] Fei Zhao,[1] Songming Huang,[1,2] and Aihua Zhang[1,2]

[1] *Department of Nephrology, Nanjing Children's Hospital, Nanjing Medical University, 72 Guangzhou Road, Nanjing, Jiangsu 210008, China*
[2] *Institute of Pediatrics, Nanjing Medical University, Nanjing, Jiangsu 210029, China*

Correspondence should be addressed to Aihua Zhang; zhaihua@njmu.edu.cn

Received 1 July 2013; Accepted 11 August 2013

Academic Editor: Zhanjun Jia

Pediatric primary nephrotic syndrome (PNS) is a chronic disease promoted by metabolic and immune dysfunctions. Peroxisome proliferator-activated receptor (PPAR) polymorphisms have been associated with a variety of metabolic and kidney disorders. We therefore hypothesized that PPAR polymorphisms might be involved in the pathophysiology of PNS. We compared the distributions of the PPAR-γ Pro12Ala and Val290Met, PPAR-γ coactivator-α (PGC-1α) Gly482Ser, and PPAR-α Leu162Val single nucleotide polymorphisms (SNPs) between children with PNS and normal controls and analyzed their correlations with clinical and metabolic indicators and steroid responsiveness. There were no significant differences in distributions of any of the polymorphisms between PNS cases and controls. However, PNS patients with the PPAR-γ (Pro12Ala) PP genotype had significantly higher fasting serum insulin, IgA, and HOMA-IR levels and lower insulin sensitivity than did patients with PA and AA genotypes. Additionally, the PGC-1α (Gly482Ser) A allele was associated with lower CD8+ T-cell counts and higher triglyceride and complement C3 levels compared with the G allele. No polymorphisms were related to hormone sensitivity. These results suggest that the PPAR-γ (Pro12Ala) and PGC-1α (Gly482Ser) SNPs may influence insulin and triglyceride metabolism in children with PNS and may thus be relevant to the prognosis of this chronic condition.

1. Introduction

Peroxisome proliferator-activated receptors (PPARs) are a group of ligand-activated nuclear transcription factors belonging to the type II nuclear receptor superfamily. Three PPAR subtypes, PPAR-α, PPAR-β, and PPAR-γ, have been identified in amphibians, rodents, and humans [1]. Recent studies have shown associations between PPAR gene polymorphisms and metabolic syndrome (MS) and the development of insulin resistance (IR). Gouda et al. [2] performed a meta-analysis of 32,849 patients with type II diabetes mellitus (T2DM) and 47,456 normal controls and found that the PPAR-γ (Pro12Ala) gene polymorphism was associated with IR and T2DM. In addition, Sparsø et al. [3] showed that the PPAR-α (Leu162Val) gene polymorphism was associated with obesity, T2DM, and abnormal lipid metabolism, while Andrulionytè et al. [4] found a link between the PPAR-γ coactivator-α (PGC-1α) Gly482Ser gene polymorphism and conversion from impaired glucose tolerance to T2DM.

Children with primary nephrotic syndrome (PNS) suffer from metabolic abnormalities including glycolipid disorders, altered hemodynamics, and immune dysfunction, and previous studies have demonstrated that these disorders promote the progression of renal diseases and the development of end-stage renal disease (ESRD) [5]. Furthermore, the Ala allele of PPAR-γ was shown to be associated with a reduced glomerular filtration rate (GFR) and increased occurrences of ESRD, cardiovascular events, and mortality in patients with diabetic nephropathy [6]. We therefore hypothesized that PPAR gene polymorphisms may be associated with

the occurrence, clinical manifestations, pathological type, and treatment response in patients with PNS. A better understanding of these relationships may provide a theoretical basis for further studies of the pathophysiological role of PPARs in PNS.

We tested this hypothesis using clinical data from children with PNS and from healthy children (normal controls, NCs). The distributions of the single nucleotide polymorphisms (SNPs) Pro12Ala and Val290Met in the PPAR-γ gene, Gly482Ser in the PGC-1α gene, and Leu162Val in the PPAR-α gene were determined in PNS and NC children. In addition, the associations between these polymorphisms and clinical metabolic indicators, proteinuria, renal pathology, and treatment response in patients with PNS were examined to investigate the pathophysiological role of PPARs in PNS and to determine the potential role of these polymorphisms in treatment planning and prognosis determination in children with PNS.

2. Subjects and Methods

2.1. Subjects. Patients with a diagnosis of PNS treated at the Nanjing Children's Hospital, China, between July 2008 and November 2010 were evaluated. Genotype determinations for Pro12Ala and Val290Met of the PPAR-γ gene and Leu162Val of the PPAR-α gene were performed in 111 PNS patients (80 male, 31 female; mean age 3.33 years, range 0.67–13.08). Genotype determination for Gly482Ser of the PGC-1α gene was performed in 108 patients (78 male, 30 female; mean age 3.47 years, 0.67–13.08). All subjects were diagnosed with PNS according to the diagnostic criteria outlined by the clinical classification diagnosis and treatment of glomerular disease in children [7]. The presence of secondary kidney disease was excluded. None of the included patients were receiving β-blockers, diuretics, calcium-channel blockers, angiotensin-converting enzyme inhibitors, angiotensin II receptor blockers, glucocorticoids, or other immunosuppressants at the time of inclusion.

All patients were followed for between 4 months and 2.5 years, and the duration of followup reflected the response to glucocorticoids. Patients who received steroids were divided into three groups: steroid-responsive nephrotic syndrome (NS), where urine was negative for protein within 8 weeks of treatment ($n = 83$), steroid-resistant NS, where urine still contained protein at 8 weeks ($n = 13$), and steroid-dependent NS, where urinary protein reappeared after the steroid dose was reduced ($n = 12$).

NCs were recruited from patients admitted to the hospital for elective surgery. Genotype determinations for Pro12Ala and Val290Met of the PPAR-γ gene and Leu162Val of the PPAR-α gene were performed in 111 healthy children who received a physical examination at our hospital (94 male, 17 female; mean age 3.5 years, range 0.80–10.75). Genotype determination for Gly482Ser of the PGC-1α gene was performed in 110 NCs (93 male, 17 female; mean age 3.54 years, range 0.80–10.75). A detailed check of medical history was performed to exclude children who had been premature and of low birth weight, had macrosomia, or whose mother had gestational diabetes mellitus or any other significant conditions. Age, sex, and body mass index (BMI) did not differ significantly between the NC and PNS children.

The local ethics committee approved the study, and informed consent was obtained from all participating children and their parents.

2.2. Detection of SNP Positions and Sequencing of PCR Products. DNA was extracted from peripheral venous blood using a genomic DNA purification kit (Qiagen Sciences, Germantown, MD, USA). The SNP genotypes were examined using polymerase chain reaction (PCR) restriction fragment length polymorphism. The primers were synthesized by Invitrogen, and the sequences were as follows: PPAR-γ Pro12Ala sense, 5′-CAAGCCCAGTCCTTTCTGTG-3′; antisense, 5′-GCCTTTCGCTAAGGAAGTGA-3′; PPAR-γ Val290Met sense, 5′-ATTCCTTAATGATGGGAGAA-3′; antisense, 5′-TCCTCTAGTGTCTCATACGGTT-3′; PPAR-α Leu162Val sense, 5′-GACTCAAGCTGGTGTATGACAAGT-3′; antisense, 5′-TAAGACAGCCTTACAGTGTGTTGC-3′; and PGC-1α Gly482Ser sense, 5′-TGCTACCTGAGAGAGACTTTG-3′; antisense, 5′-CTTTCATCTTCGCTGTCATC-3′. The cycling conditions were 95°C for 5 min followed by 30 cycles of 94°C for 30 s, 55°C for 40 s, and 72°C for 30 s. The PCR product for the Pro12Ala position of the PPAR-γ gene was 237 bp in size. Following digestion with the restriction endonuclease Hpa II, the genotypes included PP (217 bp and 20 bp), PA (237 bp, 217 bp, and 20 bp), and AA (237 bp). The size of the PCR amplification product for the Val290Met position of the PPAR-γ gene was 145 bp. Following digestion with the restriction endonuclease Nco I, the genotypes included GG (145 bp), GA (145 bp, 110 bp, and 35 bp), and AA (110 bp and 35 bp). The size of the PCR product for the Leu162Val position of the PPAR-α gene was 117 bp. Following digestion with the restriction endonuclease Hinf I, the genotypes included CC (117 bp), CG (117 bp, 94 bp, and 23 bp), and GG (94 bp and 23 bp). The size of the PCR product for the Gly482Ser position of the PGC-1α gene was 260 bp. Following digestion with the restriction endonuclease Hpa II, the genotypes included GG (149 bp and 111 bp), GA (260 bp, 149 bp, and 111 bp), and AA (260 bp). The PCR products for the Pro12Ala of PPAR-γ and Gly482Ser of PGC-1α gene were sent to BGI (Shanghai) for sequencing. The sequencing results are shown in Figures 1 and 2.

2.3. Physical Measurements. Height and weight were measured in all participants, and the mean of three measurements was used to calculate BMI (BMI = weight/height^2 (kg/m^2)). Blood pressure (BP) was measured using the brachial artery of the right arm (either in a seated position or in the mother's arms), and the process was repeated 2 min later. The mean value of both readings was recorded as the BP for each individual.

2.4. Blood Tests. Blood samples were taken from all participants following a bland meal the previous evening and an overnight fast. Fasting blood glucose (FBG), fasting serum insulin (FISN), fasting serum C-peptide (FCP), blood lipids,

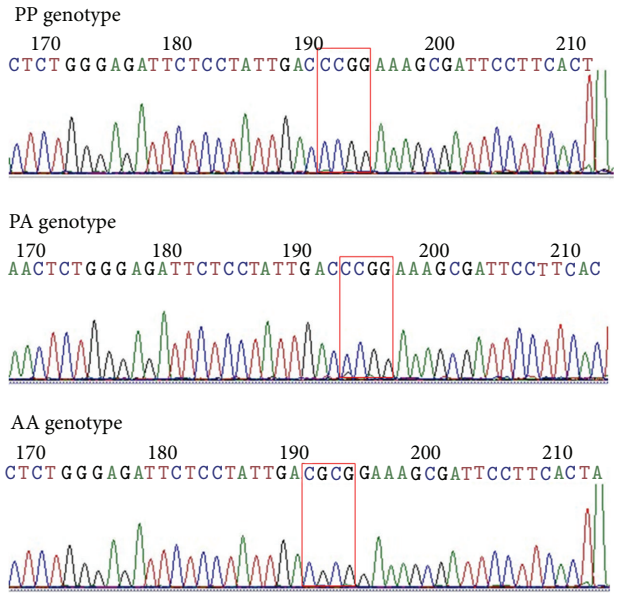

Figure 1: The sequencing map of the PCR amplification product with the PP genotype, the PA genotype, and the AA genotype of the PPAR-γ gene at the Pro12Ala position.

renal function, and coagulation were measured. All samples were obtained prior to steroid treatment. The kits for serum measurements and the 7600 automatic biochemical analyzer were provided by Hitachi (Japan). FISN and FCP were tested by chemiluminescence assays using kits and an Elecsys 2010 (Roche).

2.5. Calculation of HOMA-IR, Islet β-Cell Function, and Insulin Sensitivity Index. Homeostasis model assessment of insulin resistance (HOMA-IR), islet β-cell function (HOMA-islet), and insulin sensitivity index (ISI) were calculated using the following formulae: HOMA-IR = FBG $\times$ FISN/22.5; HOMA-islet = 20 $\times$ FISN/(FBG $-$ 3.5); ISI = ln (1/FBG $\times$ FISN) [7] (FISN mU/L; FBG mmol/L).

2.6. Statistical Analyses. The group representation of the distribution of sample genotypes was estimated using the Hardy-Weinberg equilibrium. The frequency of each genotype was calculated using the gene-counting method. Normally distributed data were presented as mean $\pm$ standard deviation, and nonnormally distributed data were presented as median (range). The means of two groups with normal distributions were compared using t-tests or analysis of variance, and nonnormally distributed data were compared using nonparametric tests. Classified data were analyzed using χ^2 tests or logistic regression. Analyses were performed using SPSS 16.0 software, and P values < 0.05 were considered statistically significant.

3. Results

3.1. Comparison of PPAR-γ (Pro12Ala) and PGC-1α (Gly482Ser) Genotypes between PNS and NC Groups. The frequencies of the PPAR-γ (Pro12Ala) and PGC-1α (Gly482Ser) genotypes in NC children conformed to the Hardy-Weinberg equilibrium. There were no significant differences in distributions of the PPAR-γ (Pro12Ala) and PGC-1α (Gly482Ser) genotypes between PNS and NC children ($P > 0.99$ and $P = 0.324$, resp.). The results are shown in Tables 1 and 2.

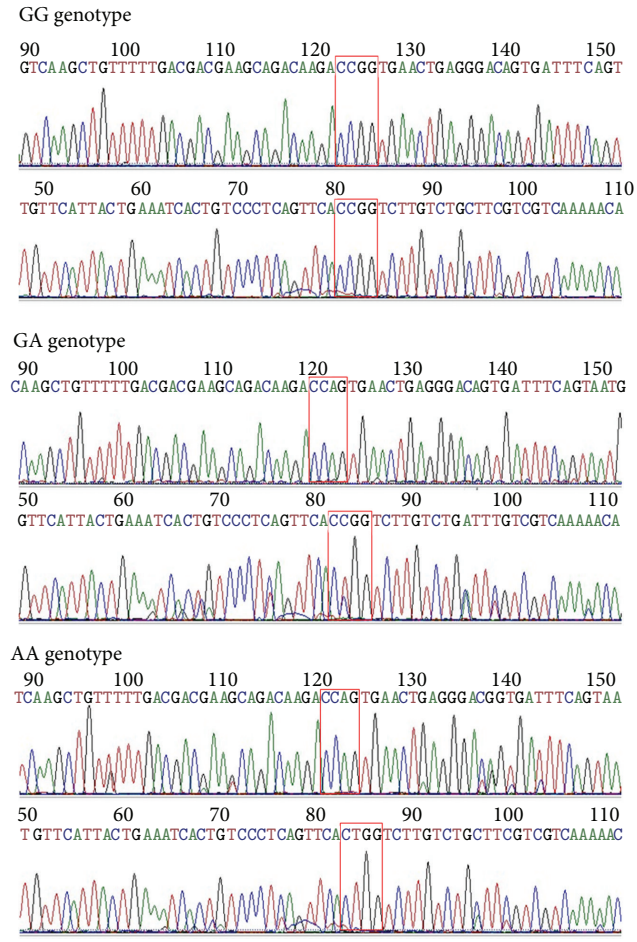

Figure 2: The sequencing map of the PCR amplification product for the GG genotype, the GA genotype, and the AA genotype of the PGC-1α gene at the Gly482Ser position.

3.2. Comparison of Clinical Data between Individuals with Different Genotypes in the PNS Group. The results of a further-stratified analysis of the PPAR-γ (Pro12Ala) genotypes in PNS children are shown in Table 3. There were no significant differences in any of the following parameters among children with PNS with different PPAR-γ (Pro12Ala) genotypes: sex, age, BMI, levels of albumin (ALB), blood urea nitrogen (BUN), serum creatinine (Scr), blood uric acid (UA), GFR, total cholesterol (TC), triglycerides (TG), high-density lipoprotein (HDL-c), fibrinogen (Fbg), FBG, FCP, immunoglobulin G/M (IgG and IgM), complement C3 and C4, frequencies of CD3+ T cells, CD4+ T cells, CD8+ T cells, NK cells, and B lymphocytes, HOMA-islet values, and 24h urine protein (24-UP). However, patients with the PP genotype demonstrated significantly higher levels of FISN,

Table 1: The distribution of PPAR-γ (Pro12Ala) genotypes among PNS and NC children.

PPAR-γ genotype	PNS group		NC group		χ^2	OR (95% CI)	P value
	n	%	n	%			
PP	103	92.8	103	92.8	1.031	1	1.000
PA/AA	8	7.2	8	7.2		1.000 (0.312–2.766)	

Table 2: The distribution of PGC-1α (Gly482Ser) genotypes among PNS and NC children.

PGC-1α genotype	PNS group		NC group		χ^2	OR (95% CI)	P value
	n	%	n	%			
GG	18	16.7	20	18.2	2.253	1.037 (0.502–2.144)	0.324
GA	59	54.6	68	61.8		0.639 (0.276–1.478)	
AA	31	28.7	22	20.0		1	

Table 3: Stratified analysis of the PPAR-γ (Pro12Ala) genotypes among PNS children.

Subjects	PPAR-γ genotype		$t/t'/\chi^2/z$	P value
	PP	PA/AA		
Gender (male/female)	74/29	6/2	0.000	1.000
Age (years)	3.67 (0.67–13.08)	3.00 (1.50–4.25)	−1.562	0.118
BMI	17.07 ± 0.22	17.24 ± 0.77	−0.205	0.838
sBP (kp)	14.28 ± 0.14	14.21 ± 0.29	0.120	0.905
dBP (kp)	9.16 ± 0.10	9.18 ± 0.37	−0.046	0.963
ALB (g/L)	17.70 (11.20–37.00)	18.95 (16.80–26.30)	−1.283	0.199
BUN (mmol/L)	4.00 (0.50–16.30)	2.60 (2.20–21.50)	−1.689	0.091
Scr (μmol/L)	37.20 (18.30–207.60)	33.45 (27.60–51.50)	−1.032	0.302
UA (mmol/L)	350.76 ± 10.96	347.88 ± 34.60	0.071	0.943
GFR (mL/(min·1.73 m^2))	137.54 ± 3.47	137.56 ± 8.75	−0.002	0.999
TC (mmol/L)	9.89 ± 0.28	9.37 ± 0.76	0.498	0.619
TG (mmol/L)	2.46 (0.77–8.03)	2.26 (1.36–6.33)	−0.160	0.873
HDL-c (mmol/L)	1.49 ± 0.06	1.46 ± 0.18	0.170	0.865
Fbg (g/L)	4.58 ± 0.16	3.37 ± 2.26	0.536	0.686
IgA (g/L)	1.06 ± 0.04	0.81 ± 0.08	2.701	**0.020***
IgG (g/L)	2.26 (1.36–11.00)	2.31 (1.46–4.79)	−0.364	0.716
IgM (g/L)	1.70 ± 0.06	1.92 ± 0.27	−0.934	0.352
C3 (g/L)	2.49 ± 1.22	1.28 ± 0.06	0.279	0.781
C4 (g/L)	0.29 ± 0.01	0.27 ± 0.02	0.484	0.629
T (CD3+) (%)	68.95 ± 1.09	60.00 ± 7.11	1.700	0.093
T (CD4+) (%)	35.62 ± 0.96	31.25 ± 6.42	0.940	0.350
T (CD8+) (%)	27.92 ± 0.76	21.50 ± 3.95	1.764	0.081
NK (%)	8.00 (2.00–44.00)	5.00 (2.00–31.00)	−0.943	0.367
BC (%)	18.85 ± 0.87	23.75 ± 6.18	−1.156	0.251
FBG (mmol/L)	4.88 ± 0.06	4.84 ± 0.26	0.162	0.872
FISN (mU/L)	2.27 (0.20–16.63)	0.92 (0.20–3.17)	−2.526	**0.012***
FCP (nmol/L)	0.47 (0.18–1.95)	0.41 (0.22–0.98)	−0.981	0.327
HOMA-IR	0.48 (0.04–4.31)	0.16 (0.05–0.82)	−2.566	0.060
HOMA-islet	38.06 (−141.54–895.56)	27.06 (2.50–90.94)	−1.460	0.144
ISI	−2.46 ± 0.10	−1.46 ± 0.33	−2.777	**0.006****
24-h UP (mg/kg)	141.15 (2.96–1179.80)	117.84 (7.41–410.00)	−0.871	0.384

$^*P < 0.05$, $^{**}P < 0.01$.

IgA, and HOMA-IR and lower levels of ISI compared with patients with PA and AA genotypes.

The results of a further-stratified analysis of the PGC-1α (Gly482Ser) genotypes among PNS children are shown in Table 4. There were no significant differences in any of the following parameters among children with PNS with different PGC-1α (Gly482Ser) genotypes: sex, age, BMI, ALB, BUN, Scr, UA, GFR, TC, HDL-c, Fbg, IgA, IgG, IgM, FBG, FISN, FCP, and C4, frequencies of CD3+ T cells, CD4+ T cells, NK cells, and B lymphocytes, HOMA-IR, HOMA-islet, ISI values, and 24-UP. However, patients with the A allele demonstrated lower levels of CD8+ T cells and higher levels of TG and complement C3 than did patients with the G allele.

The distribution of genes among children with PNS of different pathological types was analyzed by single-factor analysis of variance. There were no significant differences in PPAR-γ (Pro12Ala) and PGC-1α (Gly482Ser) genotypes between individuals with different renal pathological types. The results are shown in Tables 5 and 6.

Gene distributions among children with PNS who demonstrated different responses to hormone treatment were analyzed by χ^2 tests and single-factor analysis of variance. There were no significant differences in PPAR-γ (Pro12Ala) and PGC-1α (Gly482Ser) genotypes among patients with different responses to hormone treatment. The results are shown in Tables 7 and 8.

4. Discussion

PPAR-γ receptors can be divided into three subtypes: γl, γ2, and γ3. Several PPAR-γ2 mutations have been discovered, of which the most common is the CCA-GCA mutation at the 12th codon in exon 2, which results in the conversion of proline to alanine. This Pro12Ala gene polymorphism was first reported by Chung-Jen et al. [8] in a study of 34 Caucasian individuals. The mutation frequencies for Prol2Ala vary greatly among different ethnic groups: 12% in Caucasians, 10% in Americans, 4% in Japanese, and 2% in Chinese. Our study found the frequency of the A allele to be 3.8% and that of the P allele to be 96.2%. Other gene mutations of PPAR-γ2 (Prol15Gin, Val290Met, and Rro467Leu) exist at low frequencies and have smaller impacts on the population; however, the manifestations of these mutations include severe IR, local abnormal lipid metabolism, T2DM, and hypertension. The current study demonstrated that the Val290Met mutation in the PPAR-γ2 gene was absent in all 111 PNS and 111 NC children studied. Moreover, no patients in the current study suffered from severe IR, local abnormal lipid metabolism, T2DM, or hypertension; these observations support the rarity of this mutation.

Previous studies showed an association between the Pro12Ala mutation and blood lipid levels, cardiovascular events, insulin sensitivity, T2DM, and renal function [2, 6, 9, 10]. Compared with NC children, children with PNS demonstrated increased BP, decreased GFR, increased Scr, hyperuricemia, hyperlipidemia, increased serum C-peptide levels, and decreased islet β-cell function during the early stage of the disease, though these patients did not demonstrate IR, a hypercoagulable state, or evidence of an immune inflammatory response. These results suggest that these characteristics may be correlated with the Pro12Ala gene polymorphism. We analyzed the distributions of two different genotypes in PNS and NC children and unexpectedly found no association between the Pro12Ala gene polymorphism and PNS occurrence. A further-stratified analysis in children with PNS showed that insulin levels and islet β-cell function were decreased and insulin sensitivity was increased in patients with the A allele, after matching for age, sex, and BMI. Stefan et al. [11] demonstrated that this mutation was associated with free fatty acid-induced reduction of second-phase insulin secretion in a healthy population with normal body weight. Furthermore, a large population study in Italian and Brazilian Caucasians showed that the A allele was significantly associated with increased insulin sensitivity [12], suggesting that the A allele may have distinct effects on insulin secretion and insulin sensitivity. However, the effects of the Pro12Ala polymorphism on insulin secretion and sensitivity remain inconclusive. Although most studies have shown that patients with mutations at this site have decreased insulin secretion capacity and increased insulin sensitivity, the specific mechanisms responsible for these effects remain unclear.

Previous studies confirmed that PPAR-γ participates in the pathophysiology of kidney diseases; its activation can reduce BP, delay renal arteriosclerosis, reduce proteinuria and Scr, and reverse the process of glomerulosclerosis and interstitial fibrosis, which are closely associated with prognosis in patients with kidney diseases. The Cys161Thr polymorphism of the PPAR-γ2 gene is associated with survival in patients with nonhypertensive IgA nephropathy [13]. We analyzed the association between the Pro12Ala polymorphism of the PPAR-γ2 gene and response to treatment in PNS patients and found no differences in genotype distributions between hormone-sensitive, hormone-resistant, and hormone-dependent patients. We were therefore unable to conclude that the Pro12Ala polymorphism of PPAR-γ2 could predict response to hormone treatment. Although no mutations in this gene were detected in children in the hormone-resistant group, this could have been because of the low mutation frequency of the A allele or the small sample size. In addition, the follow-up period in this study was short, and indicators such as progression to ESRD, survival rate, and complications could not be compared. Further follow-up studies are needed to address these factors.

Evidence has shown that PGC-1α is closely associated with MS and IR, and studies in different ethnic groups have found linkage between the chromosomal fragment of the PGC-1α gene and MS-related manifestations. Our study demonstrated that the frequency of the G allele was 46.6% and that of the A allele was 53.4%. Many previous studies have shown associations between the Gly482Ser polymorphism of the PGC-1α gene and IR, obesity, and type II diabetes [4]. Compared with NC children, children with PNS demonstrated increased BP, decreased GFR, increased Scr, hyperuricemia, hyperlipidemia, increased FCP, and decreased islet β-cell function at the time of disease onset, but did not have apparent IR, a hypercoagulable state, or evidence of an immune inflammatory response. We therefore speculated that this phenomenon might be associated with

Table 4: Stratified analysis of the PGC-1α (Gly482Ser) genotypes among PNS children.

Subjects	PGC-1α gene			χ^2/F	P value
	GA	AA	GG		
Gender (male/female)	46/13	21/10	11/7	2.388	0.303
Age (years)	3.60 (1.50–13.08)	3.00 (0.67–10.58)	4.40 (1.33–9.80)	3.058	0.217
BMI	16.84 ± 0.29	17.47 ± 0.36	16.98 ± 0.54	0.874	0.420
sBP (kp)	14.18 ± 0.17	14.36 ± 0.29	14.49 ± 0.34	0.384	0.682
dBP (kp)	9.15 ± 0.13	9.14 ± 0.18	9.19 ± 0.32	0.014	0.986
ALB (g/L)	17.60 (11.20–37.00)	18.10 (12.80–26.30)	18.40 (11.30–27.60)	0.327	0.849
BUN (mmol/L)	4.10 (2.30–21.50)	3.50 (0.50–16.30)	3.85 (2.20–13.10)	3.363	0.186
Scr (μmol/L)	37.20 (18.30–67.80)	36.50 (23.00–207.60)	38.80 (25.30–69.70)	0.416	0.812
UA (mmol/L)	349.73 ± 14.53	357.90 ± 19.21	353.56 ± 27.52	0.055	0.946
GFR (mL/(min·1.73 m^2))	139.62 ± 4.11	136.34 ± 7.52	135.69 ± 7.27	0.140	0.870
TC (mmol/L)	9.60 ± 0.36	10.12 ± 0.42	10.42 ± 0.89	1.164	0.559
TG (mmol/L)	2.60 ± 0.16	3.46 ± 0.30	2.77 ± 0.35	3.766	**0.026***
HDL-c (mmol/L)	1.57 ± 0.08	1.38 ± 0.08	1.42 ± 0.11	1.299	0.277
Fbg (g/L)	4.32 ± 0.21	4.78 ± 0.42	4.79 ± 0.33	0.917	0.406
IgA (g/L)	1.03 ± 0.06	1.02 ± 0.08	1.10 ± 0.11	0.218	0.804
IgG (g/L)	2.25 (1.36–7.95)	2.30 (1.36–4.79)	1.96 (1.43–7.51)	0.044	0.978
IgM (g/L)	1.73 ± 0.09	1.75 ± 0.12	1.55 ± 0.12	0.603	0.549
C3 (g/L)	1.24 ± 0.03	1.36 ± 0.05	1.18 ± 0.07	3.193	0.045*
C4 (g/L)	0.28 (0.10–1.13)	0.28 (0.10–0.49)	0.26 (0.13–0.49)	0.412	0.814
T (CD3+) (%)	69.85 ± 1.25	64.62 ± 2.44	72.93 ± 2.13	4.755	0.093
T (CD4+) (%)	37.15 ± 1.26	33.77 ± 2.09	34.71 ± 1.50	1.312	0.275
T (CD8+) (%)	27.73 ± 0.88	25.19 ± 1.59	32.00 ± 1.86	4.469	0.014*
NK (%)	10.09 ± 1.04	10.77 ± 1.53	7.57 ± 0.94	1.012	0.368
BC (%)	17.68 ± 0.88	21.08 ± 2.00	18.07 ± 1.85	1.299	0.522
FBG (mmol/L)	4.82 ± 0.08	4.99 ± 0.13	4.85 ± 0.12	0.733	0.483
FISN (mU/L)	2.37 (0.20–9.43)	1.92 (0.57–16.63)	2.13 (0.76–12.87)	0.180	0.914
FCP (nmol/L)	0.45 (0.18–1.24)	0.50 (0.22–1.95)	0.50 (0.24–1.15)	2.386	0.303
HOMA-IR	0.68 ± 0.07	0.89 ± 0.19	0.76 ± 0.17	0.218	0.897
HOMA-islet	37.22 (−141.54–895.56)	38.47 (5.50–278.22)	28.78 (13.66–224.47)	0.192	0.908
ISI	−2.29 ± 0.14	−2.46 ± 0.18	−2.51 ± 0.19	0.468	0.628
24-h UP (mg/kg)	141.71 (11.25–1179.80)	125.88 (27.69–319.00)	176.52 (45.00–301.00)	1.064	0.587

$^*P < 0.05$, $^{**}P < 0.01$.

Table 5: The distribution of the PPAR-γ (Pro12Ala) genotypes among individuals with different renal pathological types.

PPAR-γ genotype	IgMN n (%)	MsPGN n (%)	IgAN n (%)	FSGS n (%)	C1qN n (%)	MCD n (%)	χ^2	P value
PP	5 (15.6%)	9 (28.1%)	3 (9.4%)	5 (15.6%)	5 (15.6%)	1 (3.1%)	5.698	0.285
PA/AA	2 (6.3%)	0 (0%)	2 (6.3%)	0 (0%)	0 (0%)	0 (0%)		

Table 6: The distribution of the PGC-1α (Gly482Ser) genotypes among individuals with different renal pathological types.

PGC-1α genotype	IgMN n (%)	MsPGN n (%)	IgAN n (%)	FSGS n (%)	C1qN n (%)	MCD n (%)	χ^2	P value
GG	2 (6.7%)	1 (3.3%)	1 (3.3%)	3 (10%)	0 (0%)	0 (0%)	11.633	0.252
GA	2 (6.7%)	6 (20%)	2 (6.7%)	1 (3.3%)	4 (13.3%)	0 (0%)		
AA	3 (10%)	1 (3.3%)	0 (0%)	2 (6.7%)	1 (3.3%)	1 (3.3%)		

Table 7: The distribution of the PPAR-γ (Pro12Ala) genotypes in groups with different responses to hormone treatment.

PPAR-γ genotype	Hormone-sensitive group n (%)	Hormone-resistant group n (%)	Hormone-dependent group n (%)	χ^2	P value
PP	77 (71.3%)	13 (12.0%)	11 (10.2%)	0.779	0.824
PA/AA	6 (5.6%)	0 (0%)	1 (0.9%)		

Table 8: The distribution of the PGC-1α (Gly482Ser) genotypes in groups with different responses to hormone treatment.

PGC-1α genotype	Hormone-sensitive group n (%)	Hormone-resistant group n (%)	Hormone-dependent group n (%)	χ^2	P value
GG	11 (10.5%)	3 (2.9%)	3 (2.9%)	3.500	0.473
GA	47 (44.8%)	6 (5.7%)	4 (3.8%)		
AA	24 (22.2%)	5 (4.8%)	2 (1.9%)		

the PGC1α (Gly482Ser) gene polymorphism. We analyzed the distribution of three PGC1α genotypes in PNS and NC children and found no association between the PGC-1α (Gly482Ser) genotype and PNS occurrence. However, further-stratified analysis of children with PNS showed that blood TG levels in patients with the AA genotype were significantly increased after matching for age, sex, and BMI. Previous studies have shown that PGC-1α can collaborate with PPAR-α, PPAR-γ, and the farnesoid X receptor to enhance fatty acid oxidation and regulate TG metabolism [14]. Furthermore, mutations at the Gly482Ser position of the PGC-1α gene could also induce functional changes in PGC-1α [15]. These results suggest that functional changes in the PGC-1α gene resulting from the Gly482Ser mutation may affect TG metabolism. Animal studies demonstrated that liver TG levels in PGC-1α-knockout mice were increased threefold compared with the control group [16]. The results of the current study were consistent with those of previous studies, although differences in TG levels between genotypes were inconclusive.

We further analyzed glucose metabolism in PNS children and found no differences in FBG, FISN, FCP, HOMA-IR, HOMA-islet, and ISI among GG, GA, and AA genotypes. We were therefore unable to establish an association between the Gly482Ser site of the PGC-1α gene and glucose metabolism disorders and IR. However, several previous studies have demonstrated a close correlation between mutations at the Gly482Ser site of PGC-1α and glucose metabolism, and 482Ser was shown to increase the risk of type II diabetes in the population. Muller et al. [17] analyzed the SNPs of PGC-1α in nondiabetic Pima Indians and showed that the Gly482Ser site was associated with IR. Moreover, Pima Indians with the Gly/Gly genotype had lower levels of insulin secretion following glucose loading, suggesting that the PGC-1α gene could be a candidate gene for type II diabetes. This study found that patients with the Ser/Ser genotype had slightly higher FBG and HOMA-IR values and slightly lower FISN levels compared with patients with the other two genotypes, indicating that a correlation between the Gly482Ser site and glucose metabolism remains to be confirmed.

In summary, the results of this study showed no significant correlations between the PPAR-γ (Prol2Ala) and PGC-1α (Gly482Ser) gene polymorphisms and the occurrence of PNS. However, mutation at the Pro12Ala position of the PPAR-γ gene may be associated with increased insulin sensitivity and decreased insulin secretion in children with PNS. Moreover, increased TG levels in patients with the PGC-1α (Gly482Ser) AA genotype suggest that this polymorphism may be responsible for TG abnormalities in children with PNS.

Conflict of Interests

All the authors declared no conflict of interests, including relevant financial interests, activities, relationships, and affiliations.

Authors' Contribution

Jiaping Jin and Guixia Ding contributed equally to this paper.

Acknowledgments

This work was supported by Grants from the National Basic Research Program of China 973 Program (nos. 2012CB517602 and 2013CB530604), the National Natural Science Foundation of China (nos. 81170635 and 81270785), the Natural Science Foundation of Jiangsu Province (no. BK2012001), and the Program for New Century Excellent Talents in University (no. NCET-12-0738).

References

[1] Y. Guan and M. D. Breyer, "Peroxisome proliferator-activated receptors (PPARs): novel therapeutic targets in renal disease," *Kidney International*, vol. 60, no. 1, pp. 14–30, 2001.

[2] H. N. Gouda, G. S. Sagoo, A.-H. Harding, J. Yates, M. S. Sandhu, and J. P. T. Higgins, "The association between the peroxisome proliferator-activated receptor-γ2 (PPARG2) Pro12Ala gene

variant and type 2 diabetes mellitus: a HuGE review and meta-analysis," *The American Journal of Epidemiology*, vol. 171, no. 6, pp. 645–655, 2010.

[3] T. Sparsø, M. S. Hussain, G. Andersen et al., "Relationships between the functional PPARα Leu162Val polymorphism and obesity, type 2 diabetes, dyslipidaemia, and related quantitative traits in studies of 5799 middle-aged white people," *Molecular Genetics and Metabolism*, vol. 90, no. 2, pp. 205–209, 2007.

[4] L. Andrulionytè, J. Zacharova, J.-L. Chiasson, and M. Laakso, "Common polymorphisms of the PPAR-γ2 (Pro12Ala) and PGC-1α (Gly482Ser) genes are associated with the conversion from impaired glucose tolerance to type 2 diabetes in the STOP-NIDDM trial," *Diabetologia*, vol. 47, no. 12, pp. 2176–2184, 2004.

[5] H. Kobayashi, G. Tokudome, Y. Hara et al., "Insulin resistance is a risk factor for the progression of chronic kidney disease," *Clinical Nephrology*, vol. 71, no. 6, pp. 643–651, 2009.

[6] A. Jorsal, L. Tarnow, M. Lajer et al., "The PPARγ2 Pro12Ala variant predicts ESRD and mortality in patients with type 1 diabetes and diabetic nephropathy," *Molecular Genetics and Metabolism*, vol. 94, no. 3, pp. 347–351, 2008.

[7] J. Jin, B. Jin, S. Huang et al., "Insulin resistance in children with primary nephrotic syndrome and normal renal function," *Pediatric Nephrology*, vol. 27, pp. 1901–1909, 2012.

[8] Y. Chung-Jen, B. A. Beamer, C. Negri et al., "Molecular scanning of the human peroxisome proliferator activated receptor γ (hPPARγ) gene in diabetic Caucasians: identification of a Pro12Ala PPARγ2 missense mutation," *Biochemical and Biophysical Research Communications*, vol. 241, no. 2, pp. 270–274, 1997.

[9] S. S. Deeb, L. Fajas, M. Nemoto et al., "A Pro12Ala substitution in PPARγ2 associated with decreased receptor activity, lower body mass index and improved insulin sensitivity," *Nature Genetics*, vol. 20, no. 3, pp. 284–287, 1998.

[10] J. Masugi, Y. Tamori, H. Mori, T. Koike, and M. Kasuga, "Inhibitory effect of a proline-to-alanine substitution at codon 12 of peroxisome proliferator-activated receptor-γ 2 on thiazolidinedione-induced adipogenesis," *Biochemical and Biophysical Research Communications*, vol. 268, no. 1, pp. 178–182, 2000.

[11] N. Stefan, A. Fritsche, H. Häring, and M. Stumvoll, "Effect of experimental elevation of free fatty acids on insulin secretion and insulin sensitivity in healthy carriers of the Pro12Ala polymorphism of the peroxisome proliferator-activated receptor-γ2 gene," *Diabetes*, vol. 50, no. 5, pp. 1143–1148, 2001.

[12] R. Buzzetti, A. Petrone, M. C. Ribaudo et al., "The common PPAR-γ2 Pro12Ala variant is associated with greater insulin sensitivity," *European Journal of Human Genetics*, vol. 12, no. 12, pp. 1050–1054, 2004.

[13] J. Song, M. Sakatsume, I. Narita et al., "Peroxisome proliferator-activated receptor γ C161T polymorphisms and survival of Japanese patients with immunoglobulin A nephropathy," *Clinical Genetics*, vol. 64, no. 5, pp. 398–403, 2003.

[14] Y. Zhang, L. W. Castellani, C. J. Sinal, F. J. Gonzalez, and P. A. Edwards, "Peroxisome proliferator-activated receptor-γ coactivator 1α (PGC-1α) regulates triglyceride metabolism by activation of the nuclear receptor FXR," *Genes and Development*, vol. 18, no. 2, pp. 157–169, 2004.

[15] M.-C. Vohl, A. Houde, S. Lebel, F.-S. Hould, and P. Marceau, "Effects of the peroxisome proliferator-activated receptor-γ co-activator-1 Gly482Ser variant on features of the metabolic syndrome," *Molecular Genetics and Metabolism*, vol. 86, no. 1-2, pp. 300–306, 2005.

[16] S.-H. Koo, H. Satoh, S. Herzig et al., "PGC-1 promotes insulin resistance in liver through PPAR-α-dependent induction of TRB-3," *Nature Medicine*, vol. 10, no. 5, pp. 530–534, 2004.

[17] Y. L. Muller, C. Bogardus, O. Pedersen, and L. Baier, "A Gly482Ser missense mutation in the peroxisome proliferator-activated receptor γ coactivator-1 is associated with altered lipid oxidation and early insulin secretion in Pima Indians," *Diabetes*, vol. 52, no. 3, pp. 895–898, 2003.